Collective excitations in nuclei: The isoscalar and isovector electric giant resonances and spin-isospin charge-exchange modes

Muhsin N. Harakeh

KVI-CART, University of Groningen, the Netherlands

XVI International Meeting on
“Selected Topics in Nuclear and Atomic Physics”
Fiera di Primiero, Italy
2-6 October 2017

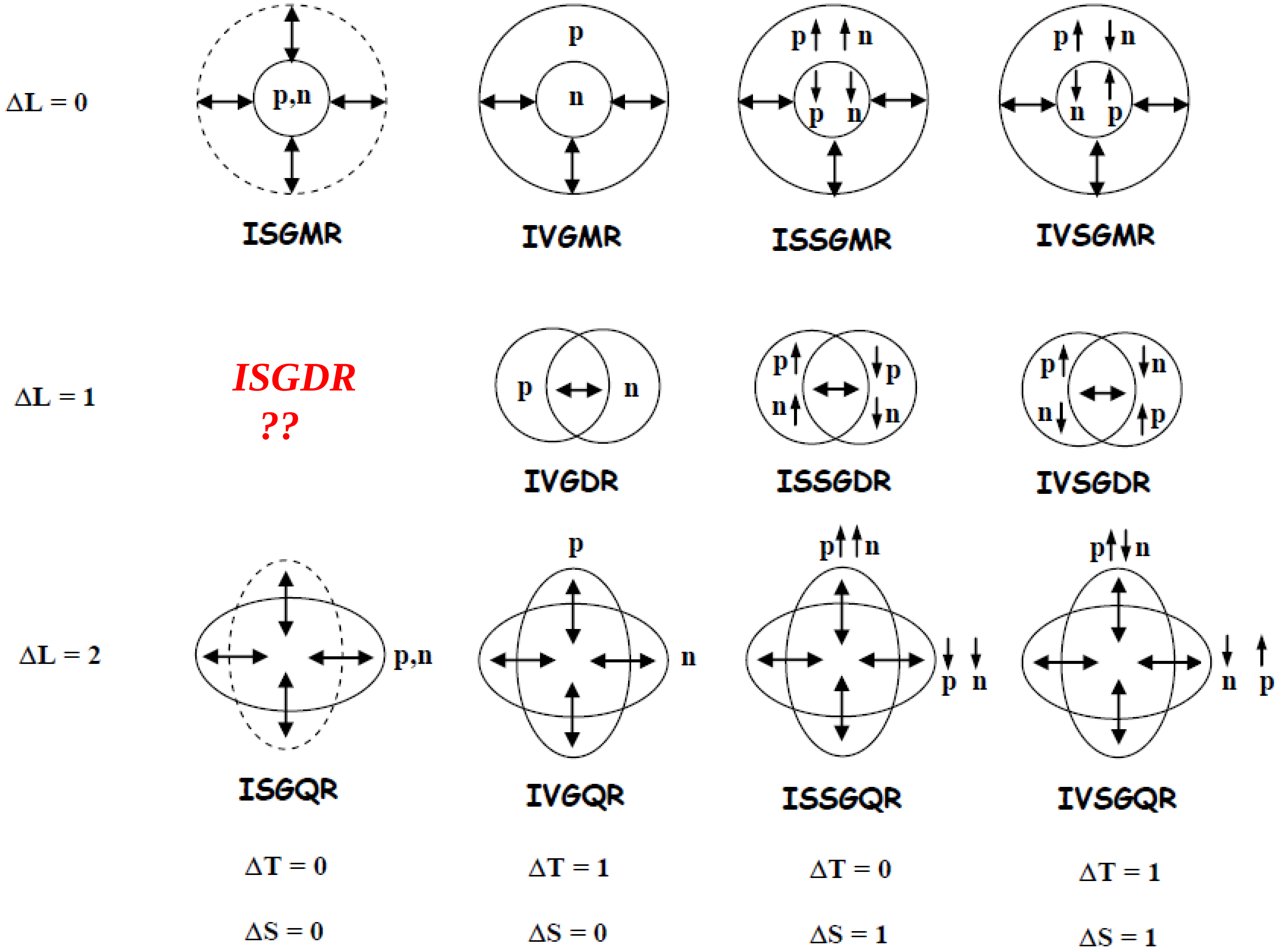
ΔL = 0
p,n
ISGMR
p
n
IVGMR
p n
p n
ISSGMR
p n
n p
IVSGMR
ΔL = 1
ISGDR
??
p
n
IVGDR
p
p
n
n
ISSGDR
p
n
n
p
IVSGDR
ΔL = 2
p,n
ISGQR
p
n
IVGQR
p n
p n
ISSGQR
p n
n p
IVSGQR
ΔT = 0
ΔS = 0
ΔT = 1
ΔS = 0
ΔT = 0
ΔS = 1
ΔT = 1
ΔS = 1

Spin-isospin excitations

Neutral (ν,ν') and charged (ν_e,e^-), (ν_e,e^+) currents

NC ⇒ Inelastic electron and proton scattering

⇒ *M0*, *M1*, *M2*

CC ⇒ Charge-exchange reactions

Isovector charge-exchange modes

⇒ IAS, GTR, IVSGMR, IVSGDR, etc.

Importance for nuclear astrophysics,

ν-physics, 2β-decay, *n*-skin thickness, etc.

(*p*,*n*), (^{3}He,*t*) {GT^-}; (*n*,*p*), (*d*,^{2}He) & (*t*,^{3}He) {GT^+}

Nucleus → **Many-body system with a finite size**

Vibrations → **Multipole expansion with r, Y_{lm}, τ, σ**

	ΔS=0, ΔT=0	ΔS=0, ΔT=1	ΔS=0, ΔT=1	ΔS=1, ΔT=1	ΔS=1, ΔT=1
***L=0*: Monopole**	ISGMR r^2Y_0	IAS τY_0	IVGMR τr^2Y_0	GTR $\tau\sigma Y_0$	IVSGMR $\tau\sigma r^2Y_0$
***L=1*: Dipole**	ISGDR $(r^3 - 5/3\langle r^2\rangle r)Y_1$		IVGDR τrY_1		IVSGDR $\tau\sigma rY_1$
***L=2*: Quadrupole**	ISGQR r^2Y_2		IVGQR τr^2Y_2		IVSGQR $\tau\sigma r^2Y_2$
***L=3*: Octupole**	LEOR, HEOR r^3Y_3				

Dropped ΔS=1, ΔT=0 operators because excitations are very weak

Non-Energy-Weighted Sum Rules

Intermezzo: Sum rules

Fermi, Gamow-Teller and higher multipole non-energy-weighted sum rules (NEWSR):

Gamow-Teller operator

$$\beta_{\pm}(\mu) = \frac{1}{2}\sum_{k=1}^{A} \sigma_{\mu k}\tau_{\pm k}$$

$$(\mu = -1, 0, +1), \qquad \tau_{\pm} = (\tau_x \pm i\tau_y)$$

$$\frac{1}{2}\tau_{-}|n\rangle = |p\rangle, \qquad \frac{1}{2}\tau_{+}|p\rangle = |n\rangle, \;\; \tau_{-}|p\rangle = \tau_{+}|n\rangle = 0$$

$$S_{\pm}(GT) = \sum_{f,\mu} \left|\langle f|\beta_{\pm}(\mu)|i\rangle\right|^{2}$$

$$S_{\pm}(GT) = \sum_{f,\mu} \langle f|\beta_{\pm}(\mu)|i\rangle^{*} \langle f|\beta_{\pm}(\mu)|i\rangle$$

$$S_{\pm}(GT) = \sum_{f,\mu} \langle i|\beta_{\pm}^{\dagger}(\mu)|f\rangle \langle f|\beta_{\pm}(\mu)|i\rangle$$

Using closure:

$$S_{\pm}(GT) = \sum_{\mu} \langle i | \beta_{\pm}^{\dagger}(\mu) \beta_{\pm}(\mu) | i \rangle$$

$$\tau_{\mp}^{\dagger} = \tau_{\pm}$$

$$S_{-}(GT) - S_{+}(GT) = \sum_{\mu} \langle i | \beta_{-}^{\dagger}(\mu) \beta_{-}(\mu) - \beta_{+}^{\dagger}(\mu) \beta_{+}(\mu) | i \rangle$$

$$S_{-}(GT) - S_{+}(GT) = \frac{1}{4} \langle i | \sum_{k=1}^{A} \sum_{\mu=-1}^{+1} \left[\sigma_{\mu k}^{\dagger} \tau_{+k} \sigma_{\mu k} \tau_{-k} - \sigma_{\mu k}^{\dagger} \tau_{-k} \sigma_{\mu k} \tau_{+k} \right] | i \rangle$$

$$S_{-}(GT) - S_{+}(GT) = \frac{1}{4} \langle i | \sum_{k=1}^{A} \left[\sigma_{k}^{2} \tau_{+k} \tau_{-k} - \sigma_{k}^{2} \tau_{-k} \tau_{+k} \right] | i \rangle$$

$$S_{-}(GT) - S_{+}(GT) = \frac{3}{4} \langle i | \sum_{k=1}^{A} [\tau_{+k} \tau_{-k} - \tau_{-k} \tau_{+k}] | i \rangle$$

$$\sigma^2 = \sum_{\mu=-1}^{+1} [\sigma_\mu^\dagger \sigma_\mu] \, ; \quad expectation\ value\ of\ \sigma^2\ is\ 3.$$

$$\tau_+\tau_-|n\,\rangle = 4|n\,\rangle$$

$$, \qquad \tau_-\tau_+|p\,\rangle = 4|p\,\rangle, \;\; \tau_+\tau_-|p\,\rangle = \tau_-\tau_+|n\,\rangle = 0$$

$$S_-(GT) - S_+(GT) = \frac{3}{4} \times 4\,(N-Z) = 3(N-Z)$$

This is the Ikeda sum rule. For the Fermi sum rule:

$$S_\pm(F) = \frac{1}{4} \sum_{f,\mu} \left| \langle f | \tau_\pm | i \rangle \right|^2$$

$$S_-(F) - S_+(F) = \frac{1}{4} \times 4\,(N-Z) = (N-Z)$$

Isovector non-spin-flip and isovector spin-flip higher multipole operators:

$$O_{\pm}^{\lambda t}(M) = \frac{1}{2}\sum_{k=1}^{A} r_k^{\lambda} Y_{\lambda M}(\hat{r}_k)\tau_{\pm k}$$

$$O_{\pm}^{\lambda \sigma t}(M\mu) = \frac{1}{2}\sum_{k=1}^{A} r_k^{\lambda} [Y_{\lambda}(\hat{r}_k)\otimes\vec{\sigma}_k]_{J^{\pi}}\tau_{\pm k}$$

$$S_{-}^{\lambda J} - S_{+}^{\lambda J}(GT) = \frac{3(2J+1)}{2\pi}\left(N\langle r_n^{2\lambda}\rangle - Z\langle r_p^{2\lambda}\rangle\right)$$

If spin-flip is involved the sum over possible *J*-values yields a factor $3(2\lambda+1)$.

Gamow-Teller excitations and Astrophysical Implications

Spin-isospin excitations

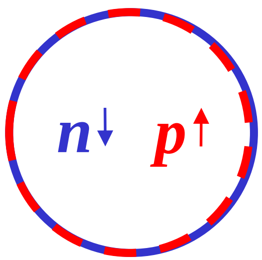

***ΔL* = 0 *ΔS* = 1 *ΔT* = 1**

GTR

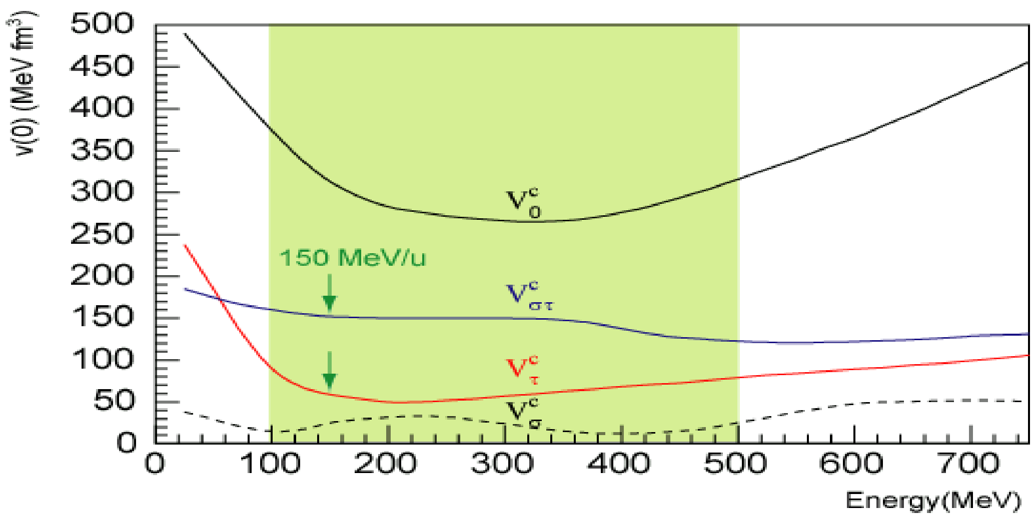

- **Gamow-Teller transitions;**
  Isospin (*ΔT* = 1)
  Spin (*ΔS* = 1)

Advantages

- **Cross section peaks at θ = 0° (*ΔL* = 0)**
- **Strong excitation of GT states at *E* = 100-500 MeV/u**

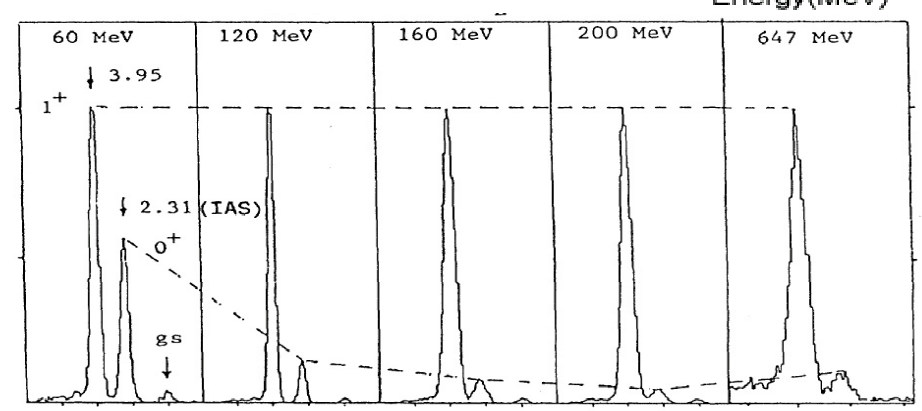

FIG. 4. Zero-degree cross-section spectra for the $^{14}C(p,n)^{14}N$ reactions at the indicated bombarding energies. The spectra have been arbitrarily normalized. From Gaarde (1985) and Rapaport (1989).

J. Rapaport, E. Sugarbaker, Annu. Rev. Nucl. Part. Sci. 44 (1994) 109

Spin-flip & GT transitions

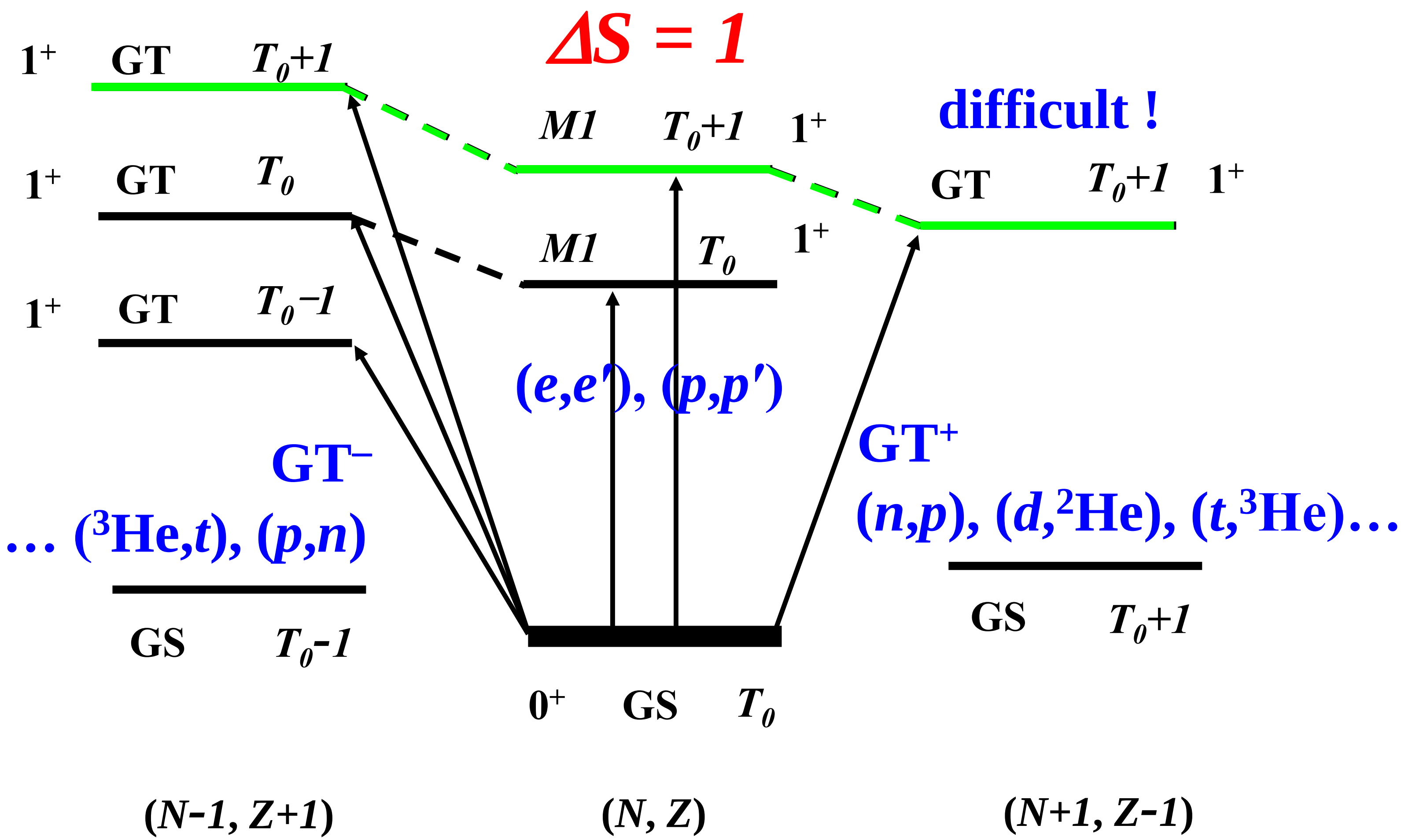

Charge-exchange probes

(p,n)-type ($\Delta T_z = -1$)

- β^--decay
- (p,n)
- (^{3}He,t)
- heavy ion

(n,p)-type ($\Delta T_z = +1$)

- β^+-decay
- (n,p)
- (d,^{2}He)
- (t,^{3}He)
- heavy ion; (^{7}Li,^{7}Be)

- Energy per nucleon (> 100 MeV/u)
- Spin-flip versus non-spin-flip
- Complexity of reaction mechanism
- Experimental considerations

The (p,n) reaction at 0 degree

- **Cross sections at $E_p \geq 100$ MeV, $q = 0$ for (p,n) reactions**

$$\frac{d\sigma}{d\Omega} = \frac{\mu_i \mu_f}{(\pi\hbar^2)^2}\left(\frac{k_f}{k_i}\right)(N_\tau^D \,|\, J_\tau \,|^2\, B(F) + N_{\sigma\tau}^D \,|\, J_{\sigma\tau} \,|^2\, B(GT))$$

T. N. Taddeucci *et al.*, Nucl. Phys. A469 (1987) 125
I. Bergqvist *et al.*, Nucl. Phys. A469 (1987) 648

- **Neutrino absorption cross sections**

$$\sigma = \frac{1}{\pi \hbar^4 c^3}\left[G_V^2 B(F) + G_A^2 B(GT)\right] \times F(Z,E_e) p_e E_e$$

$F(Z,E_e)$ is the relativistic Coulomb barrier factor

Importance of charge-exchange reactions at intermediate energies

Time of flight (ToF) neutron spectra for $^{90}Zr(p, n)^{90}Nb$ reaction

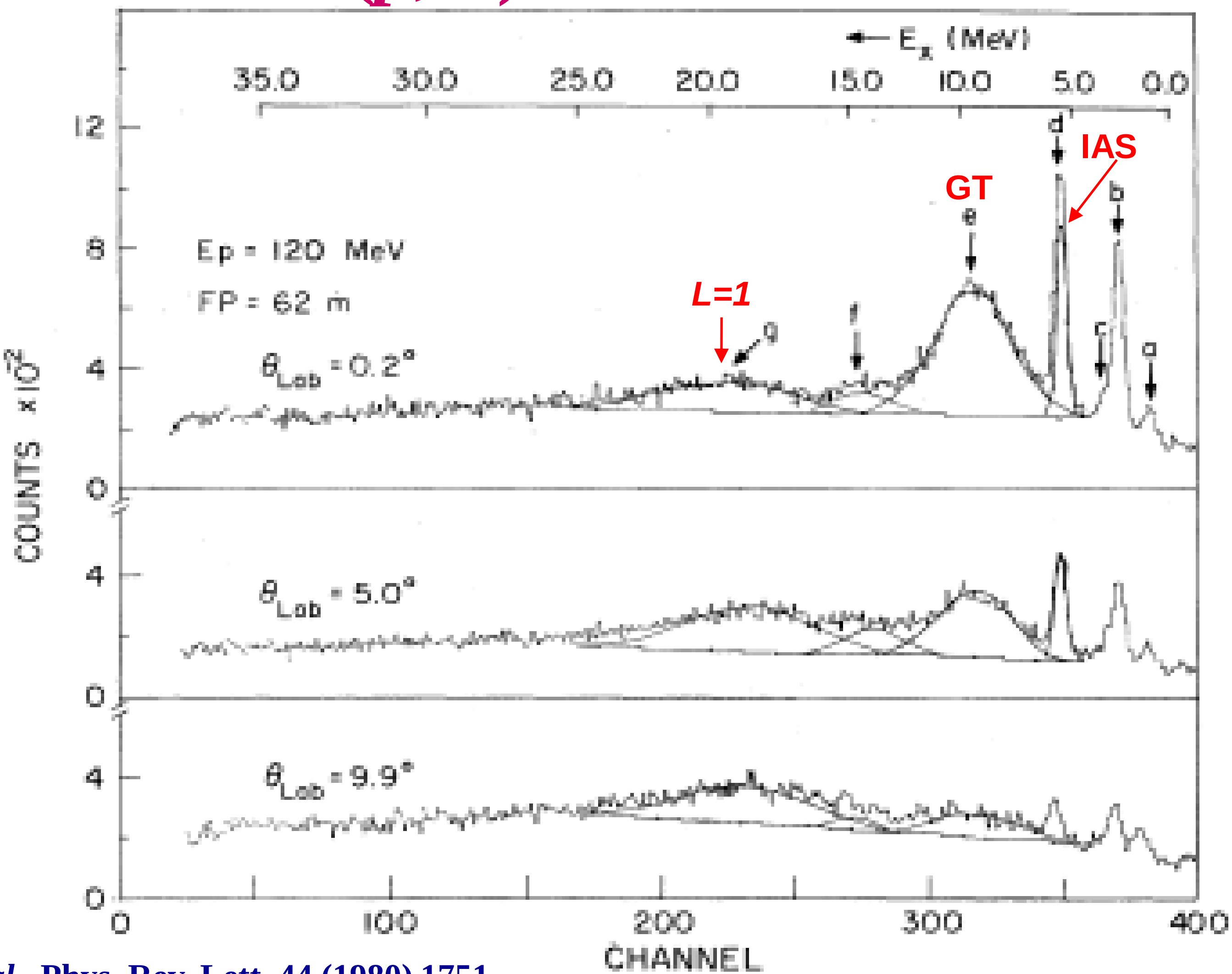

D.E. Bainum *et al.*, Phys. Rev. Lett. 44 (1980) 1751

(p, n) excitation-energy spectra for Fe and Ni Isotopes from ToF measurements

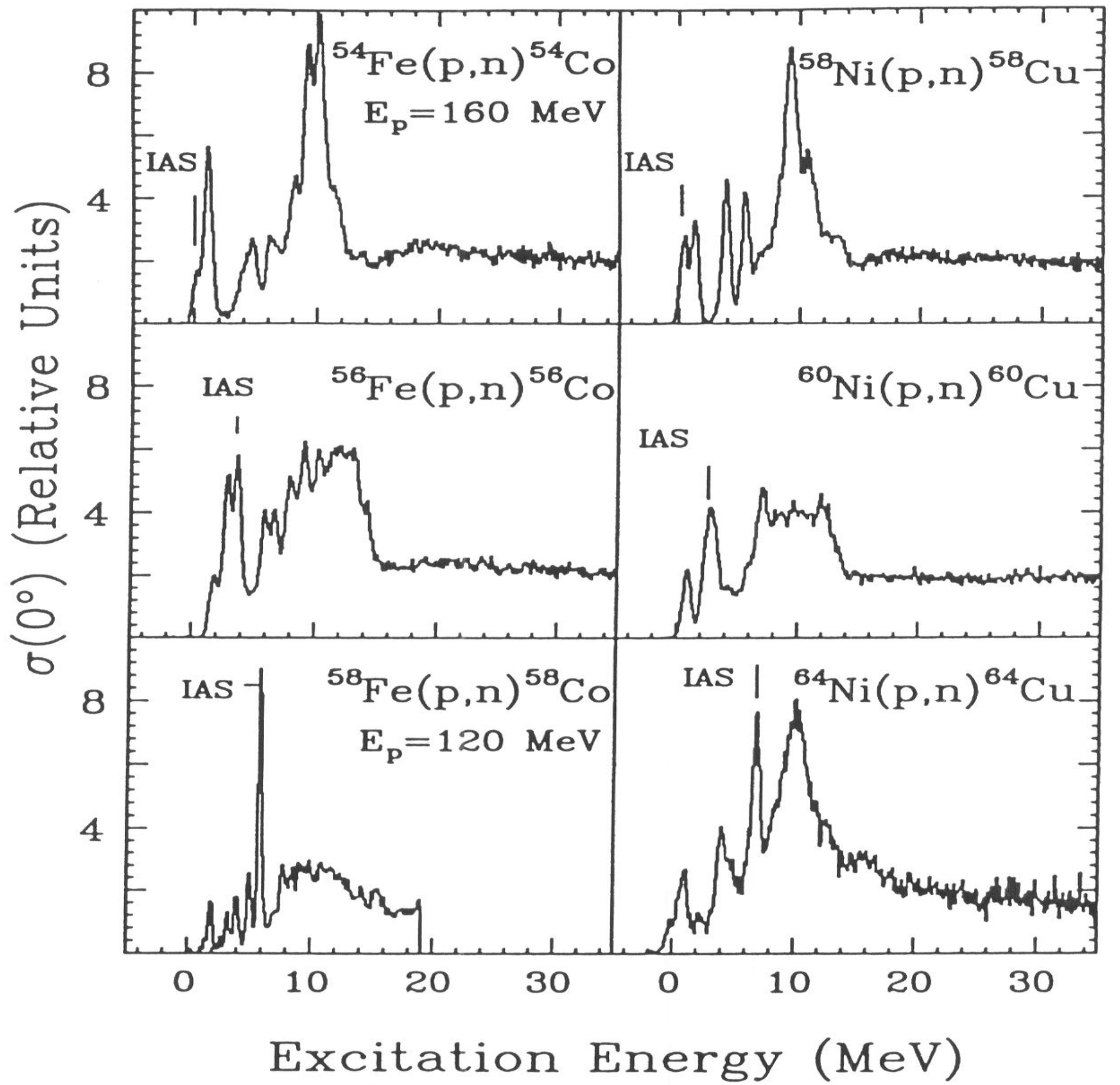

J. Rapaport, E. Sugarbaker, Annu. Rev. Nucl. Part. Sci. 44 (1994) 109

situation before 1997

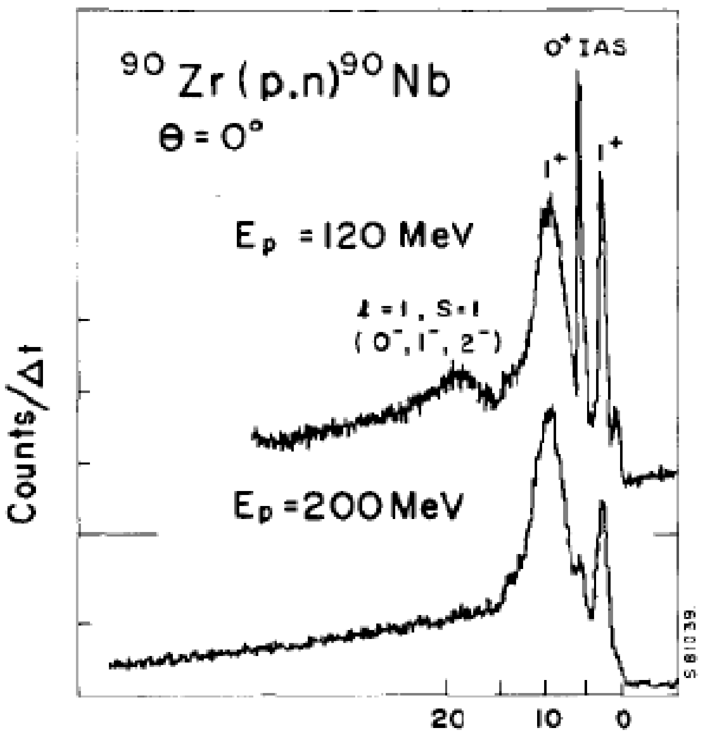

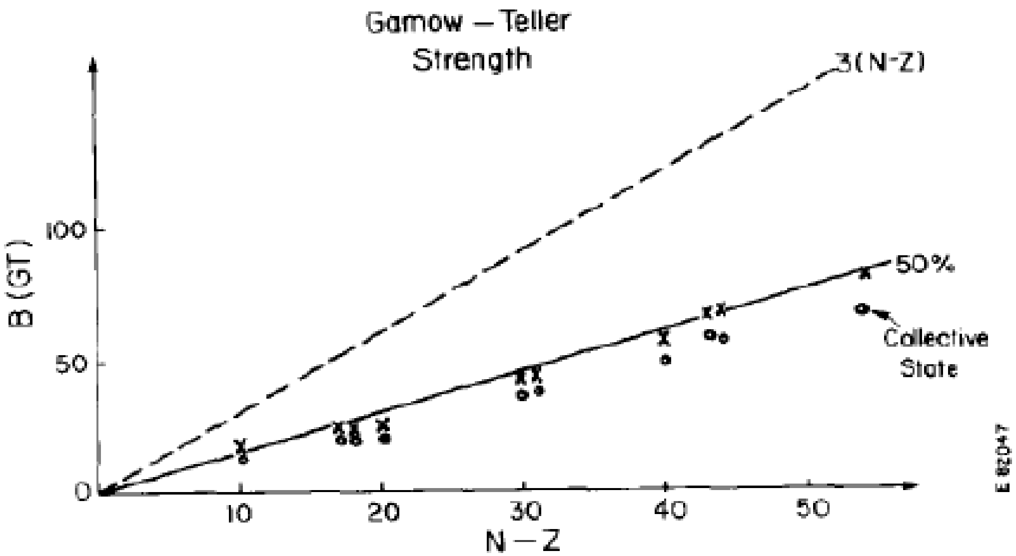

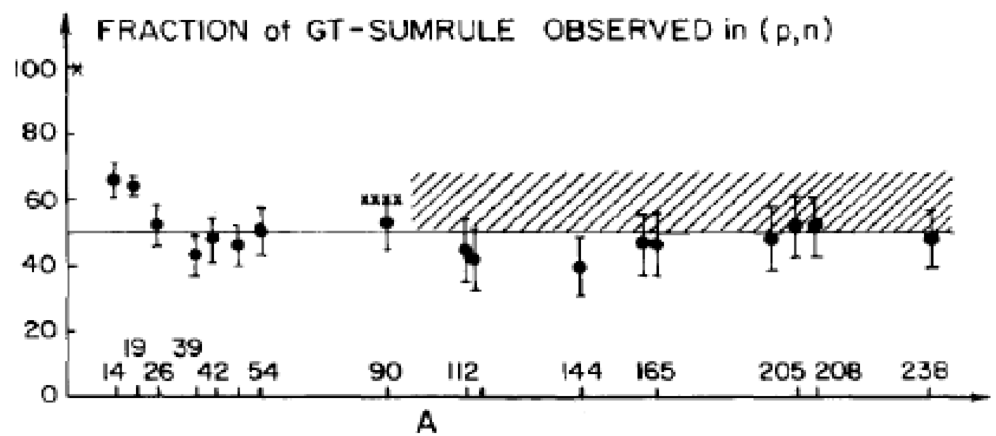

The quenching problem of GT strength

1- Pushed to higher energies by tensor force, or

2- Coupling to Δ resonance

C. Gaarde, Nucl. Phys. A396 (1983) 127c

^{90}Zr (p,n) ^{90}Nb

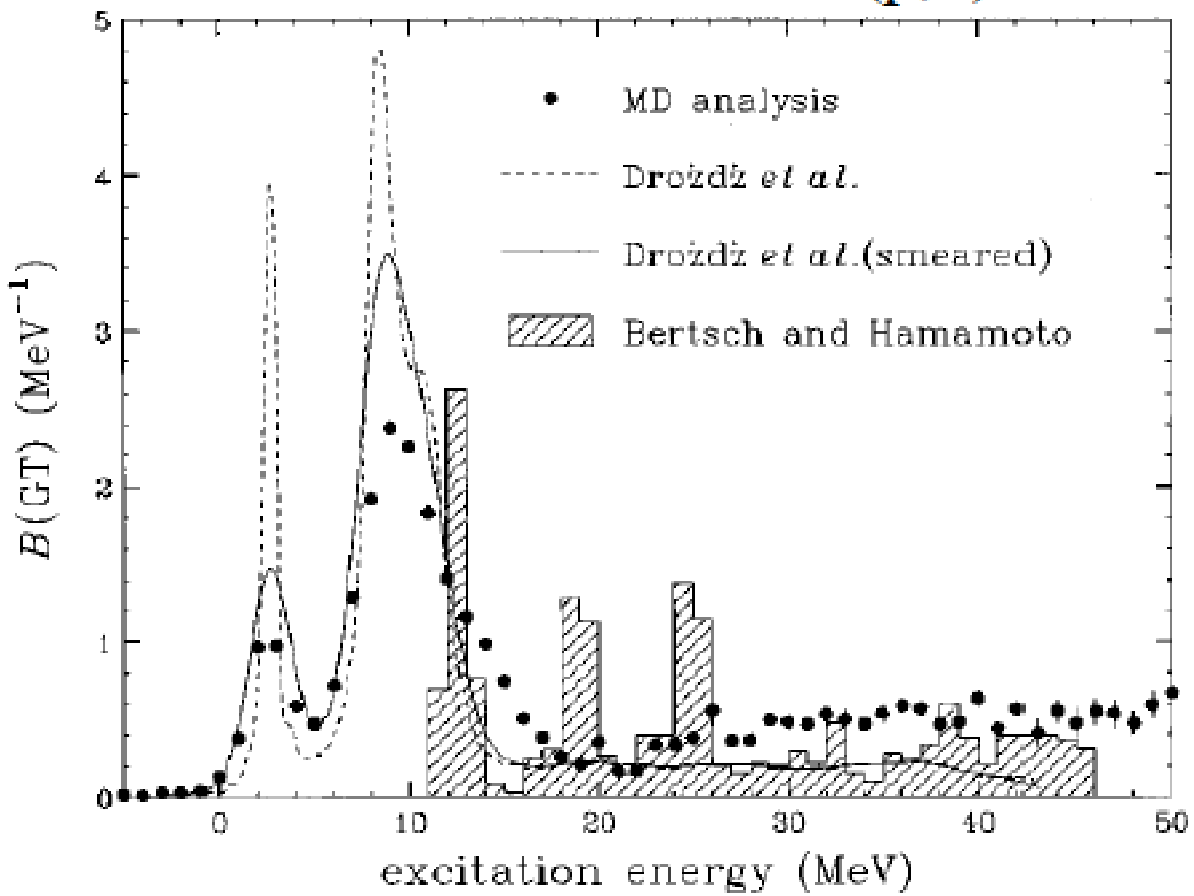

T. Wakasa et al., PRC55 ('97) 2909

$S_- - S_+ = 27.0 \pm 1.6 = (90 \pm 5)\%$ of Ikeda sum rule

⇒ *Δ* contribution is small

T. Wakasa *et al.*, Phys. Rev. C 55 (1997) 2909

(^{3}He,t) Reaction ≥ 100 MeV/u

- **Energy dependence of effective interactions.**

- **At RCNP, Osaka**

  $E(^3\text{He}) \approx 150$ MeV/u

  - **V_0 part: Minimum.**
  - **$V_{\sigma t}$ part: Relatively large.**
  - **V_t part: Minimum.**
  - **V_σ part: Negligible**

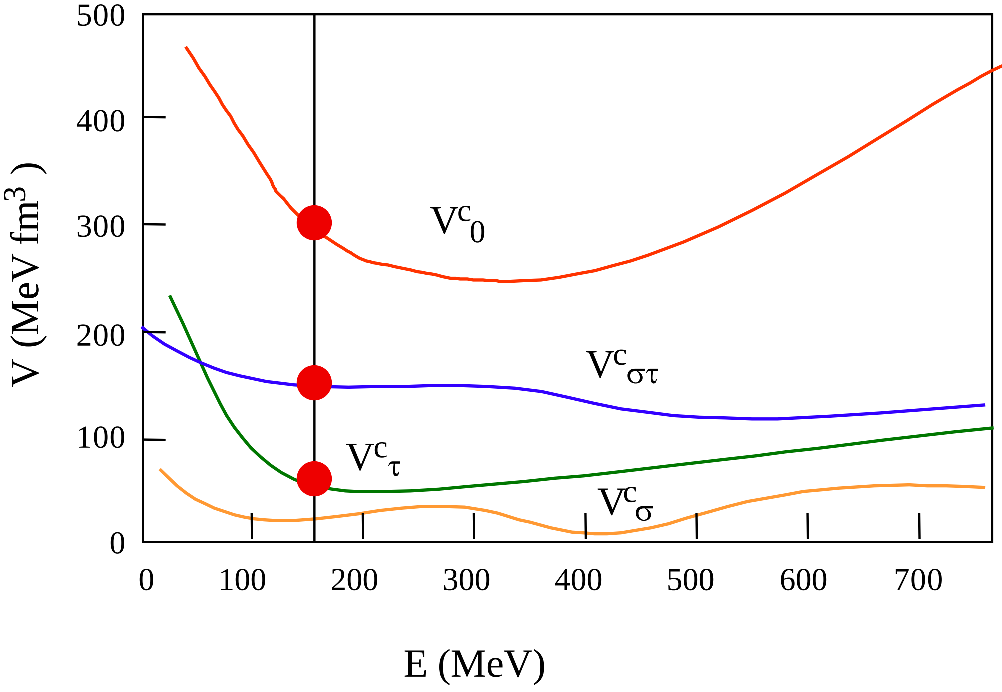

The (^{3}He,*t*) reaction at 0 degree
Measuring GT strengths

Cross sections at E(^{3}He) = 450 MeV, q = 0 for (^{3}He,t) reactions

$$\frac{d\sigma}{d\Omega}(q=0) = K N_D \left| J_{\sigma\tau} \right|^2 B(GT)$$

- K: kinematic factor
- N_D: distortion factor
- $J_{\sigma\tau}$: nucleon-nucleus interaction
- $B(GT)$: Gamow-Teller strength

Calibration of *B(GT)* to cross section for known transitions (e.g., from β-decay)

Experiments at RCNP, Osaka University

- **(^{3}He,*t*) reaction at 420 MeV**
  - **High-resolution spectrometer "Grand Raiden"**
  - **$\Delta E \sim 30$ keV**

Used ^{164}Dy(^{3}He,t)^{164}Ho (g.s., 1+) reaction for calibration: logft 4.6 → $B(GT)$ = 0.293±0.006

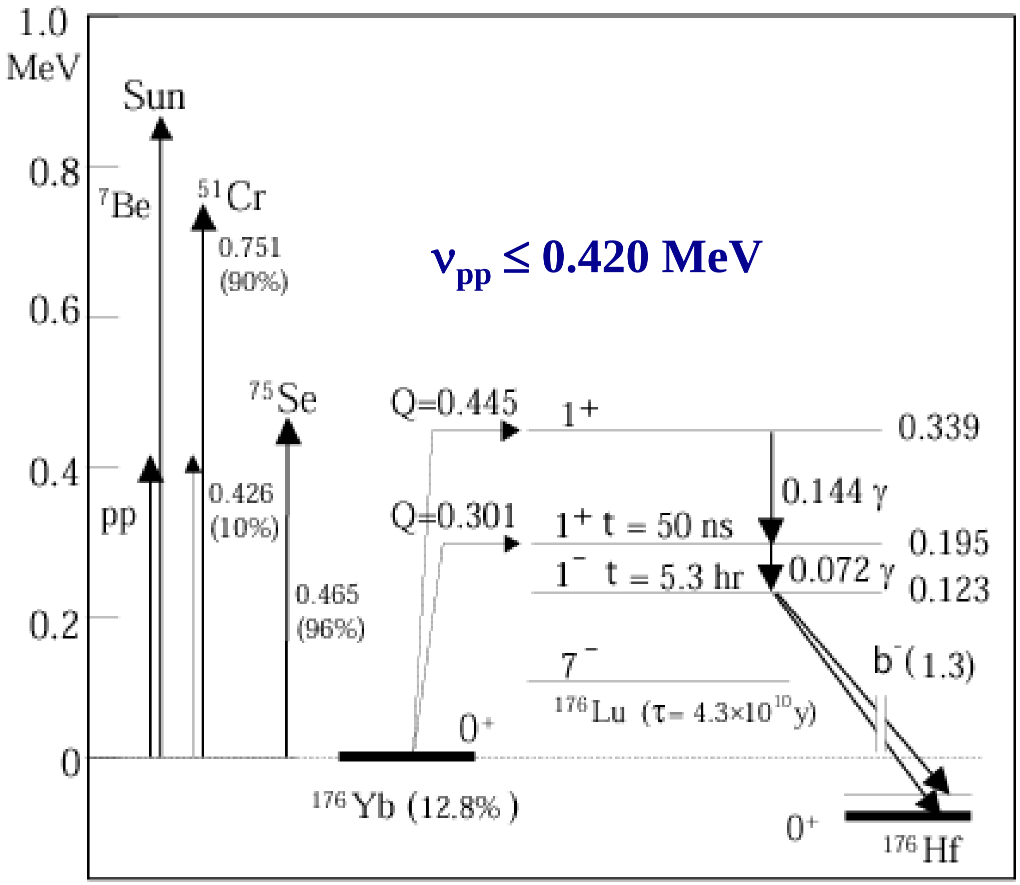

M. Fujiwara *et al.*, PRL 85 (2000) 4442

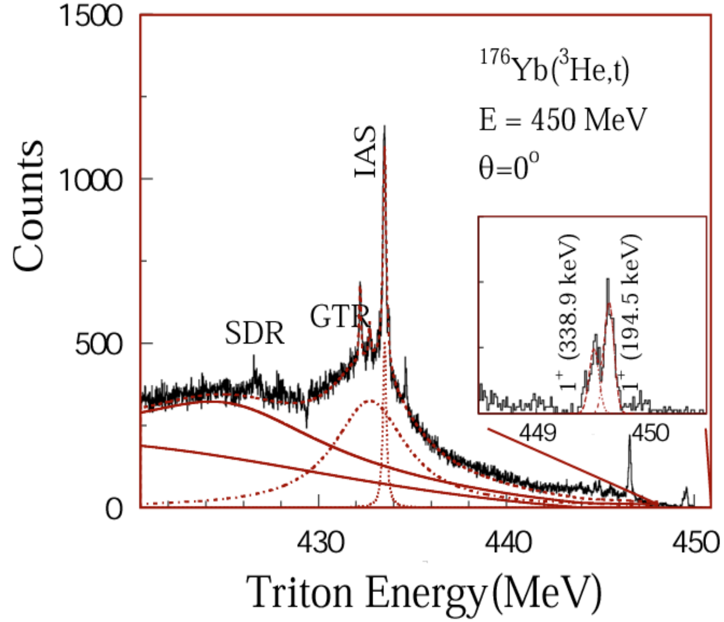

Resolution ≈ 100 to 130 keV

E_x(MeV)	0.195+0.339 (p,n)	0.195 (^{3}He,t)	0.339 (^{3}He,t)
$B(GT)$	0.32±0.04	0.20±0.04	0.11±0.02

Beam line WS-course

Grand-Raiden Spectrometer

M. Fujiwara *et al*., NIM A422 (1999) 484

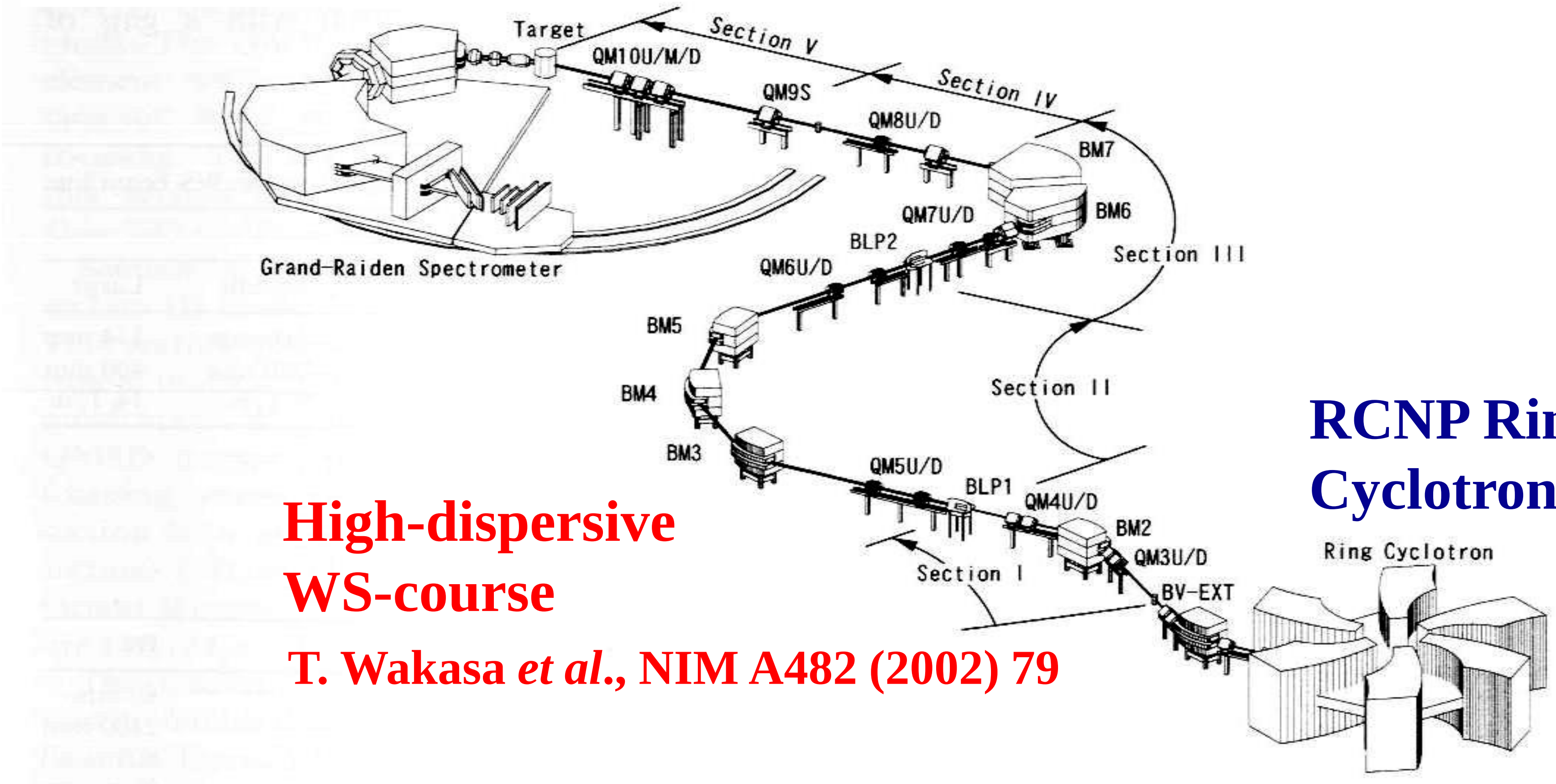

RCNP Ring Cyclotron

High-dispersive WS-course

T. Wakasa *et al*., NIM A482 (2002) 79

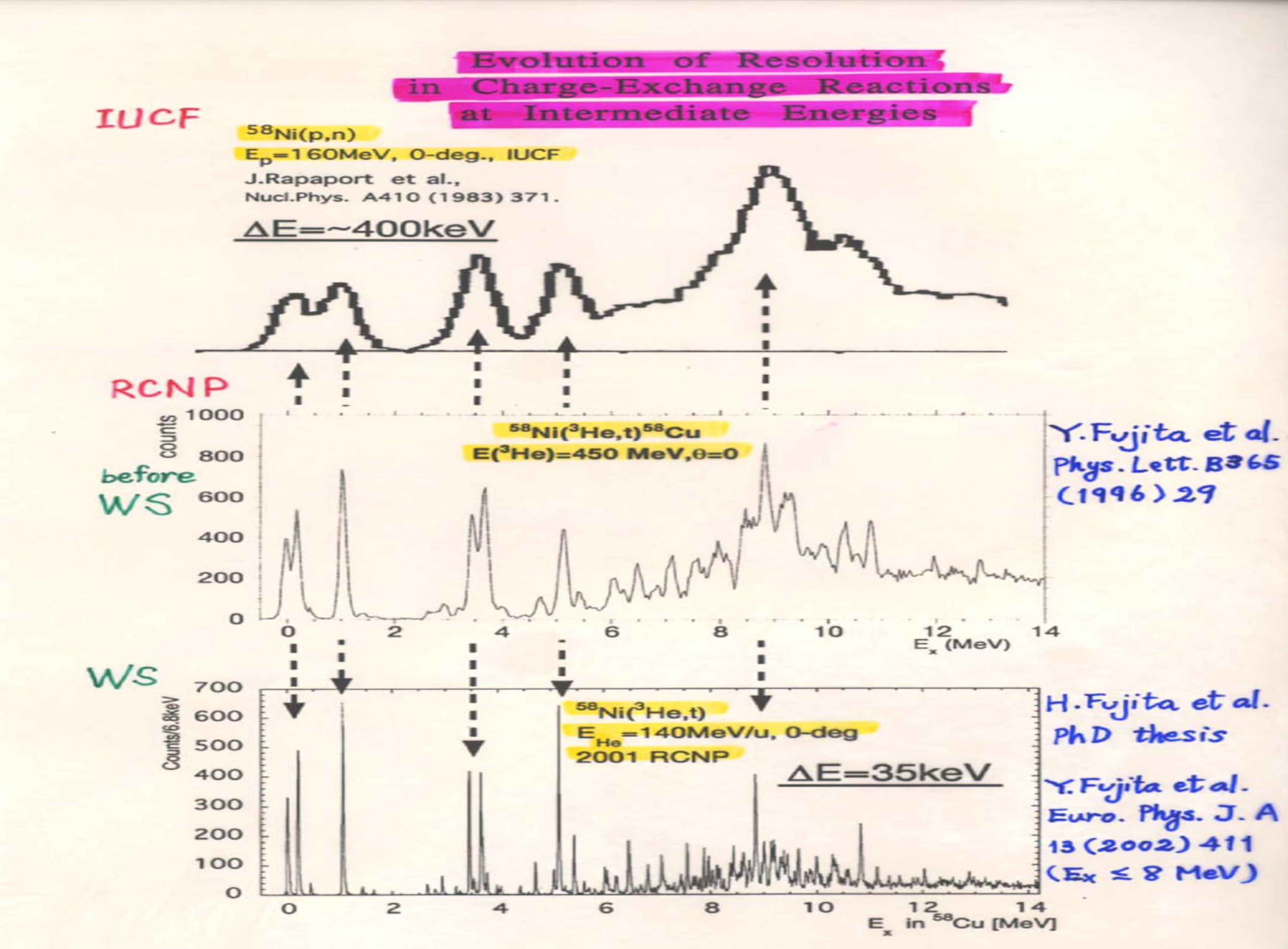
Evolution of Resolution
in Charge-Exchange Reactions
at Intermediate Energies
IUCF
58Ni(p,n)
Ep=160MeV, 0-deg., IUCF
J.Rapaport et al.,
Nucl.Phys. A410 (1983) 371.
ΔE=~400keV
RCNP
before WS
58Ni(3He,t)58Cu
E(3He)=450 MeV,θ=0
counts
Ex (MeV)
Y. Fujita et al.
Phys. Lett. B365
(1996) 29
WS
Counts/6.8keV
58Ni(3He,t)
EHe=140MeV/u, 0-deg
2001 RCNP
ΔE=35keV
Ex in 58Cu [MeV]
H. Fujita et al.
PhD thesis
Y. Fujita et al.
Euro. Phys. J. A
13 (2002) 411
(Ex ≤ 8 MeV)

Decomposition of the isospin components of the excited states in ^{58}Cu.

- Isospin of ^{58}Ni g.s. : $T_0 = 1$
- In principle, comparison among (n,p), (p,p'), (p,n) spectra
  → separates isospin components

But, very difficult in practice
because of high level density for
$T = 1$ and $T = 2$ states.

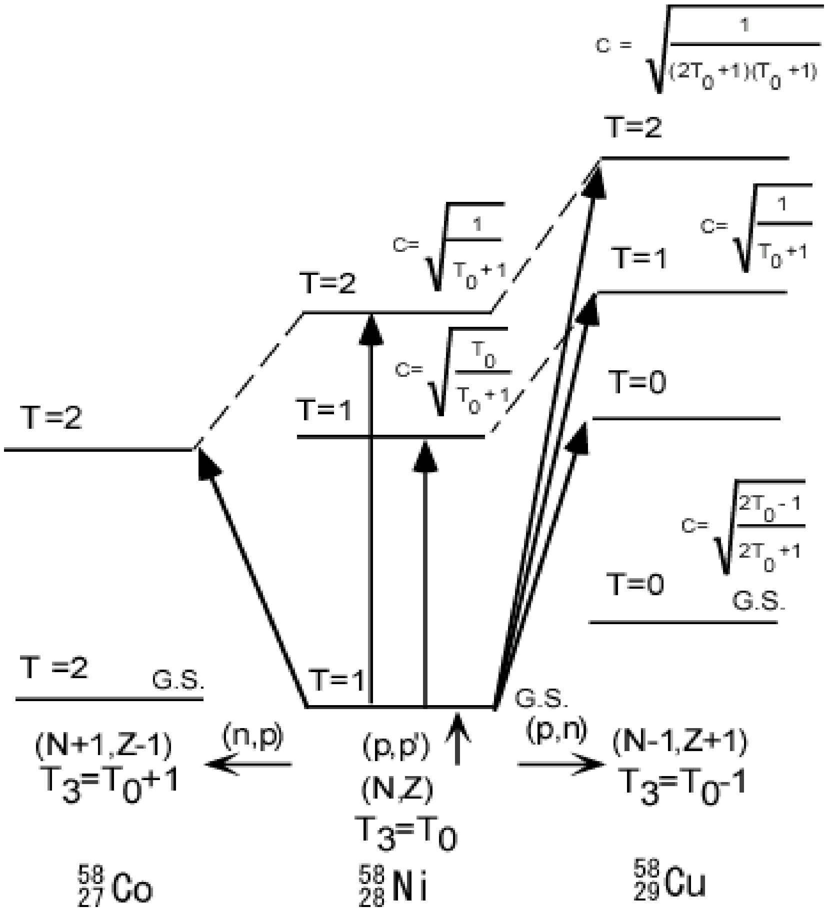

- Clebsch-Gordon coefficients for ($T_0 = 1$)

⇒ $\sigma_{T=0}:\sigma_{T=1}:\sigma_{T=2}$ = 2:3:1 for (p,n)

⇒ $\sigma_{T=1}:\sigma_{T=2}$ = 1:1 for (p,p'), (e,e')

Comparison of (^{3}He,*t*) and (*e*,*e*′) spectra

- **Comparison of 1^+ levels in (^{3}He,*t*) with (*e*,*e*′) and (*t*,^{3}He) spectra**
  - **➔ Try to separate isospin components**
- **Fig. (b) is shifted by 0.20 MeV (IAS)**
  - **b-1) B(M1) distribution obtained in (*e*,*e*′)**
  - **b-2) B(M1) convoluted with 140 keV resolution**
  - **In b-1) 1^+ levels observed in (*t*,^{3}He) spectra are marked with small circles**
  - **Furthermore, comparing with (*n*,*p*) spectra assume all levels above 11.5 MeV have *T*=2**
  - **b-3) Same as b-2) but with *T*=2 strength reduced artificially by a factor 3**
- **At E_x ~ 6-10 MeV (*T=1* region)**
  - **Rather good correspondence**
- **At E_x ~ 10-15 MeV (*T=2* region)**
  - **Reasonable correspondence**

Y. Fujita *et al*., Phys. Lett. B365 (1996) 29
Y. Fujita *et al*., Eur. Phys. J. A13 (2002) 411

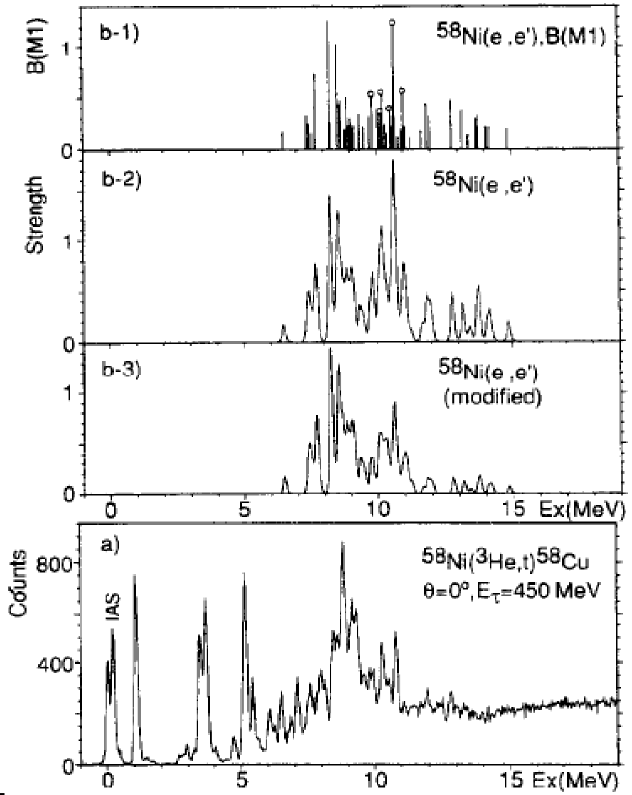

B(M1) distribution

Γ_{FWHM} = 30 keV

σ(T=1):σ(T=2) = 1 : 1

σ(T=1):σ(T=2) = 3 : 1

Γ_{FWHM} = 140 keV

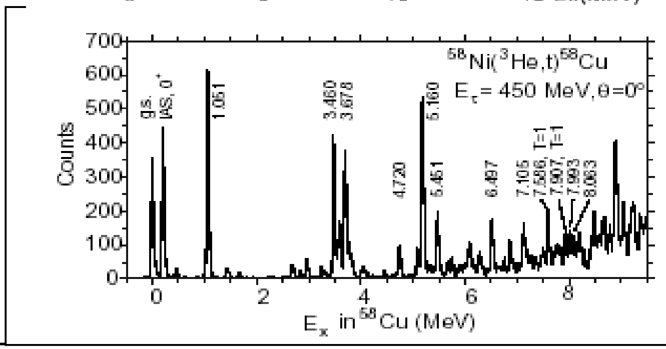

WS beam line

Γ_{FWHM} = 50 keV

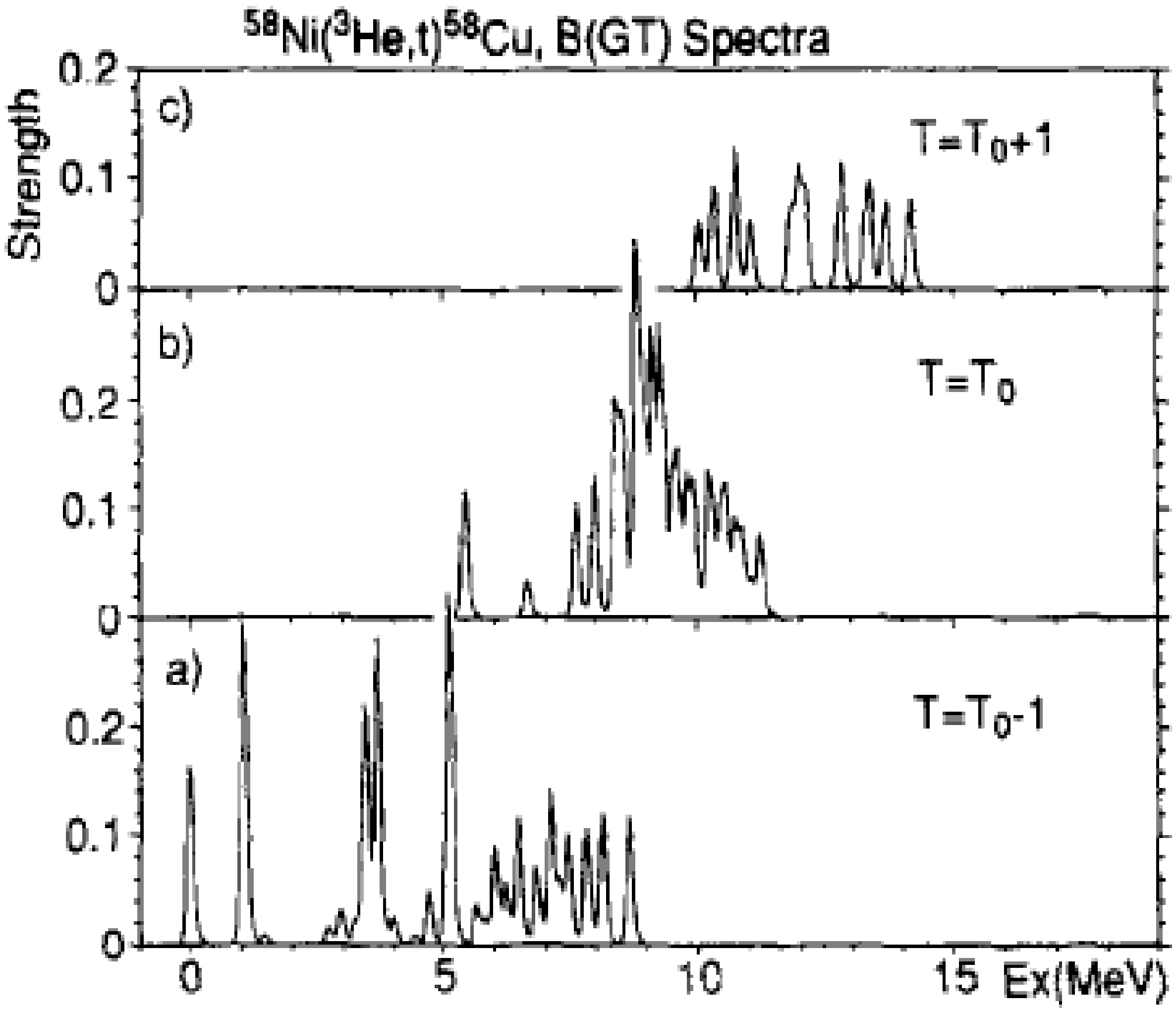

Disentangling the isospin components of the GT strength in 58Cu

See: Y. Fujita *et al*., Phys. Lett. B365 (1996) 29

^{26}Mg(p,n)^{26}Al & ^{26}Mg(^{3}He,t)^{26}Al spectra

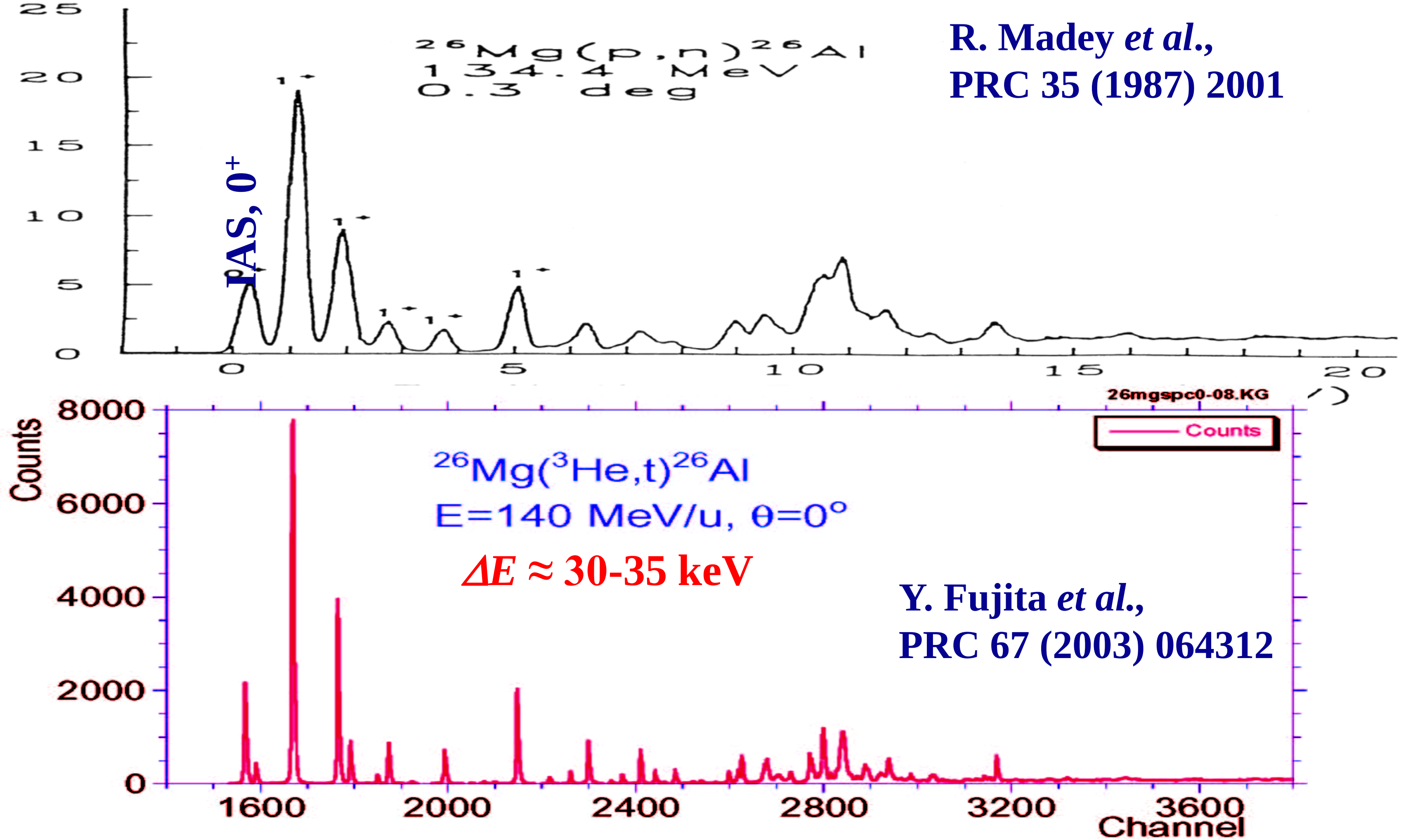

Prominent states are GT states and the IAS !

^{54}Fe(p,n) & ^{54}Fe(^{3}He,t)

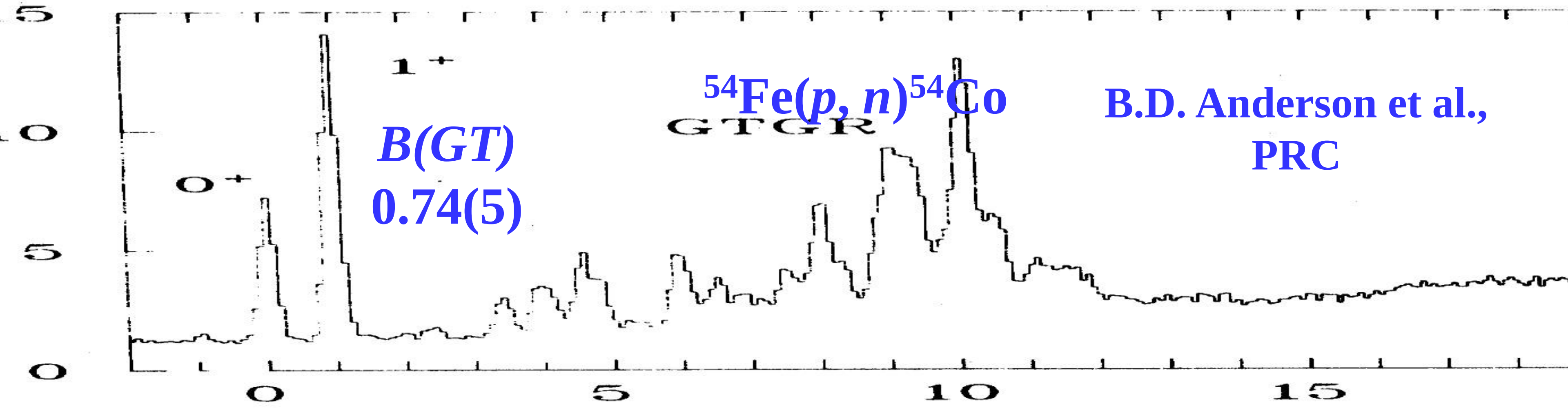

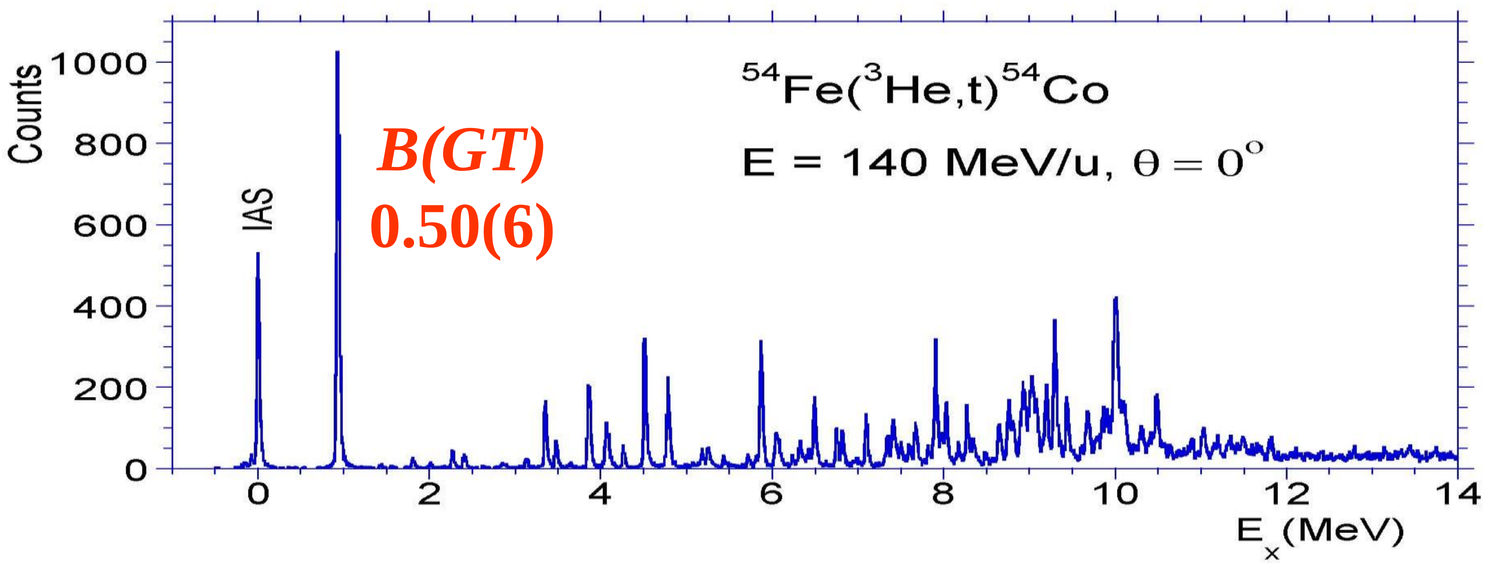

Why are Gamow-Teller transitions in *fp*-shell nuclei important ?

- **Role of *fp*-shell nuclei in supernova explosions: Core of supernova star is composed of *fp*-shell nuclei.**

  $\Rightarrow$ electron capture

- **Neutrino absorption cross sections by *fp*-shell nuclei are essential in understanding of nucleosynthesis in Supernova explosions in cosmos.**

➔ **Difficulties in shell-model calculations for *fp*-shell nuclei.**

➔ **Importance to measure spin-isospin responses of *fp*-shell nuclei to gauge theoretical calculations.**

Determination of GT^+ Strength and its Astrophysical Implications

In supernova explosions, electron capture (EC) on *fp*-shell nuclei plays a dominant role during the last few days of a heavy star with $M > 10\ M_{\odot}$

Presupernova stage; deleptonization ⇒ core collapse ⇒ subsequent type IIa Supernova (SN) explosion

H.A. Bethe *et al*., Nucl. Phys. A324 (1979) 487

Nuclear processes and energy household of supernovae

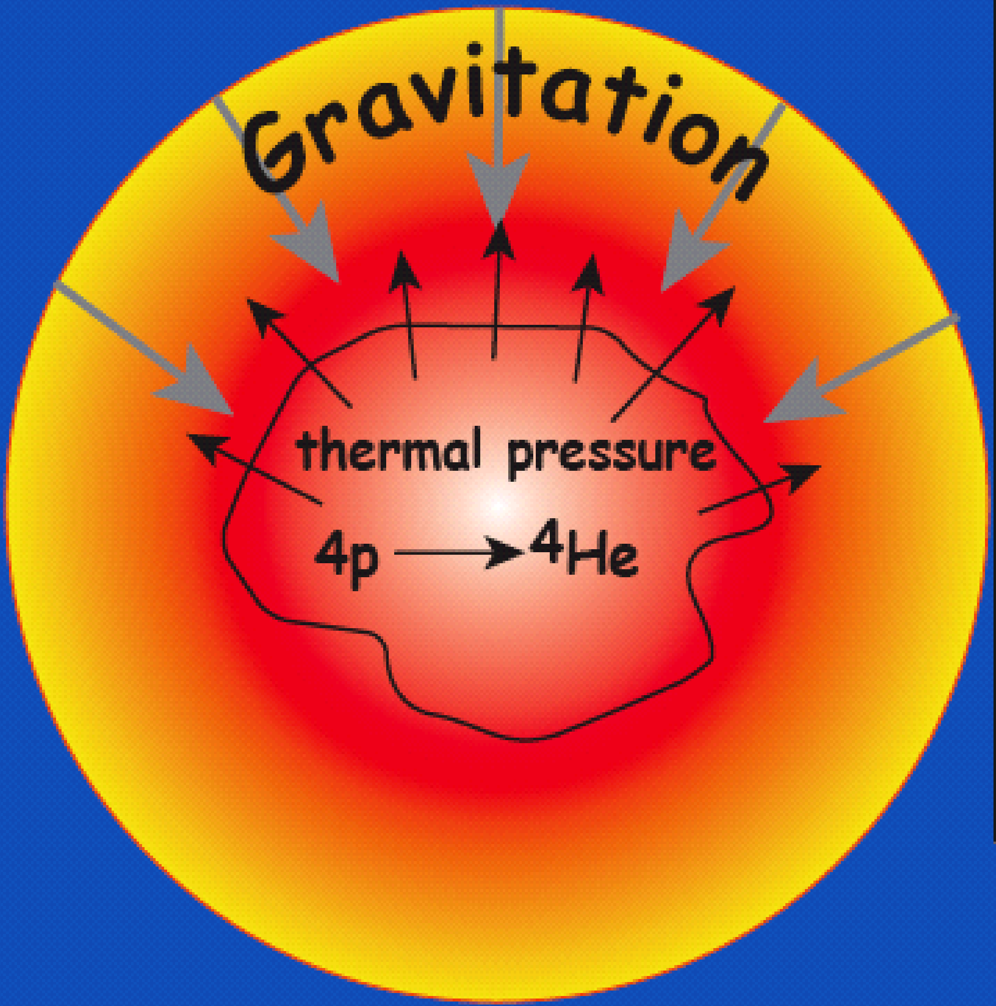

initial condition:
$M > 10\,M_\odot$

energy:
fusion $4p \rightarrow {}^4He$

at: $T \sim 10^7 - 10^8$ K

lifetime: $10^6 - 10^7$ y

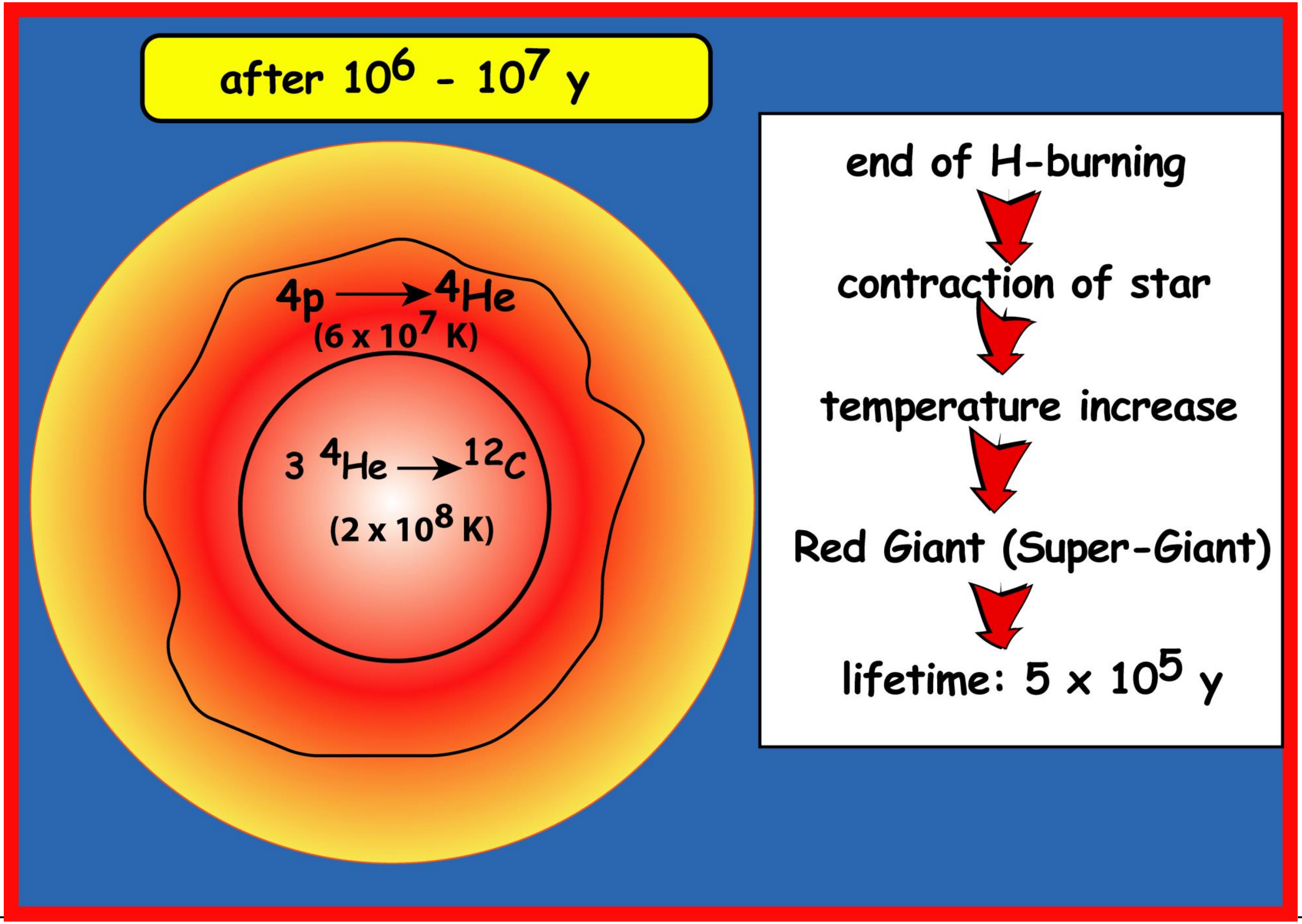
after 10^6 - 10^7 y
4p → ^{4}He
(6 x 10^7 K)
3 ^{4}He → ^{12}C
(2 x 10^8 K)
end of H-burning
contraction of star
temperature increase
Red Giant (Super-Giant)
lifetime: 5 x 10^5 y

end of stellar evolution $M_{star} \sim 15\ M_\odot$

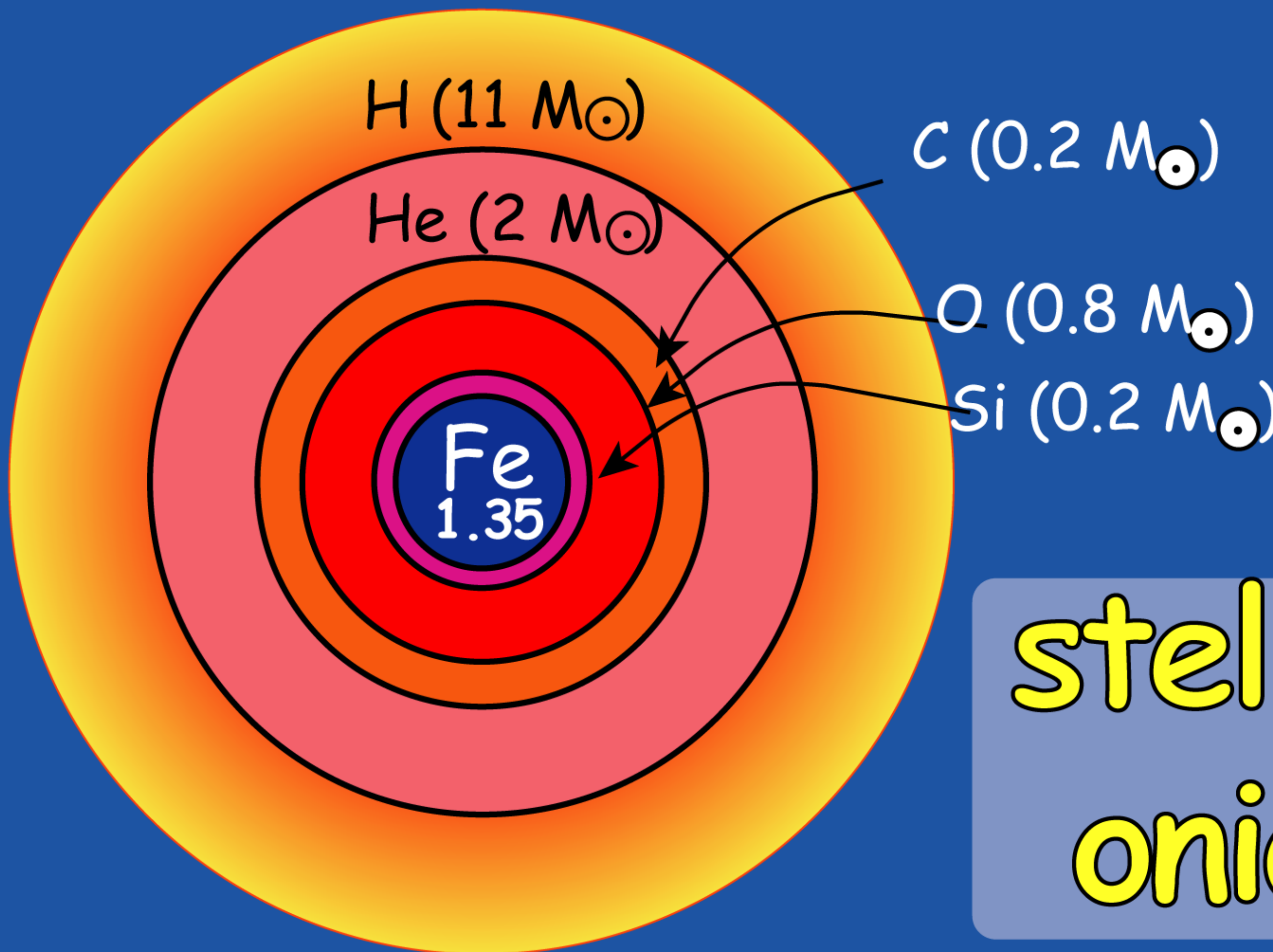

stellar onion

Determination of GT Strength is imperative

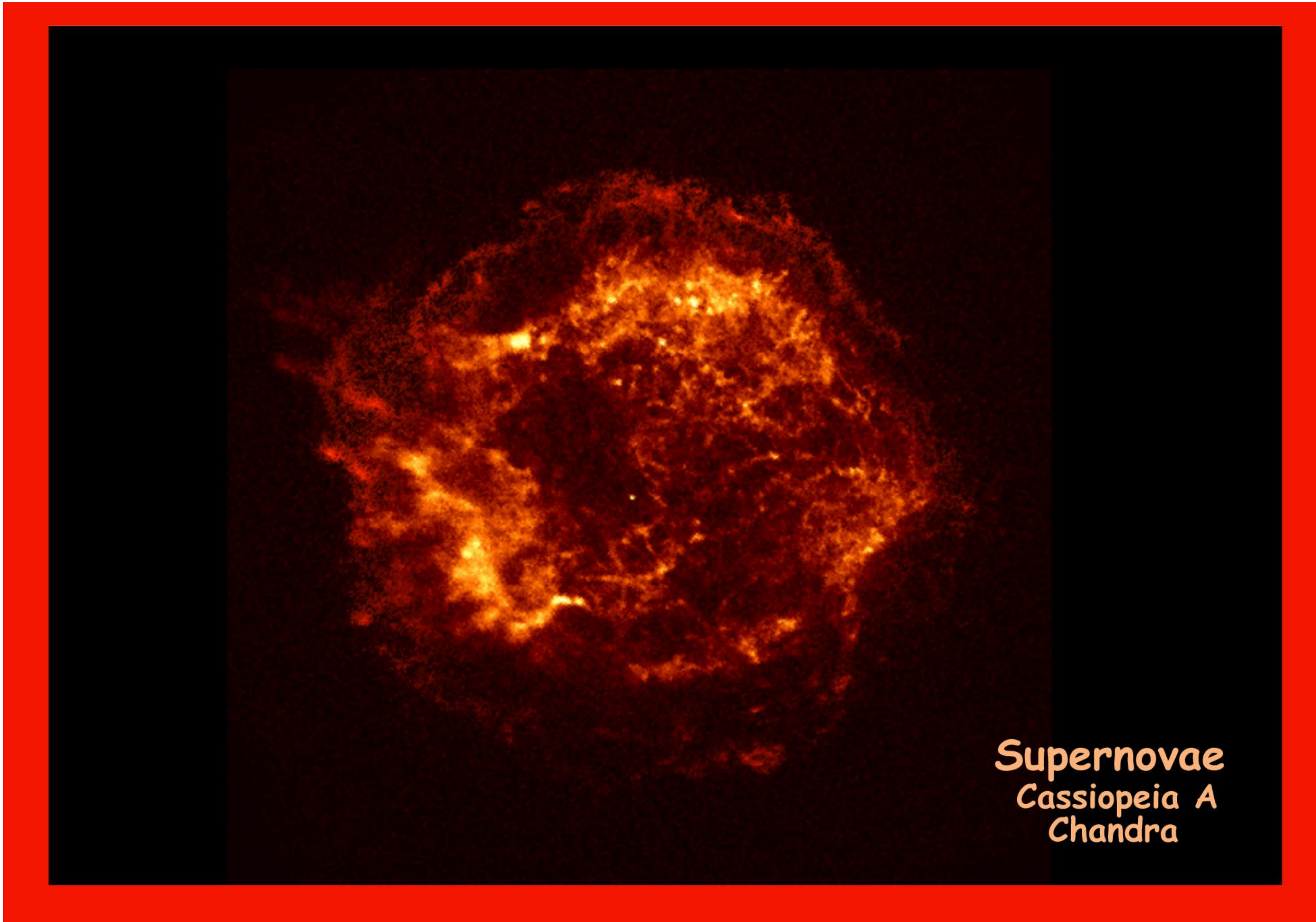

Courtesy of D. Frekers

Supernova Simulatie

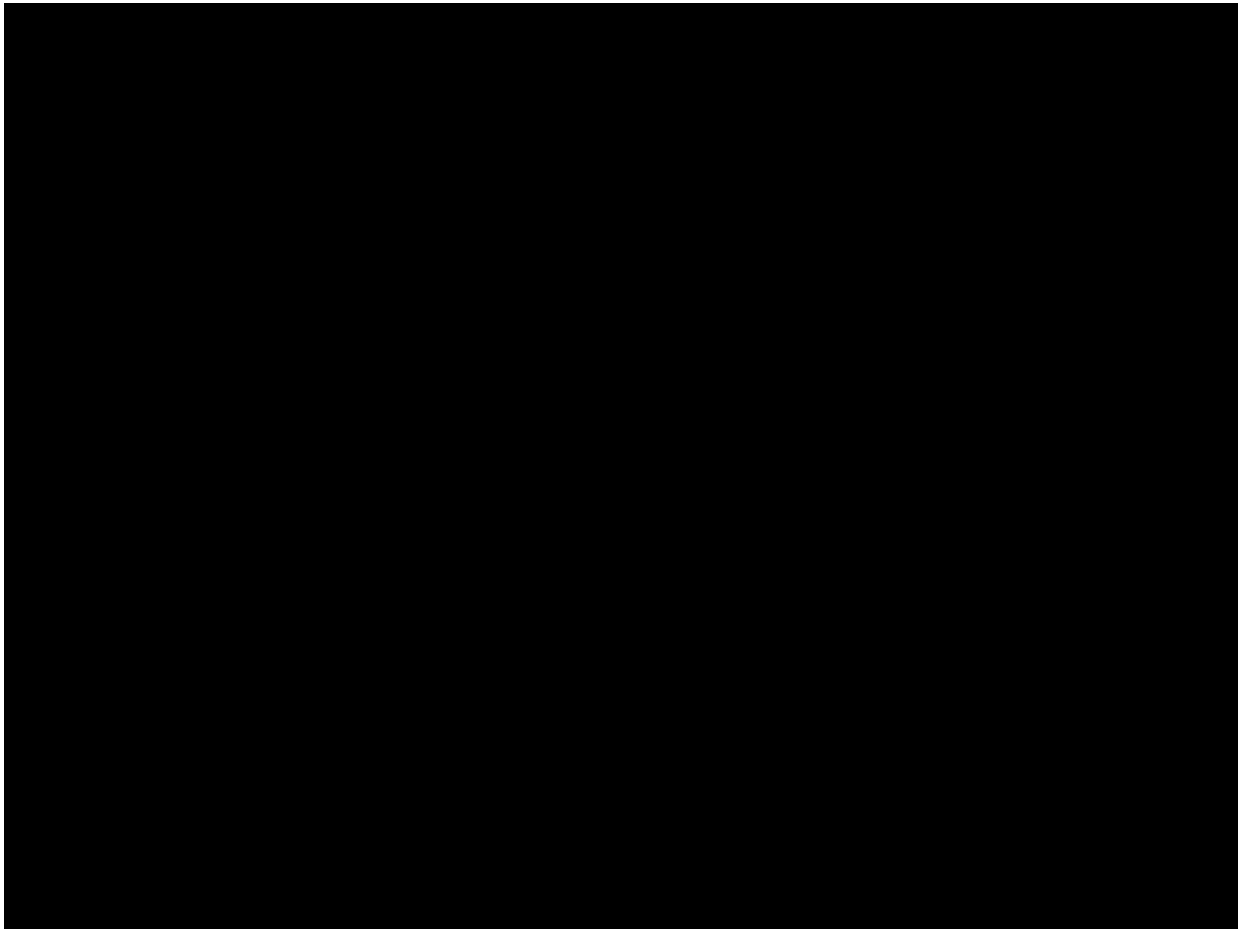

Electron capture in *fp*-shell

- **The rate for EC is governed by the GT^+ strength distribution at low excitation energy; not accessible to β-decay.**

- **Fuller, Fowler and Newman (FFN) (1982-1985); estimates of stellar rates in stellar environments using s.p. model.**

- **Caurier *et al*., Martínez-Pinedo & Langanke (1999), Otsuka *et al*. ⇒ Large shell-model calculations ⇒ marked deviations from FFN EC rates; generally smaller EC rates.**

- **Experiments and theory relied on (*n*,*p*) data (TRIUMF) which have a rather poor energy resolution.**

fp-shell nuclei: large scale shell model calculations

E. Caurier *et al.*, NPA 653 (1999) 439

- Stellar weak reaction rates with improved reliability
- Large scale shell model (SM) calculations
- Tuned to reproduce GT^+ strength measured in (*n*,*p*)

- (*n*,*p*) data from TRIUMF
- GT^+ strength from SM
- Folded with 1 MeV energy resolution

Case study: ^{58}Ni

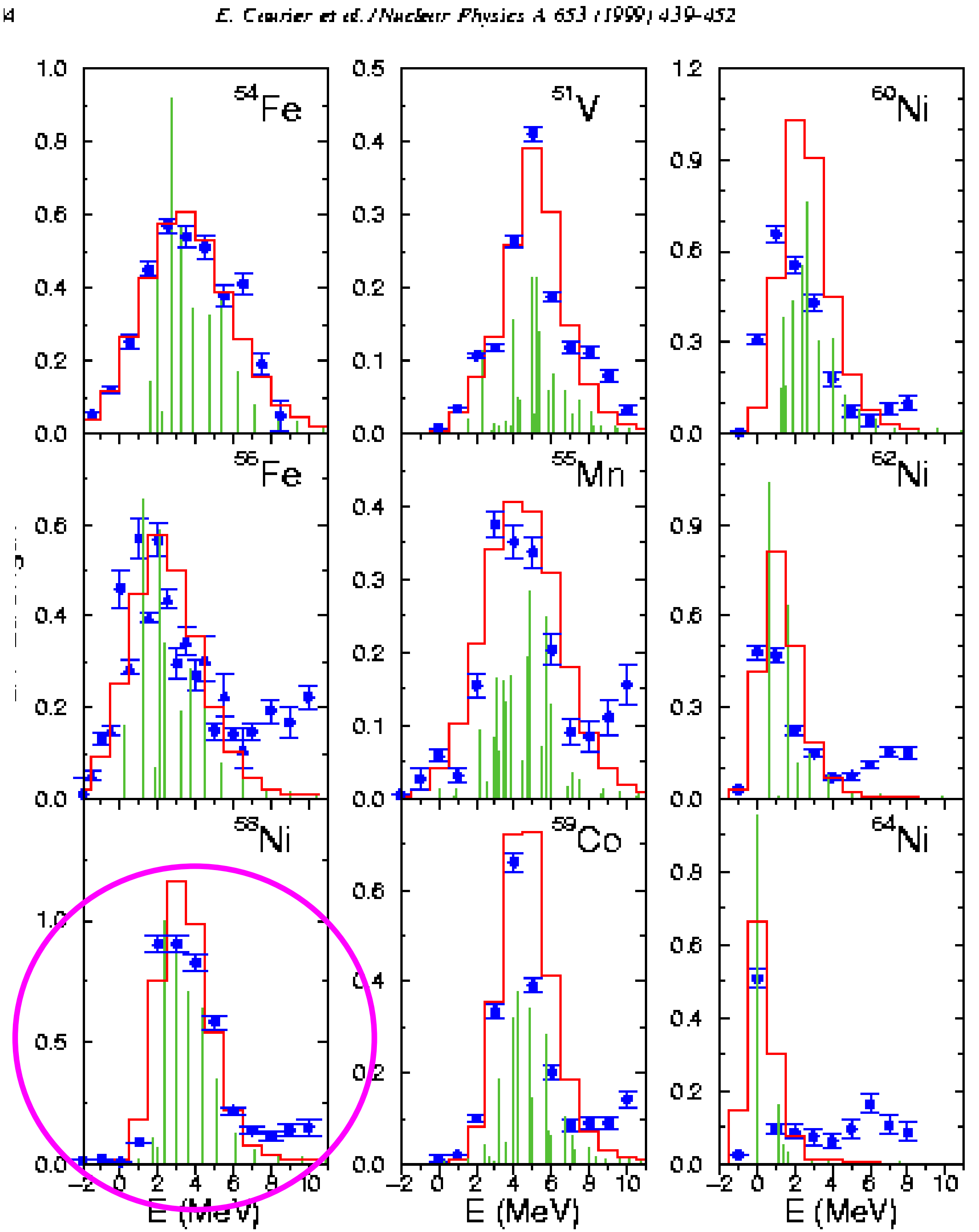

Exclusive excitations $\Delta S = \Delta T = 1$: (d,^{2}He)

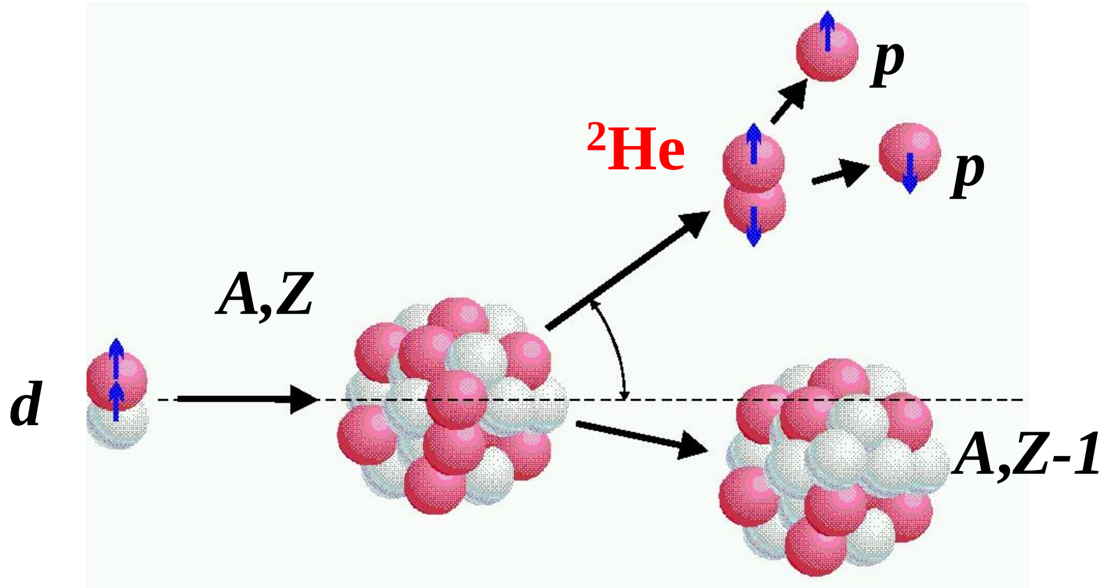

$^3S_1$ deuteron $\Rightarrow$ $^1S_0$ di-proton (^{2}He)

$^1S_0$ dominates if (relative) 2-proton kinetic energy $\varepsilon < 1$ MeV

(n,p)-type probe with exclusive $\Delta S=1$ character (GT$^+$ transitions)

But near 0°, tremendous background from d-breakup

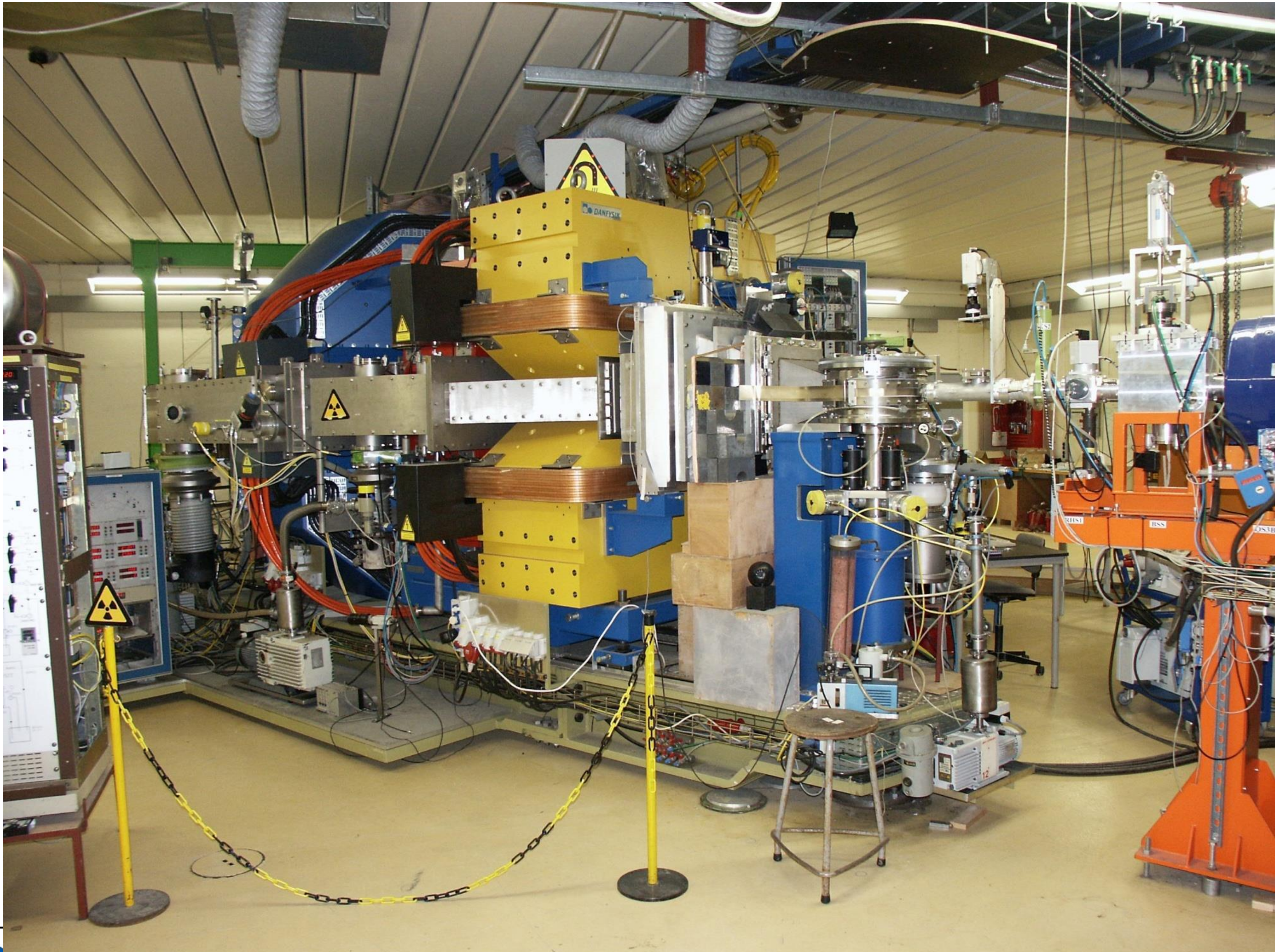
DANFYSIK

Si-ball
16 Si-detectors at
10 cm from the target
total solid angle: 1 sr

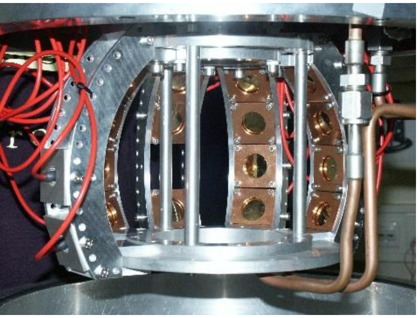

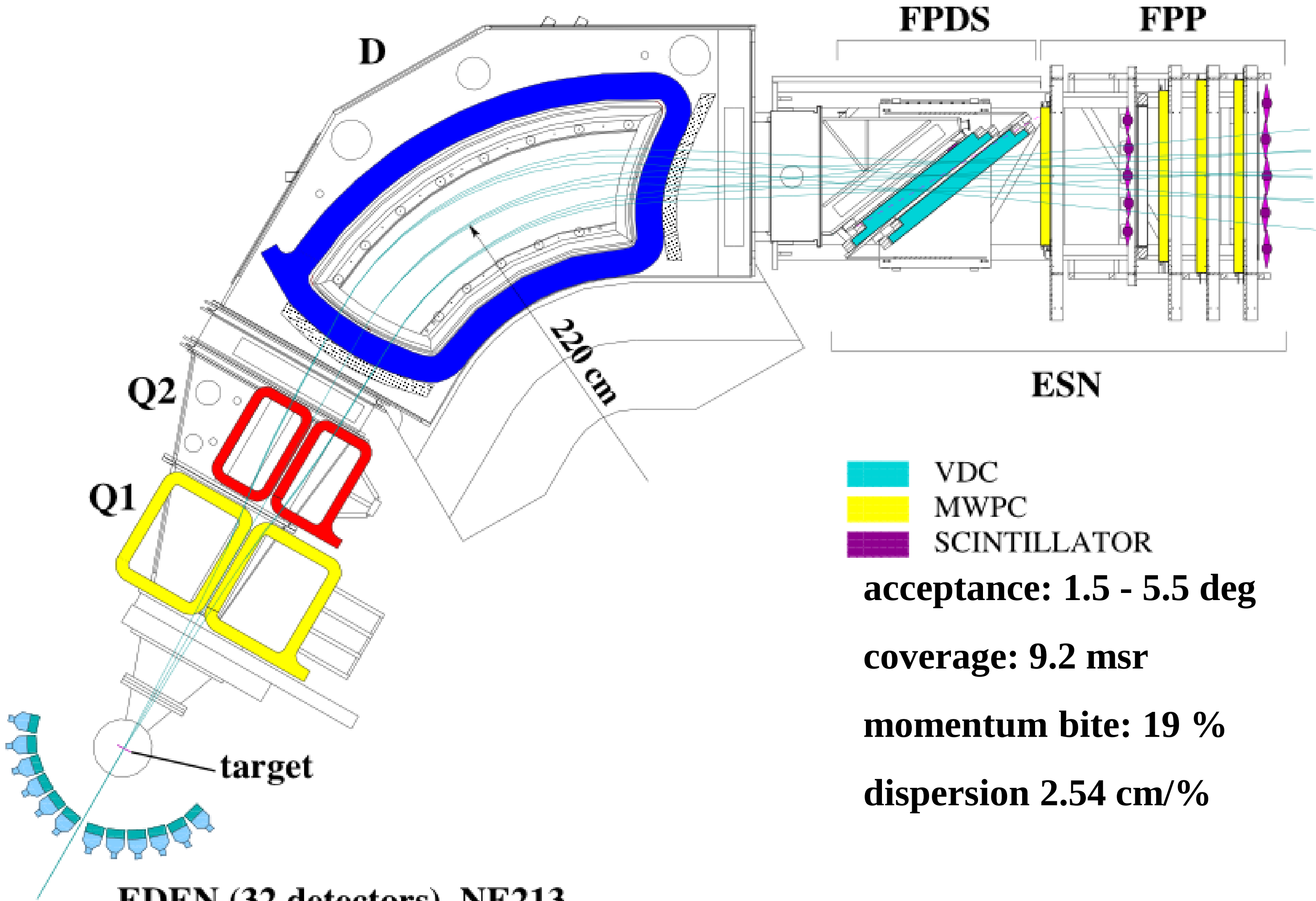

acceptance: 1.5 - 5.5 deg

coverage: 9.2 msr

momentum bite: 19 %

dispersion 2.54 cm/%

EDEN (32 detectors), NE213

total solid angle: 0.37 sr

KVI Big-Bite Spectrometer (BBS)

Setup: ESN detector

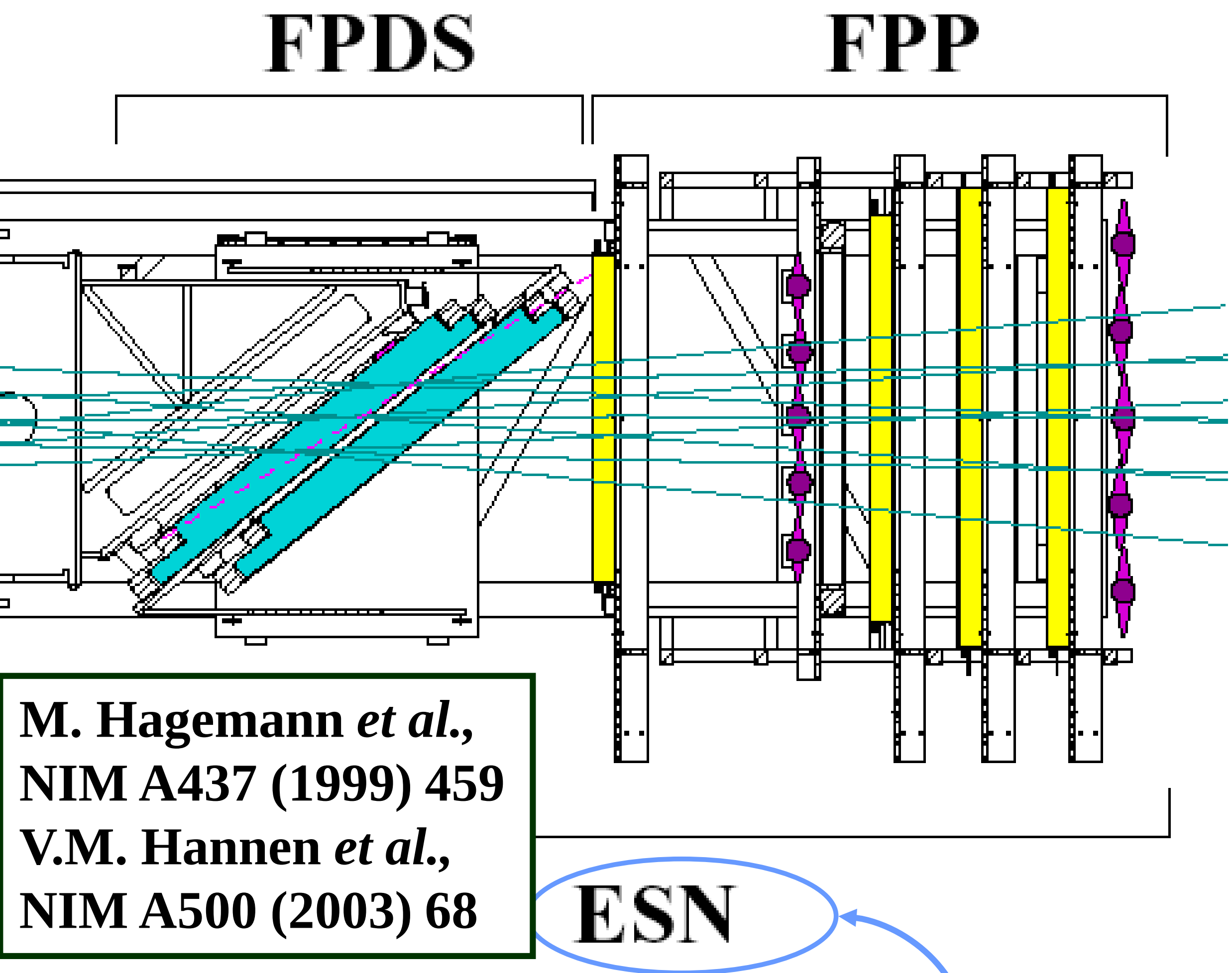

Focal-Plane Detector:
(FPDS): 2 VDCs

Focal-Plane Polarimeter:
(FPP): 4 MWPCs & graphite analyzer

Features:
- **fast readout**
- **VDC readout pipeline TDC's**
- **VDC decoding using imaging techniques**
- **DSP based online analysis**

M. Hagemann *et al.*, NIM A437 (1999) 459
V.M. Hannen *et al.*, NIM A500 (2003) 68

Bari, Darmstadt, Gent, Iserlohn, KVI, Milano, Münster, TRIUMF

- **Good double tracking**
- **Use VDC information**
- **Good phase-space coverage for small relative proton energies**

S. Rakers *et al.*,
NIM A481 (2002) 253

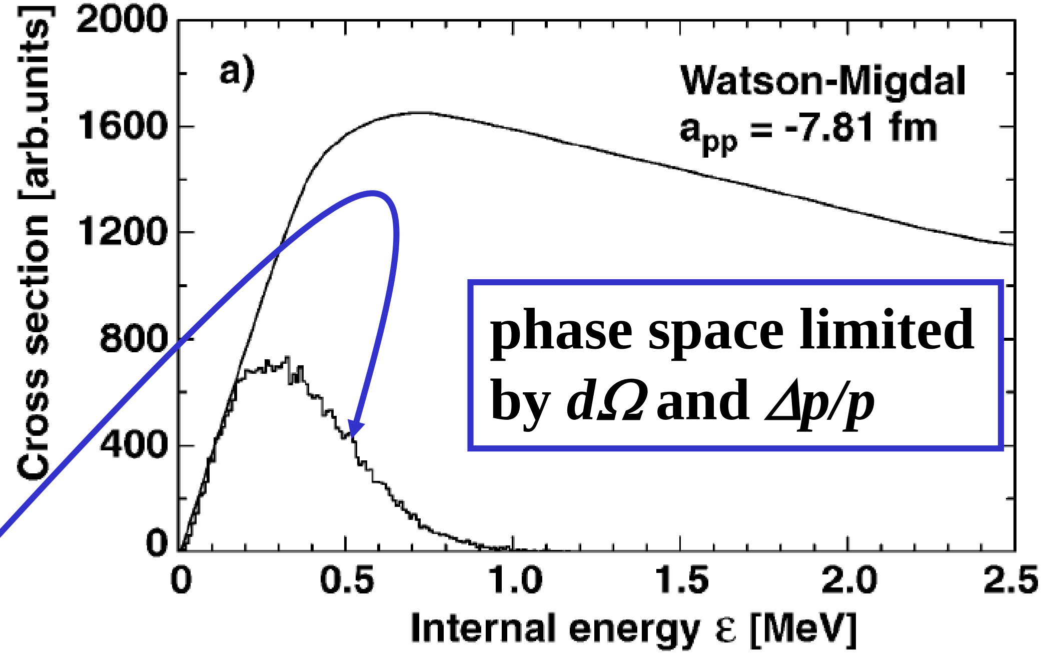

measured

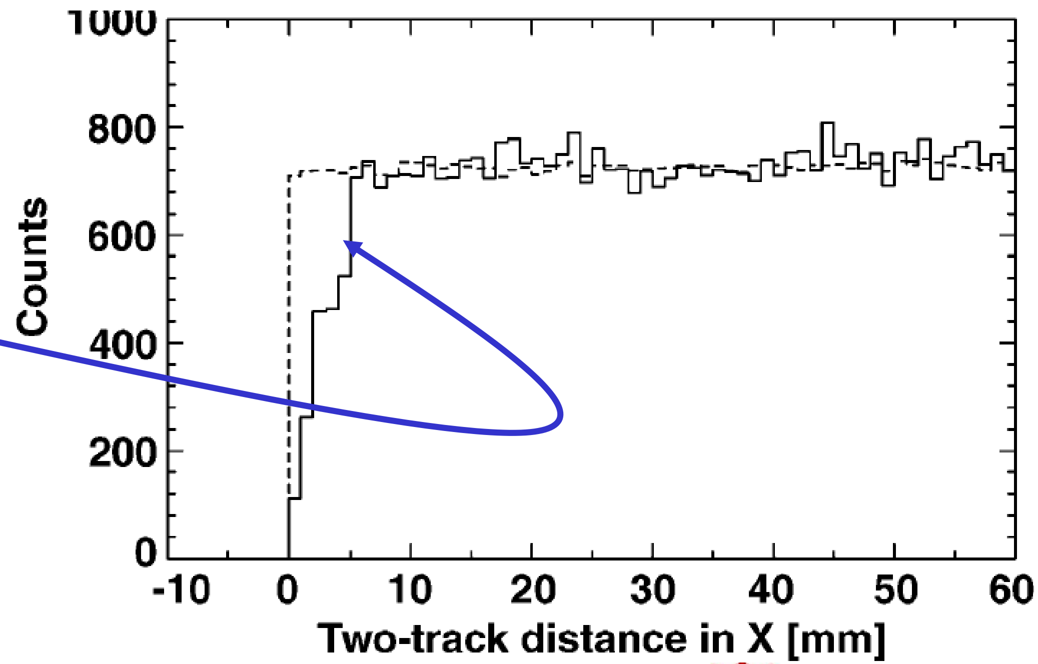

Exclusive measurement of *ΔS* = *ΔT* = 1 strength

$^{12}C(d,^{2}He)^{12}B$

E_0 = 171 MeV, θ = 0°

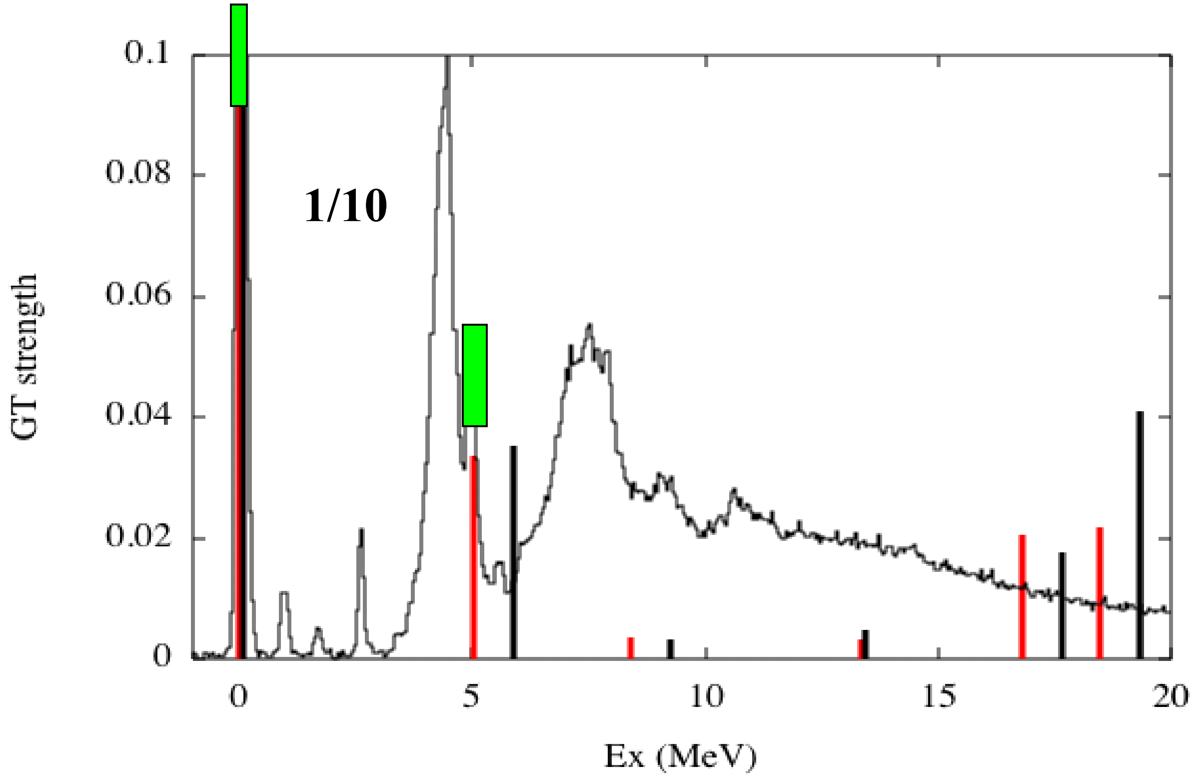

- **shell model calculations 4ħω & 6ħω (G. Martinez-Pinedo)**
- ***B (GT⁺)*** **(S. Rakers)**

(p,n) vs ($d,^2$He): calibration

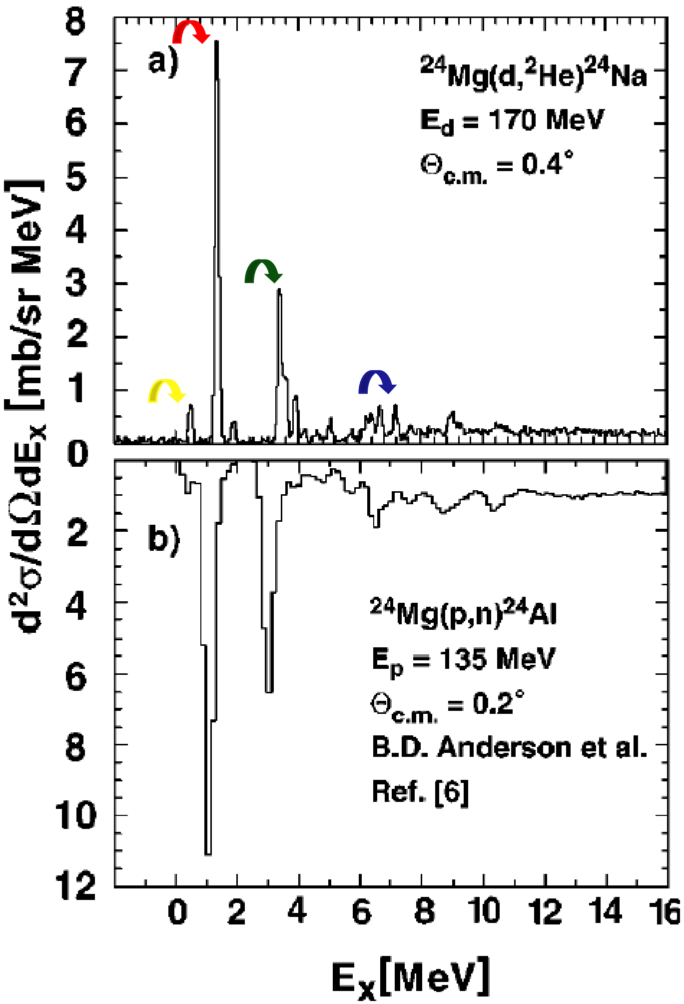

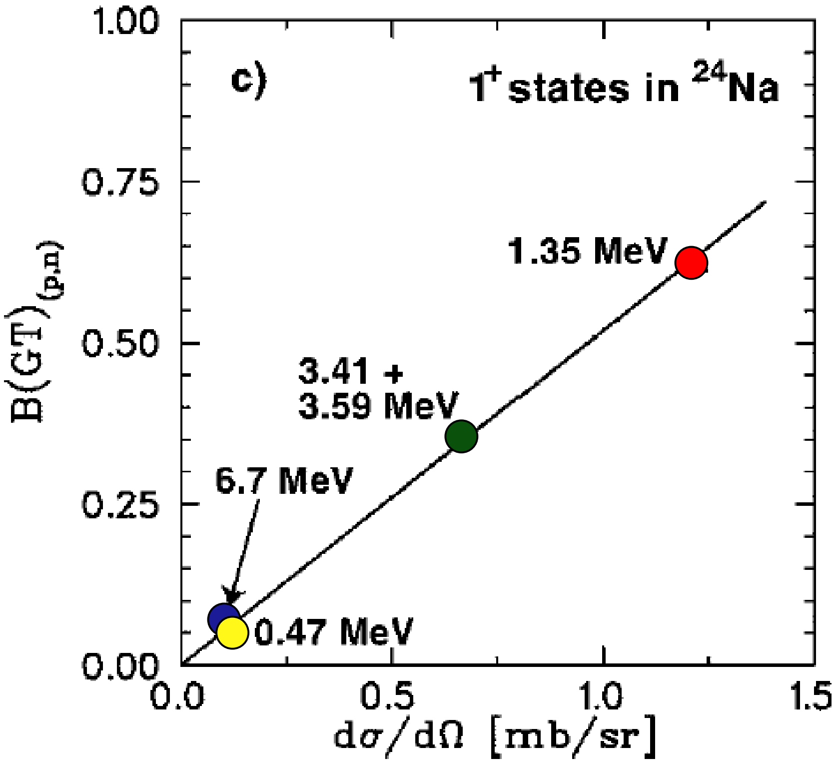

Self-conjugate ^{24}Mg

S. Rakers *et al.*, PRC 65 (2002) 044323

Experimental cross section and GT strength

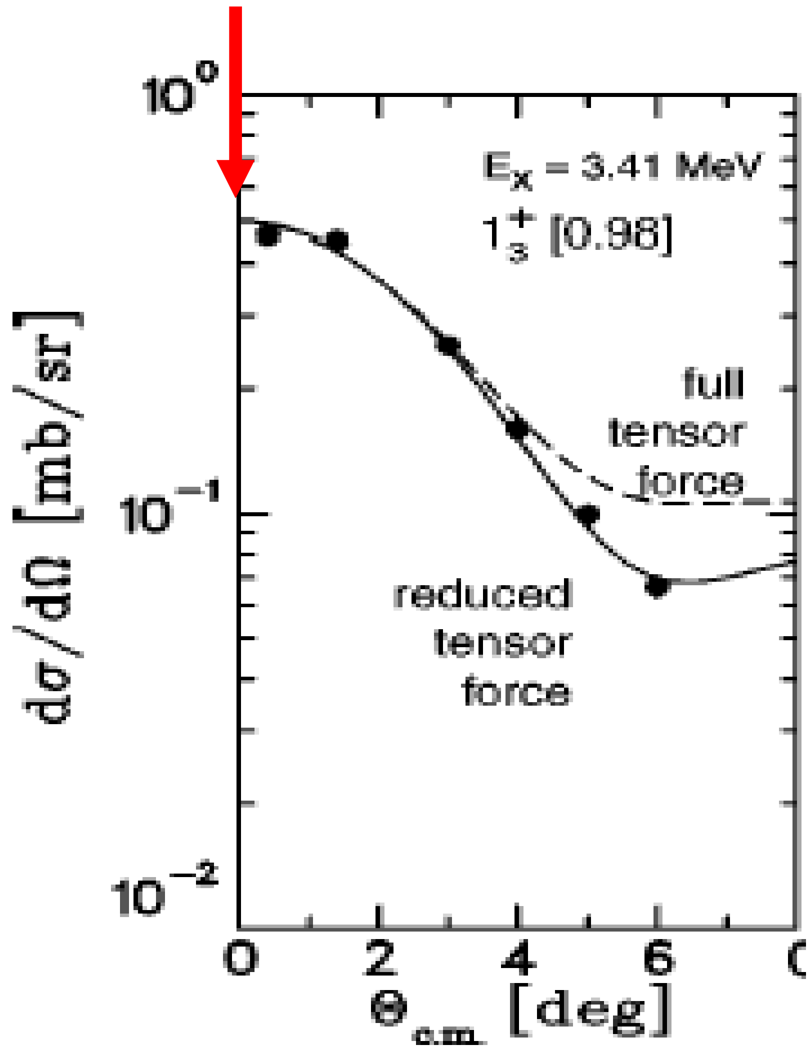

$$\mathbf{B}_{\mathrm{exp}}(\mathrm{GT+}) = \frac{\mathrm{d}\sigma(q=0)}{d\Omega} \cdot \left[\frac{d\sigma(GT)}{d\Omega}\right]^{-1}$$

extrapolated (DWBA)

unit cross section

GT Strength in ^{12}B and ^{24}Na from (d,^{2}He) reaction

Target	Reference data		Present data			
	E_x [MeV]	$B(GT_-)$	E_x [MeV]	$d\sigma/d\Omega(q=0)$ [mb/sr]	$\sigma(L=0)/\sigma(\tau o \tau)$ (q=0)	$B(GT_+)$ (C=0.267)
^{12}B	0.00	0.998	0.00	2.580±0.138	0.988	0.930±0.050
			5.00	0.138±0.010	0.976	0.050±0.004
^{24}Na	0.44	0.050	0.47	0.138±0.012	0.821	0.049±0.004
	1.07	0.613	1.35	1.563±0.085	0.948	0.654±0.035
	1.58	0.020	1.89	0.087±0.026	0.649	0.025±0.008
	2.98	0.362	3.41	0.667±0.039	0.980	0.290±0.016
			3.59	0.266±0.018	0.806	0.095±0.006
	3.33	0.059	3.92	0.193±0.058	0.809	0.070±0.022
	4.69	0.015	5.06	0.093±0.027	0.561	0.024±0.007
			6.24	0.086±0.026	0.818	0.031±0.010
	6.46	0.068	6.70	0.161±0.012	0.972	0.071±0.005
	6.87	0.029	7.20	0.173±0.013	0.642	0.050±0.004

(*d*,^{2}He) as GT$^+$ probe in *fp*-shell nuclei

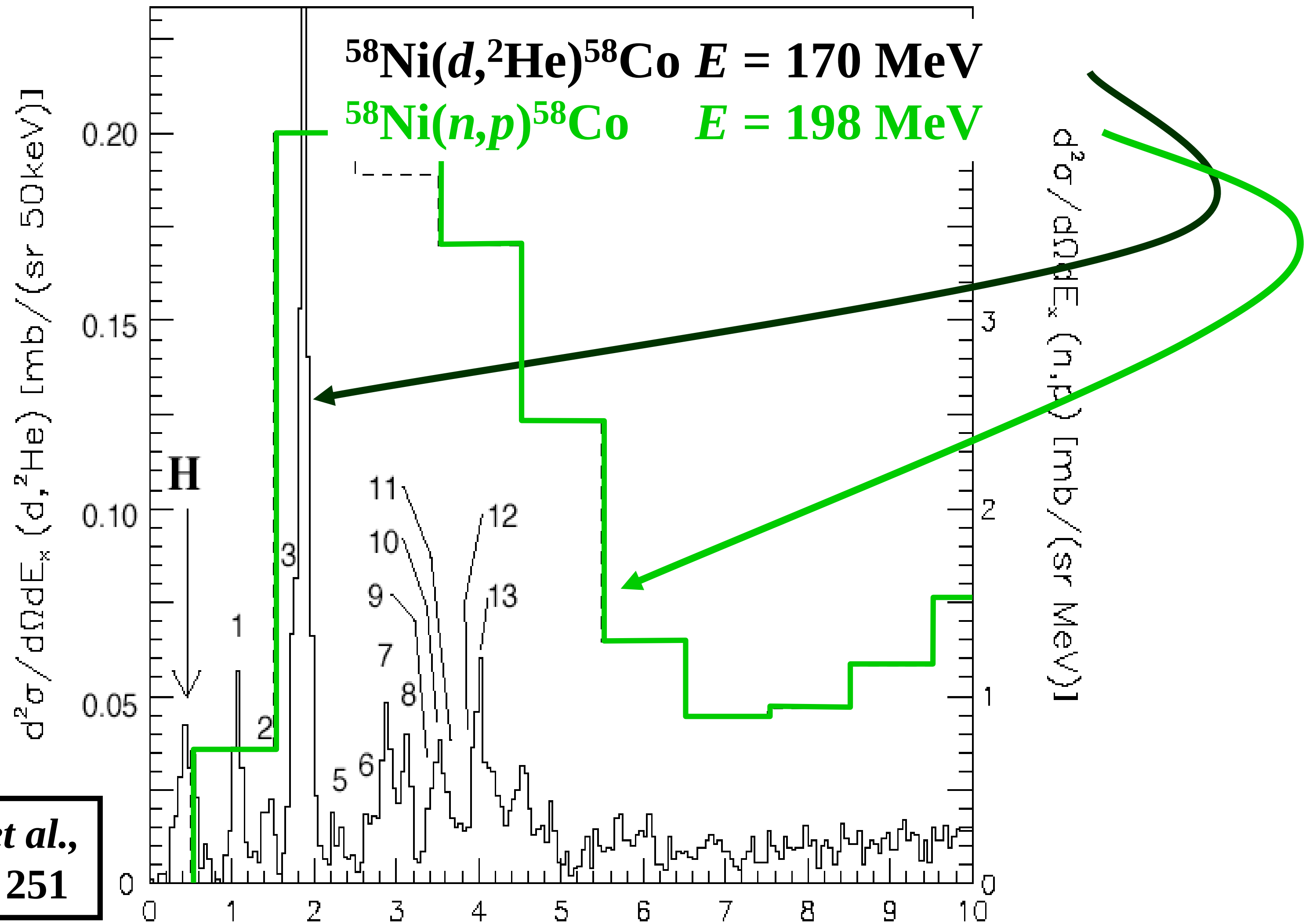

M. Hagemann *et al.*, PLB 579 (2004) 251

$^{58}Ni(d,{}^{2}He)^{58}Co \quad E_d = 170$ MeV

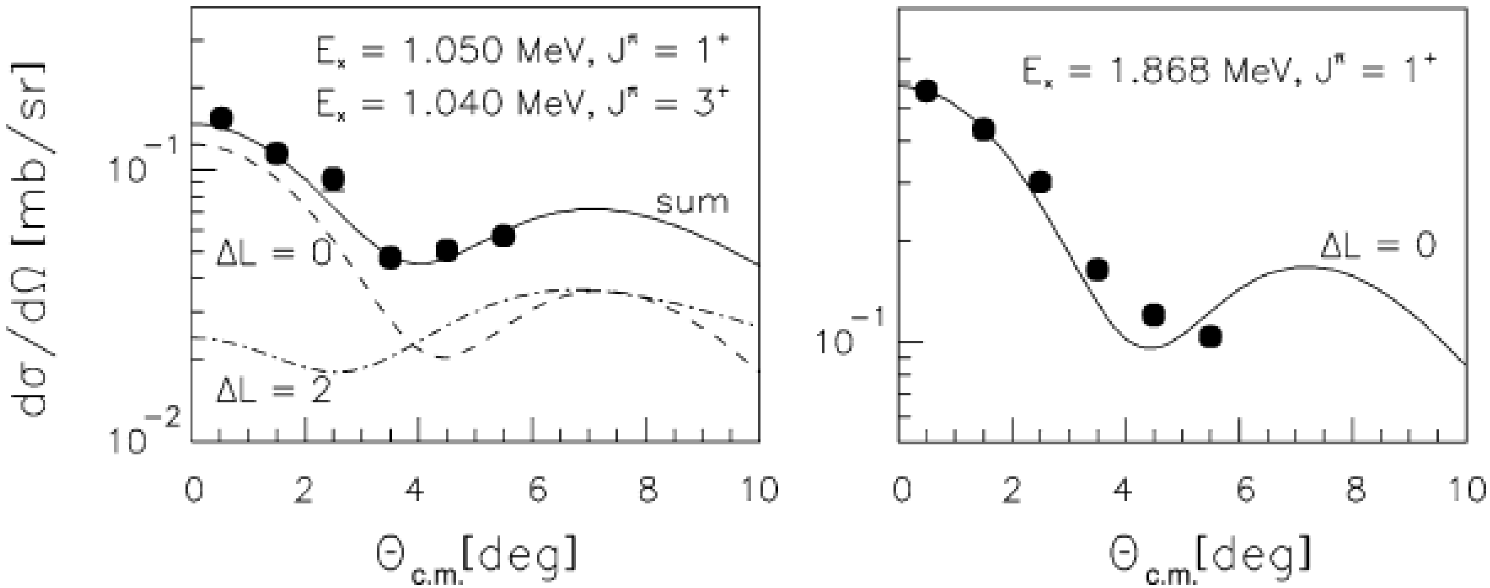

$$\mathbf{B}_{\mathrm{exp}}(\mathrm{GT}+) = \frac{\mathrm{d}\sigma(q=0)}{d\Omega} \cdot \left[\frac{d\hat{\sigma}(GT)}{d\Omega} \right]^{-1}$$

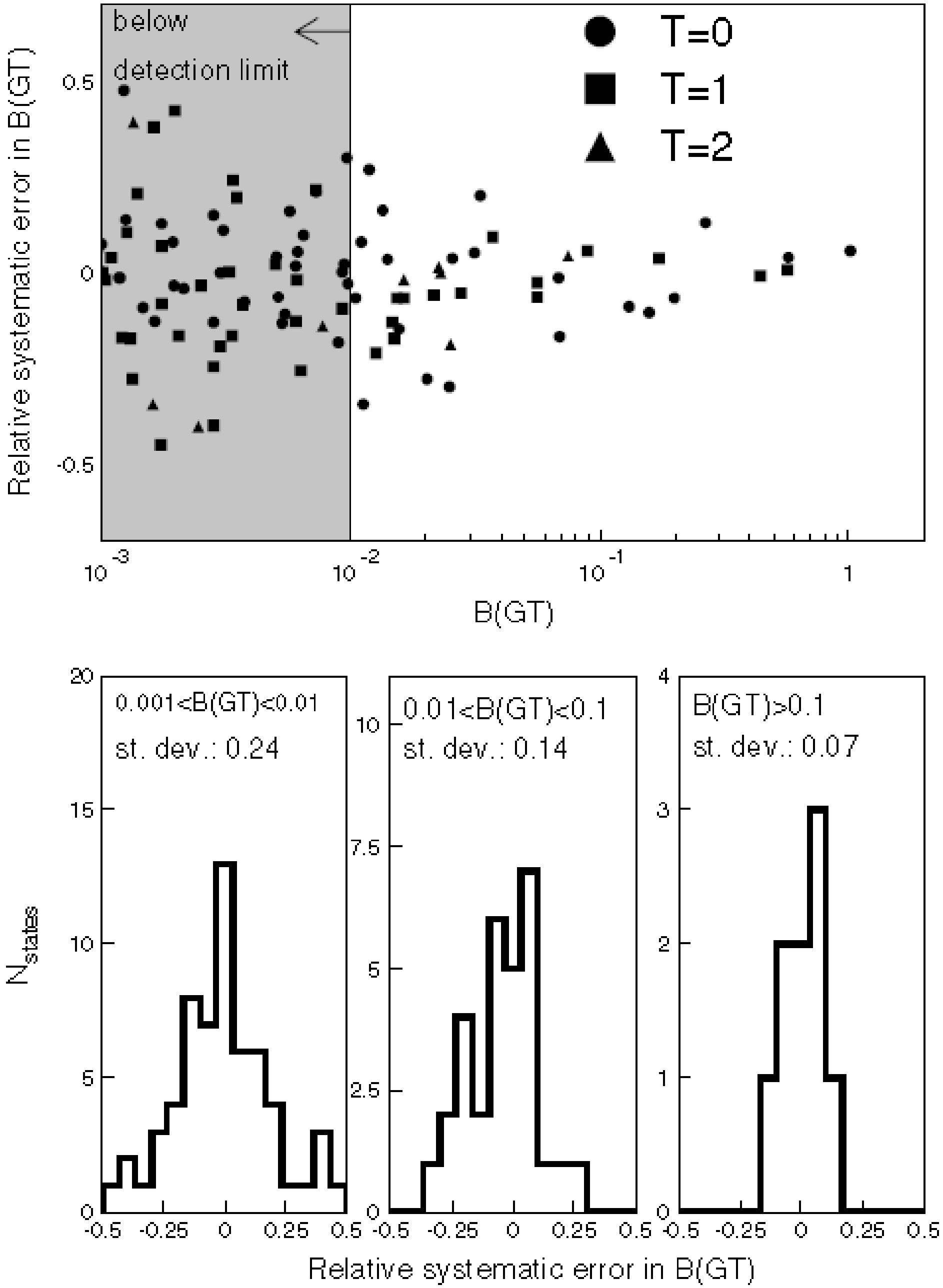

Theoretical Study ^{26}Mg(^{3}He,*t*)^{26}Al

Effects of $\Delta L = 2$, $\Delta S = 1$ contributions, mediated via the T_τ interaction, that interfere with $\Delta L = 0$, $\Delta S = 1$ contributions to Gamow-Teller transitions.

$$\text{Rel. syst. error} = \frac{B(GT)_{DWBA} - B(GT)_{SM}}{B(GT)_{SM}}$$

R.G.T. Zegers *et al.*, PRC74 (2006) 024309

GT Strength in ^{58}Co from (d,^{2}He) reaction

E_x [MeV]	dσ/dσ(0.5°) [mb/sr]	σ(L=0)/σ(τοτ)	B(GT+)
1.050	0.159±0.009	0.88	0.15±0.01
1.435	0.078±0.006	1.00	0.09±0.01
1.729	0.148±0.014	1.00	0.16±0.02
1.868	0.648±0.020	1.00	0.72±0.05
2.249	0.047±0.004	1.00	0.05±0.01
2.660	0.057±0.005	0.96	0.06±0.01
2.860	0.145±0.009	0.99	0.17±0.01
3.100	0.126±0.008	0.99	0.15±0.01
3.410	0.065±0.007	0.96	0.07±0.01
3.520	0.080±0.009	0.95	0.09±0.01
3.625	0.067±0.007	0.87	0.07±0.01
3.900	0.062±0.006	0.97	0.07±0.01
4.030	0.155±0.010	1.00	0.19±0.01
4.05-5.00	0.381±0.061		0.49±0.09

GT$^+$ strength: comparison (*n*,*p*), (*d*,^{2}He) & theory

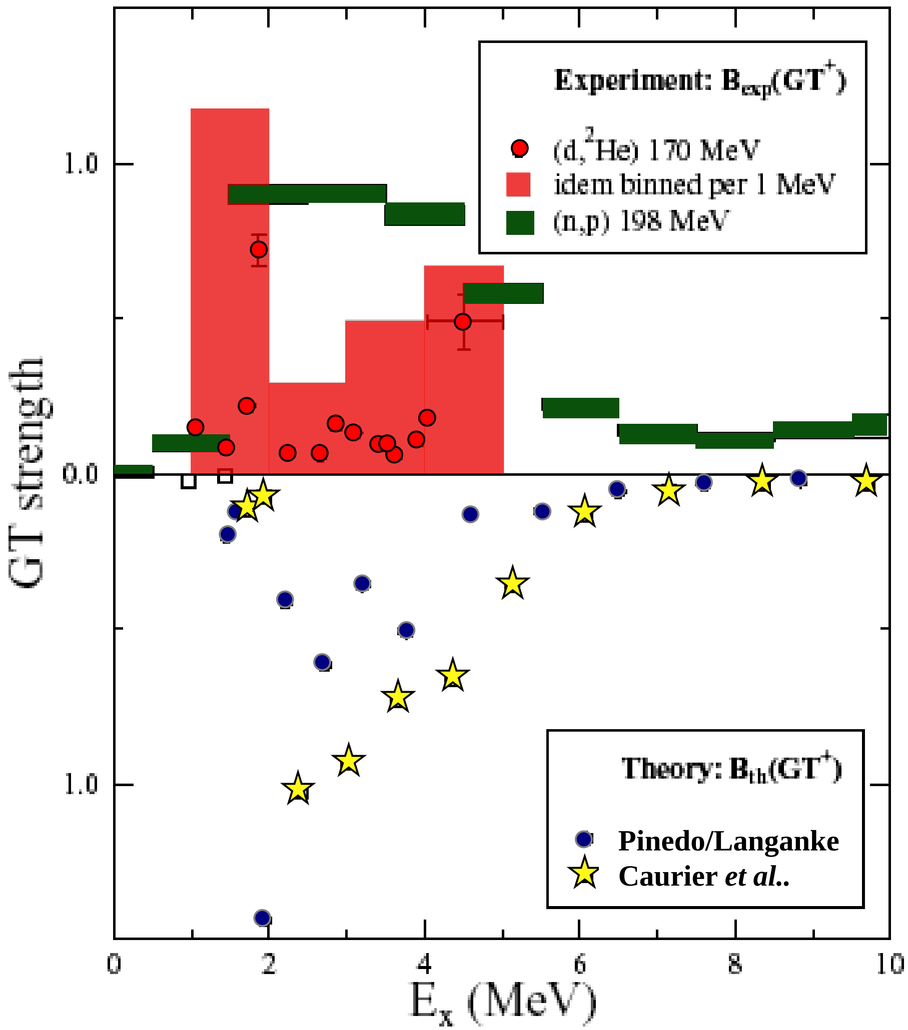

Up to 4 MeV excitation:

13 GT transitions measured in (*d*,^{2}He)

Strength re-binned in 1 MeV bins

Significant differences

Updated shell model calculations by Martínez-Pinedo/Langanke using KB3G interaction

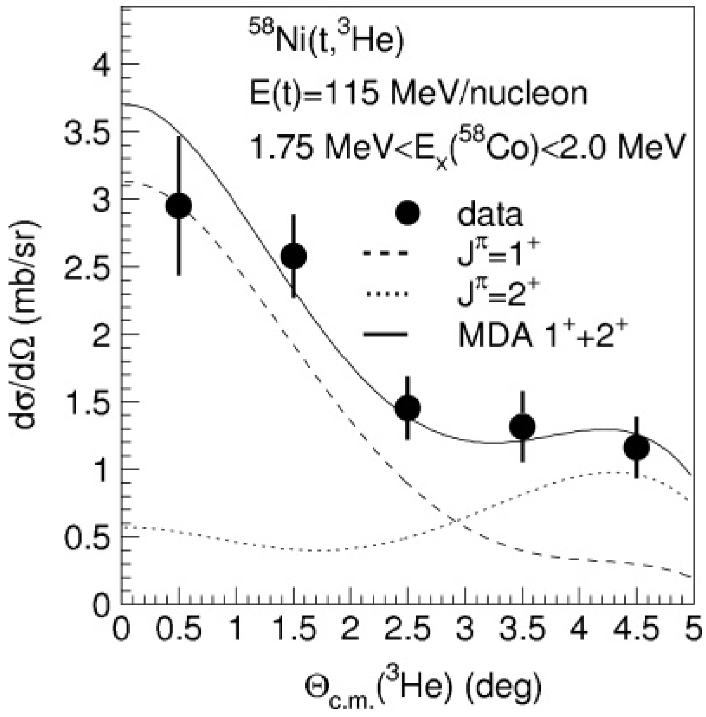

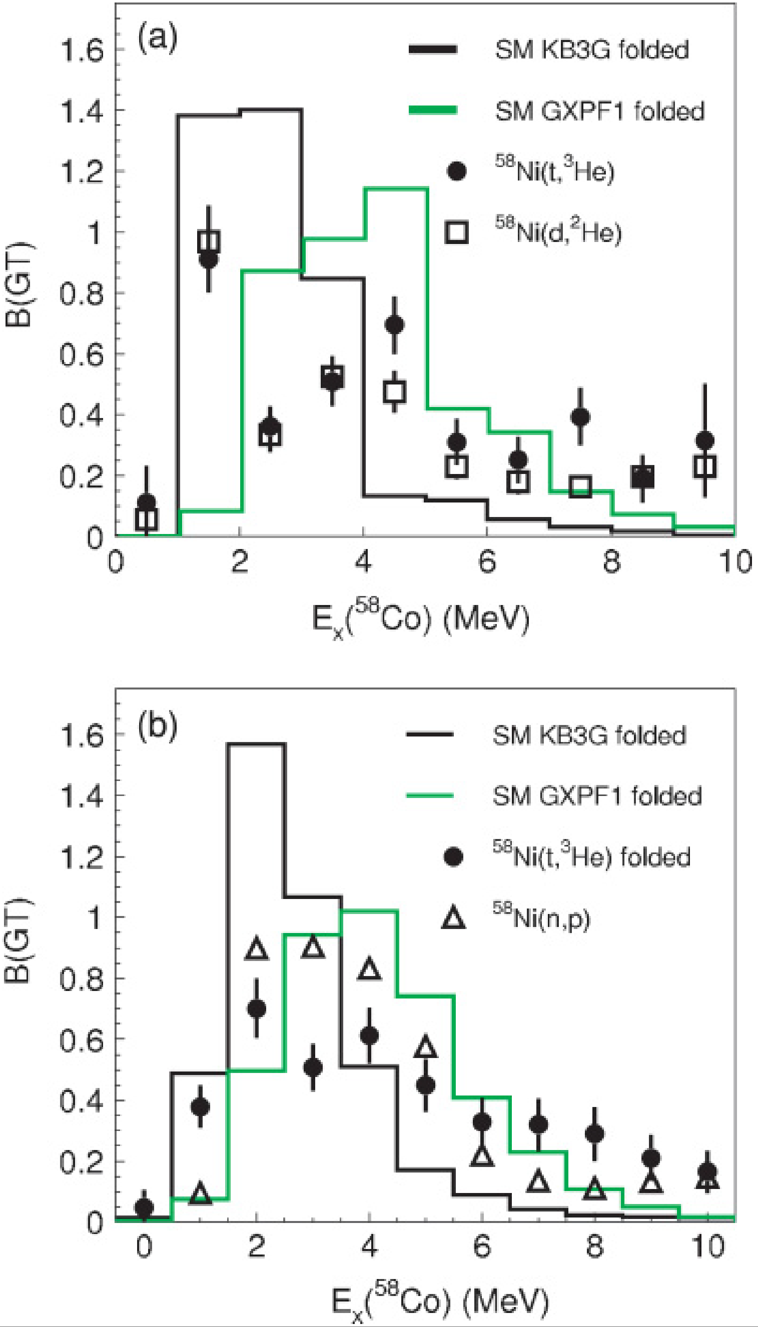

^{58}Ni(t,^{3}He)^{56}Co

***E_t* = 115 MeV/u**

Resolution = 250 keV

A.L. Cole *et al.*, PRC74 (2006) 034333

Electron capture rate

$$\lambda_{ec} \approx \sum_i B_i(GT) \int_{\omega_l}^{\infty} \omega p \left(Q_i + \omega\right)^2 F(Z,\omega) S_e(\omega,T) d\omega$$

With

- **$B_i(GT)$ Gamow-Teller strength distribution**
- **ω and p energy and momentum of electrons**
- **$F(Z,\omega)$ is the relativistic Coulomb barrier factor**
- **$S_e(\omega,T)$ Fermi-Dirac distribution electron gas at temperature T**

e^{-}-capture rates using experimental strengths

(Martínez-Pinedo, Langanke)

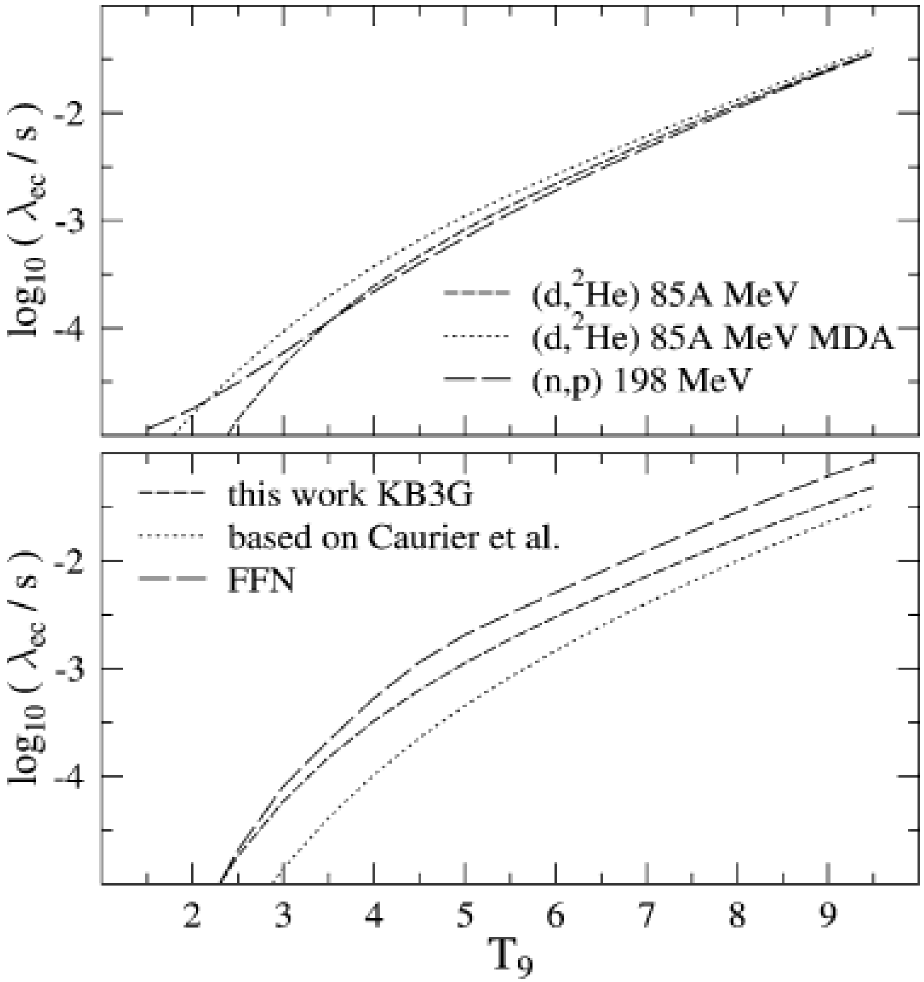

Evolution of core of 25 $M_\odot$ star. Conditions following silicon depletion.

$T_9 = 4.05$

$\rho = 3.18\times10^7$ g/cm^3

$Y_e = 0.48$

[Heger *et al.*, Astrophys. J. 560 (2001) 307]

Calculate EC rates as function of T_9 for GT transitions from $^{58}Ni_{g.s.}$

Strength deviations at low excitation ⇒ rates deviation at low *T*

^{58}Ni: comparison of *e*-capture rates theory/experiment

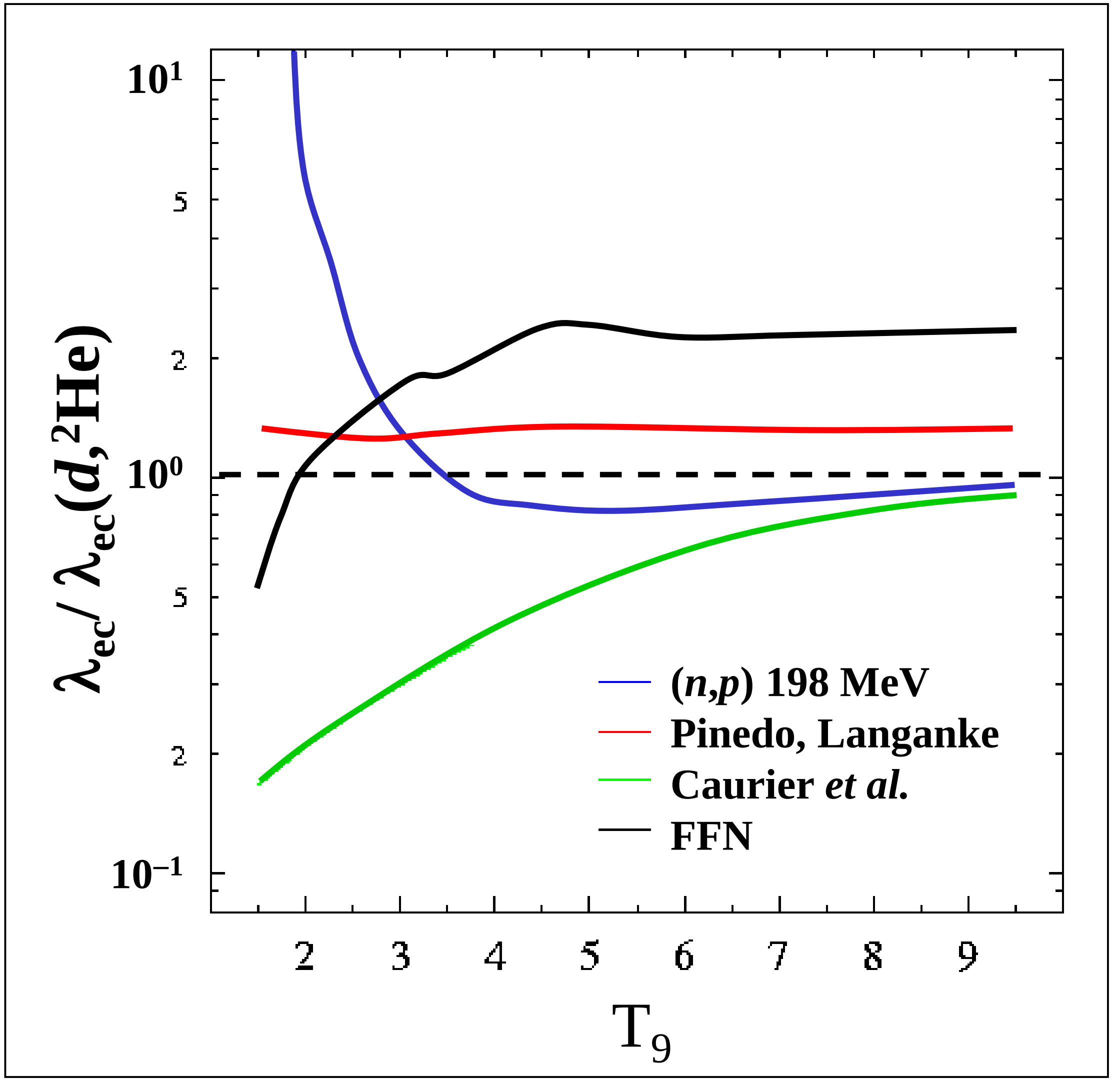

- **Influence of GT strength distribution on calculated capture rate is dramatic, especially at low temperatures**
- **rates vary up to a factor 5-6**
- **FFN not too far off**
- **large scale shell-model calculations fail at low T**
- **calculations with improved residual interaction (KB3G) in reasonable agreement**

^{51}V(*d*,^{2}He)^{51}Ti: *B(GT$^+$)* for proton-odd *fp*-shell nucleus

^{51}V g.s. ($J^\pi=7/2^-$, $T=5/2$) ⇒ ^{51}Ti ($J^\pi=5/2^-$, $7/2^-$, $9/2^-$, $T=7/2$)

Independent single-particle model (FFN): E_x(GTR)=3.83 MeV

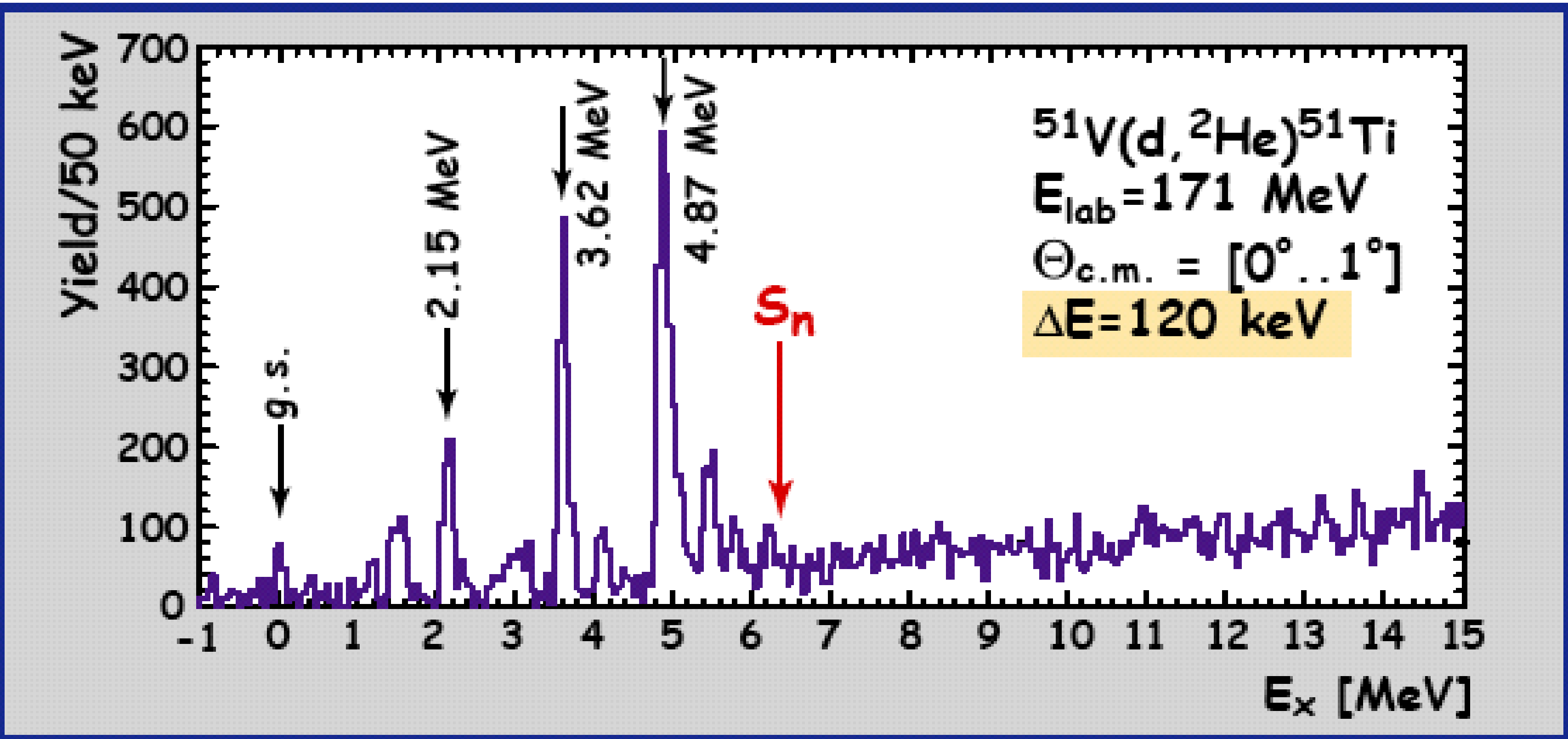

C. Bäumer *et al.*, PRC 68 (2003) 031303(R)

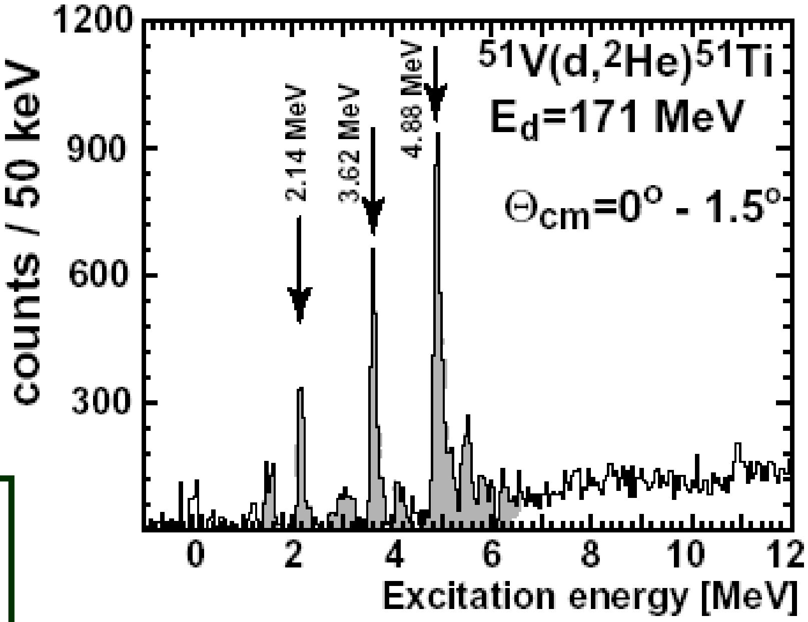

C. Bäumer *et al.*,
PRC 68 (2003) 031303(R)

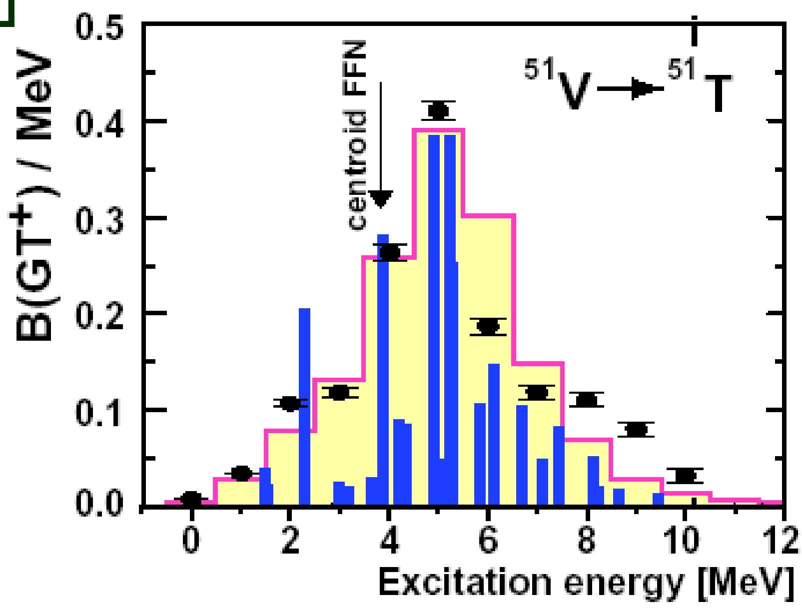

^{51}V(d,^{2}He): Angular distributions of $d\sigma/d\Omega$

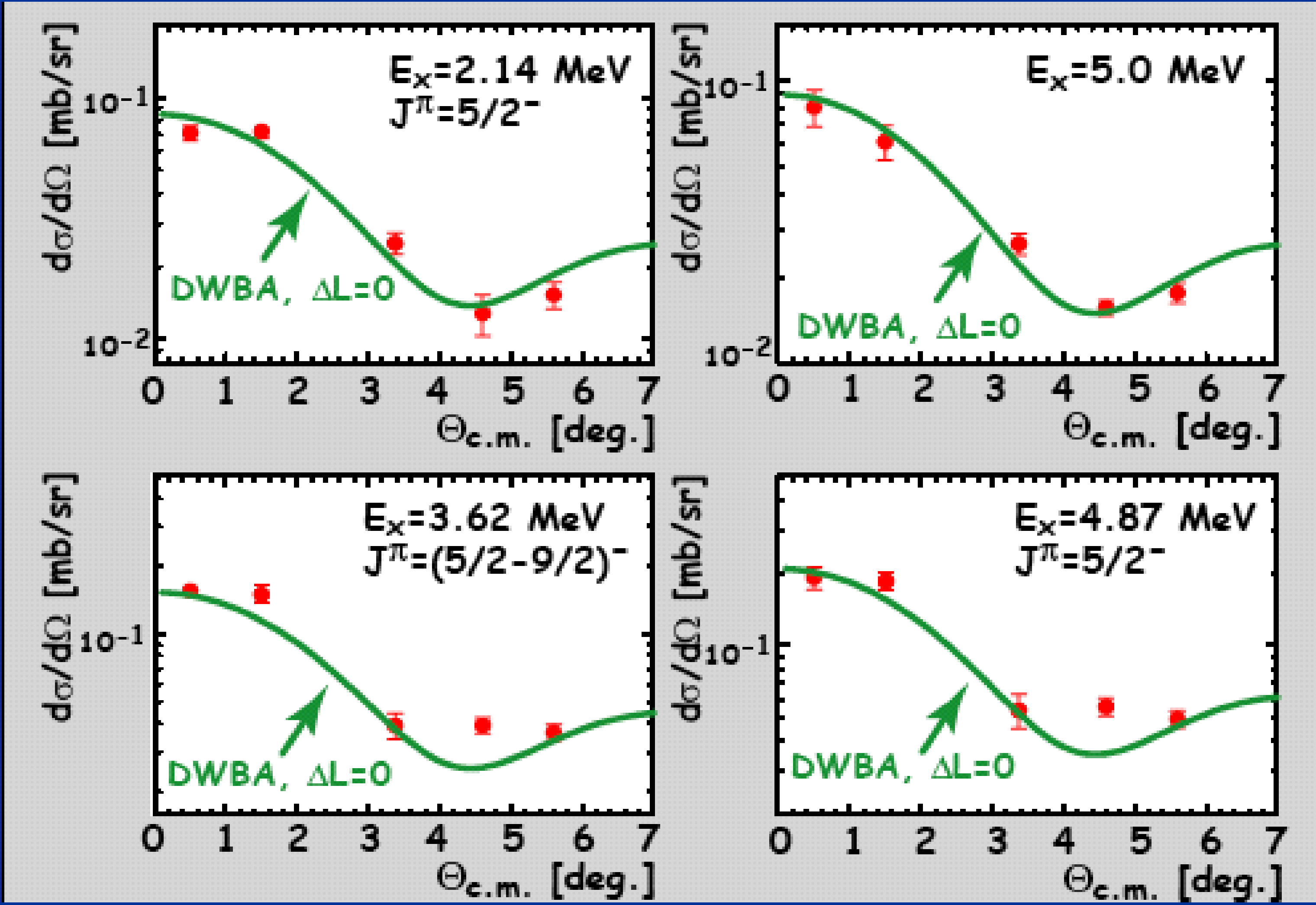

$^{51}V(d,^{2}He)$: Comparison with shell-model calculations

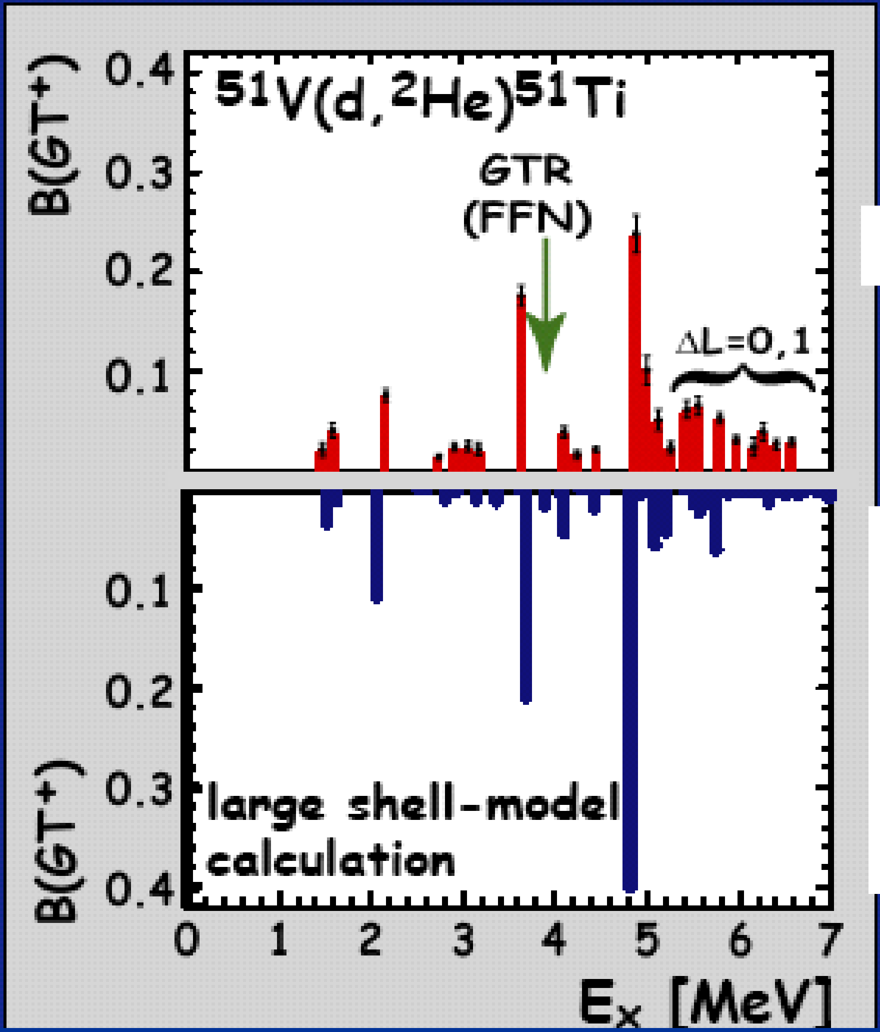

← Experimental result

← Full *fp*-shell model calculations
quenching factor $(0.74)^2$
G. Martínez-Pinedo, K. Langanke

$^{50}V(d,^{2}He)$: GT^{+} transitions from odd-odd nucleus

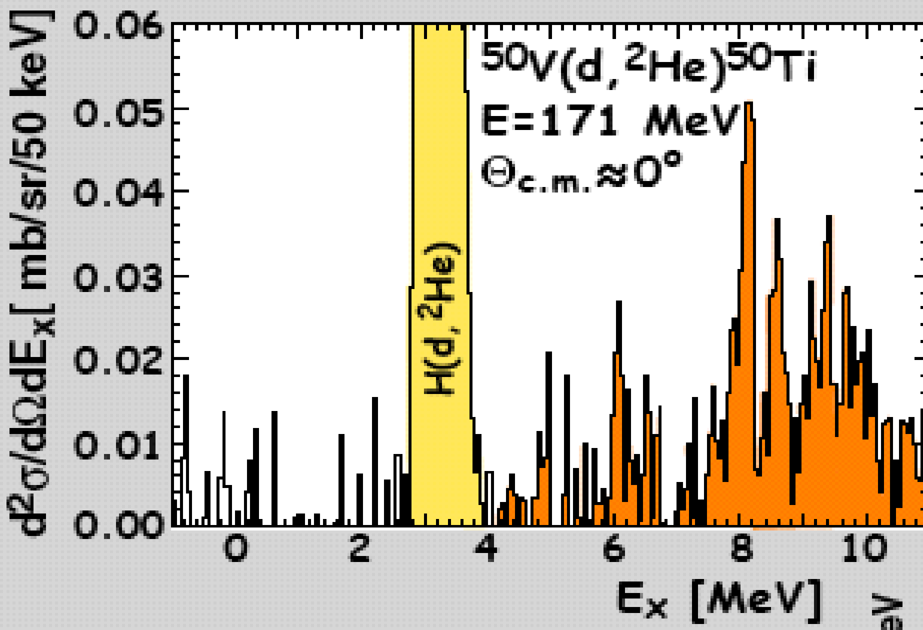

^{50}V	GT^{+}	^{50}Ti
$J^{\pi}=6^{+}$	→	$J^{\pi}=5^{+}, 6^{+}, 7^{+}$
$T=2$		$T=3$

GT-centroid located at ~ 9 MeV

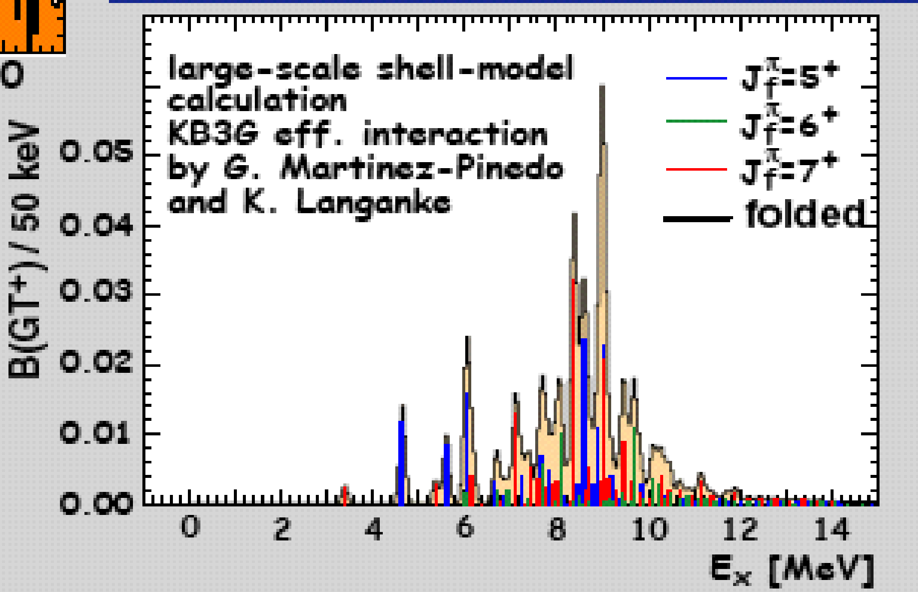

^{56}Fe(d,^{2}He): Comparison with shell-model calculations

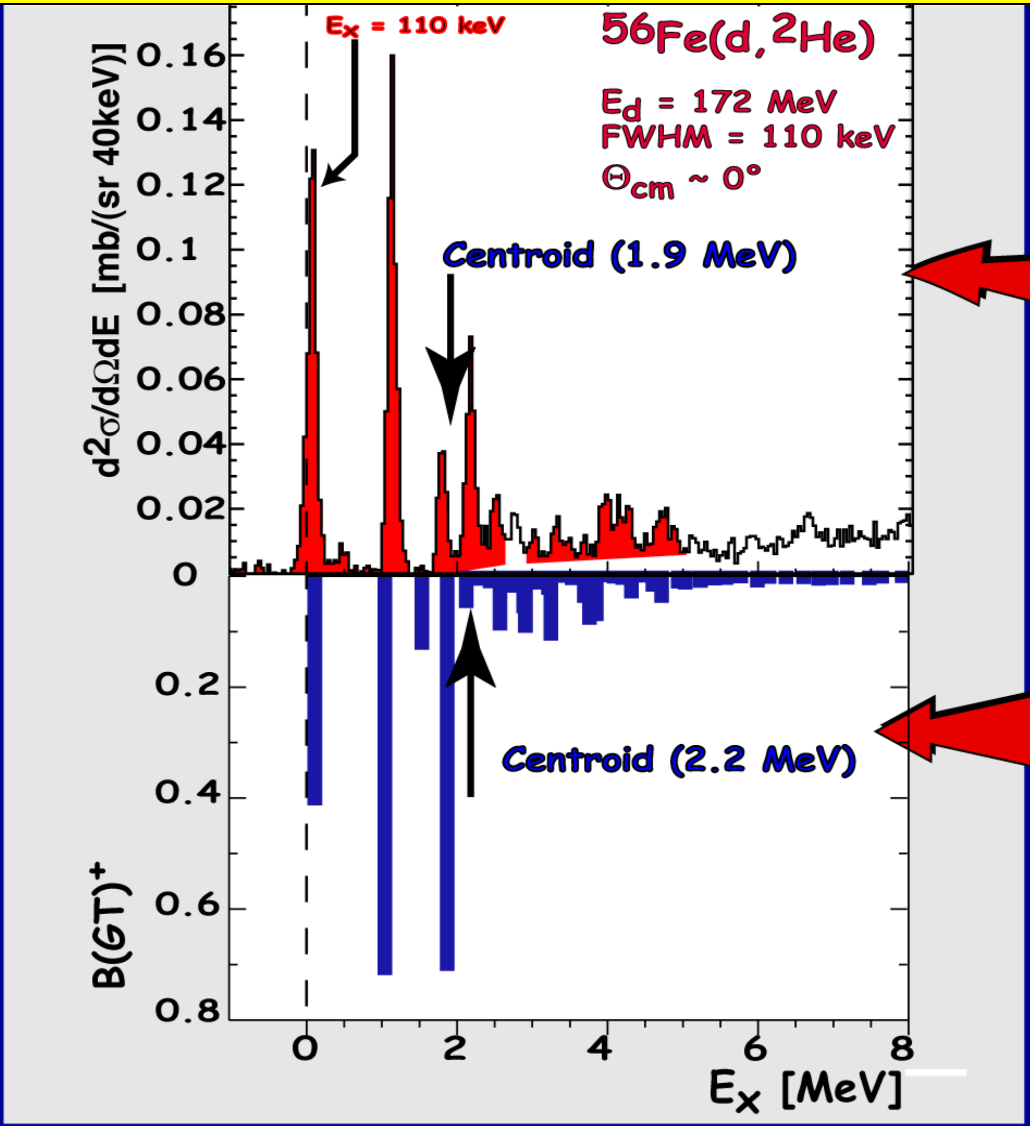

Experiment

Full *fp*-shell model calculations (KB3G) (G. Martínez-Pinedo)

^{61}Ni(d,^{2}He)^{61}Co: GT$^+$ distribution

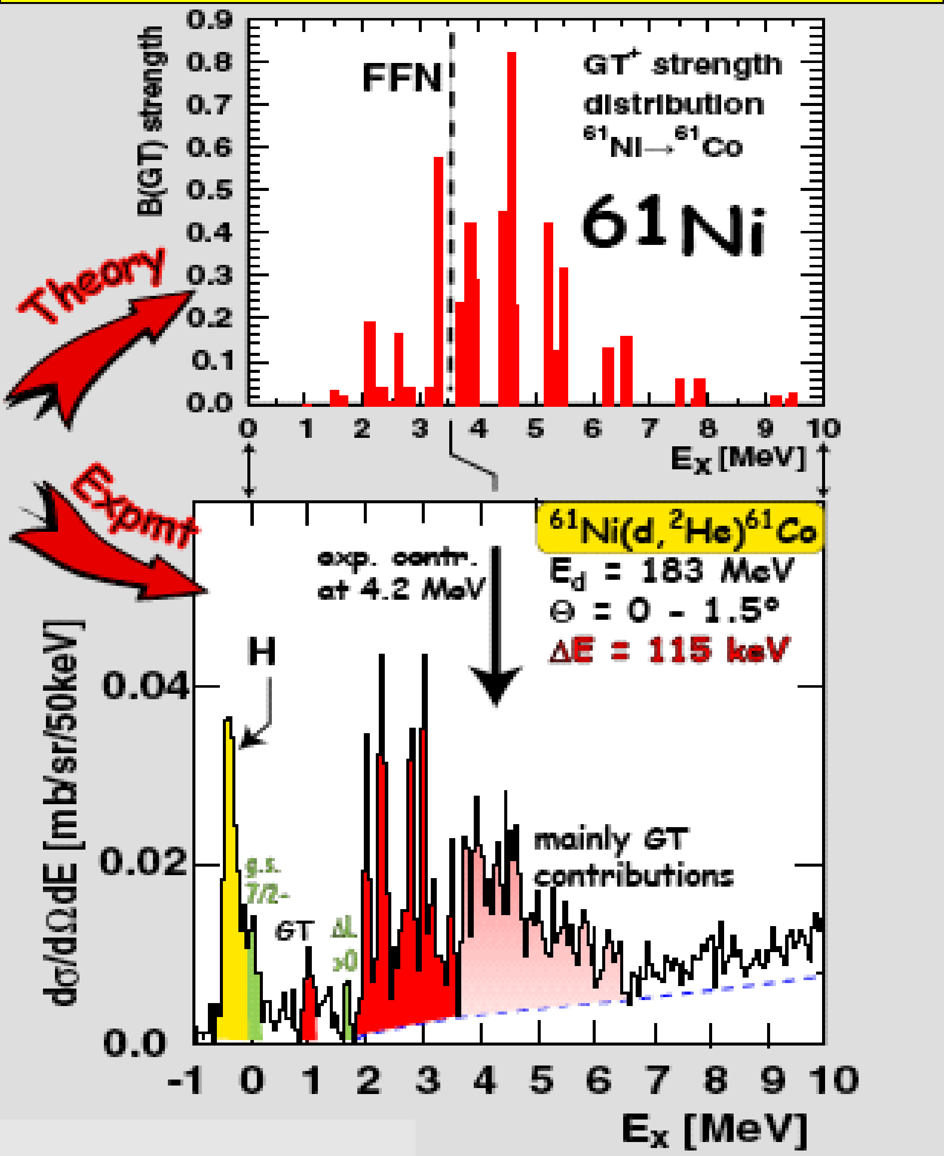

^{57}Fe(d,^{2}He)^{57}Mn: GT$^+$ distribution

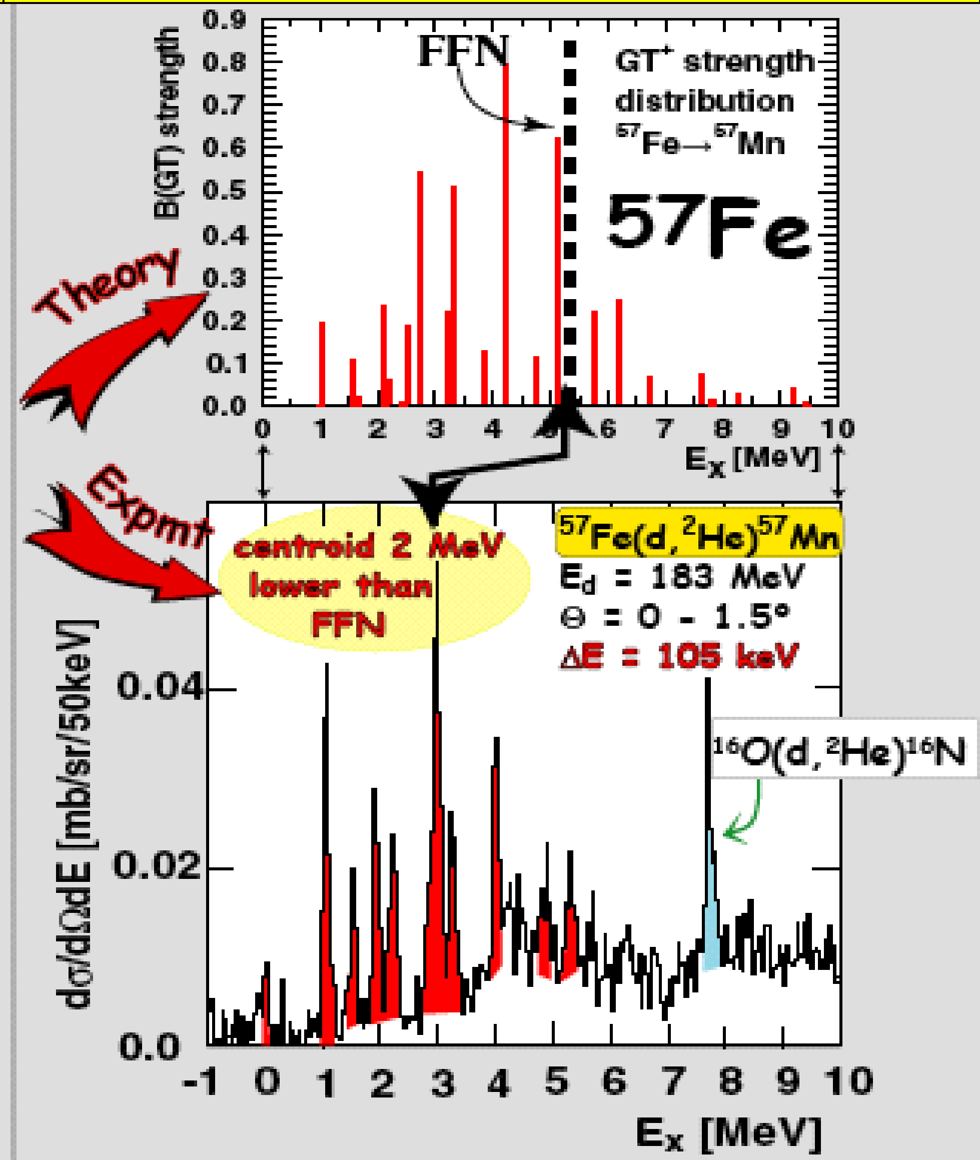

$^{67}Zn(d,^{2}He)^{67}Cu$: GT^{+} distribution

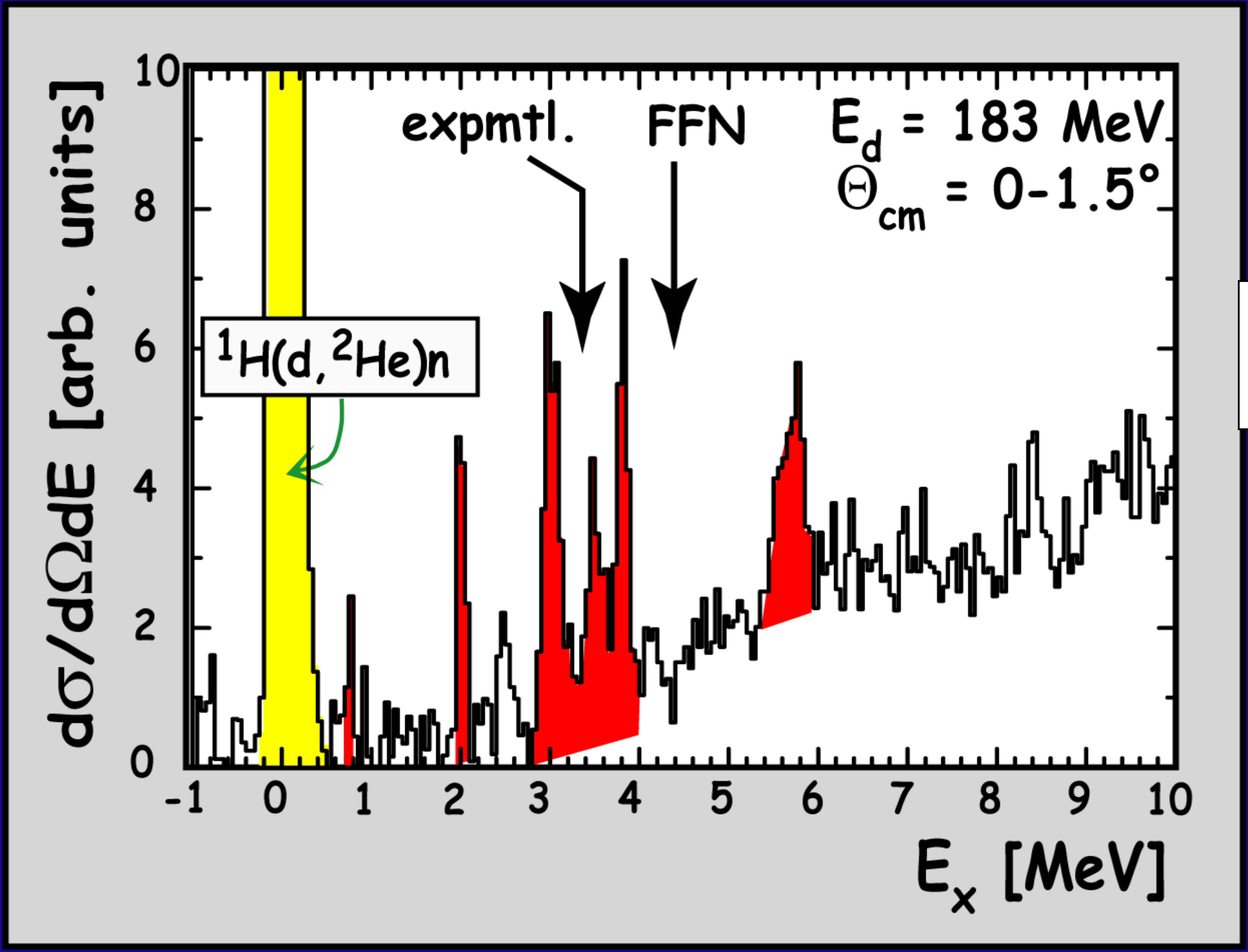

No shell-model calculations yet

Comparison of centroids (MeV) of GT$^+$ Strength distribution

	Nucleus	FFN	SM	Exp.
Even-Even	^{56}Fe	3.8	2.2	1.9
	^{58}Ni	3.8	3.6	3.4
Odd *A*-Odd *p*	^{51}V	3.8	4.7	4.1
Odd *A*-Odd *n*	^{57}Fe	5.3	4.1	2.9
	^{61}Ni	3.5	4.6	4.2
	^{67}Zn	4.4	--	3.4
Odd-Odd	^{50}V	9.7	8.5	8.8

WW = Woosley-Weaver Model calculations (FFN rates)

LMP = Langanke-Martínez-Pinedo Large shell-model calculations {G. Martínez-Pinedo *et al*., NPA 777 (2006) 395}

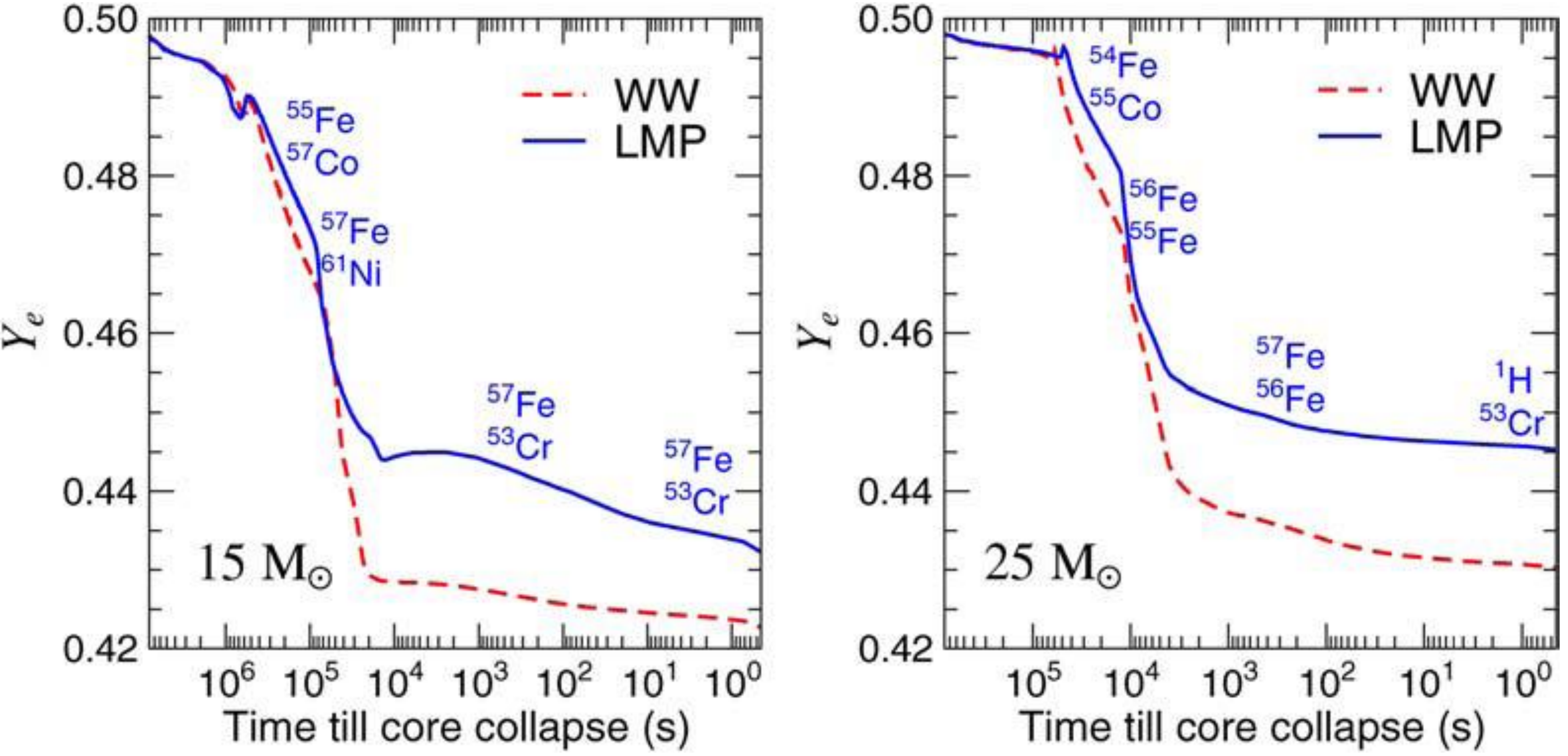

Conclusions

- **Presupernova models depend sensitively on EC rates.**
- **GT$^+$ transitions in *fp*-shell nuclei play a decisive role in determining EC rates and thus provide input into modeling of explosion dynamics of massive stars.**
- **Large shell-model calculations are needed especially as function of T. (Caurier *et al*.; Martínez-Pinedo & Langanke [KB3G]; Otsuka *et al*. [GXPF]) $\Rightarrow$ smaller EC rates for *A*=45-60 than FFN $\Rightarrow$ Larger Y_e (electron to baryon ratio) and smaller iron core mass (Heger *et al*.)**
- **New high resolution (d,^{2}He) experiments provide essential tests for shell model calculations at 0 *T*.**

Double-Beta Decay

ββ decay

2νββ decay

Allowed in SM and observed in many cases

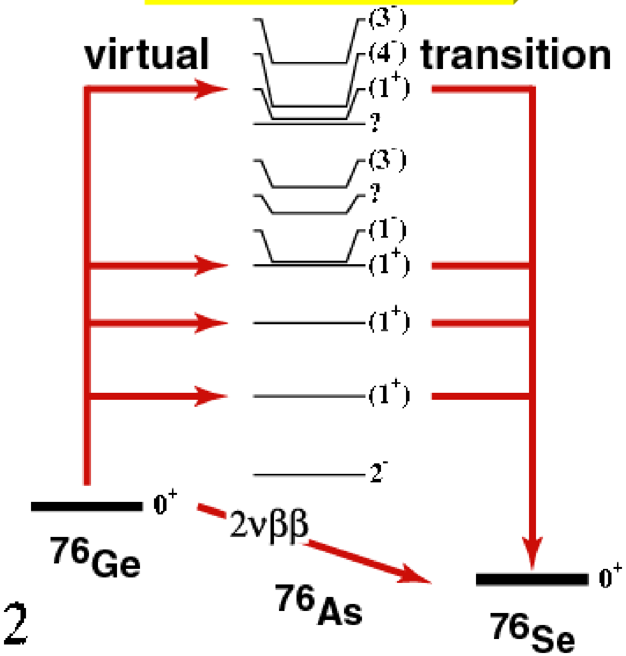

$$[t_{1/2}^{(2\nu)}]^{-1} = G^{(2\nu)}|M_{\mathrm{DGT}}^{(2\nu)}|^2 ,$$

$$M_{\mathrm{DGT}}^{(2\nu)} = \sum_m \frac{(0_{\mathrm{g.s.}}^{(f)}\|\sum_i\sigma(i)\tau^{\pm}(i)\|1_m^+)(1_m^+\|\sum_i\sigma(i)\tau^{\pm}(i)\|0_{\mathrm{g.s.}}^{(i)})}{[\frac{1}{2}Q_{\beta\beta}(0_{\mathrm{g.s.}}^{(f)}) + E(1_m^+) - M_i]/m_e + 1}$$

Accessible through charge-exchange reactions in (n,p) and (p,n) direction [e.g. (d,^{2}He) or (^{3}He,t)]

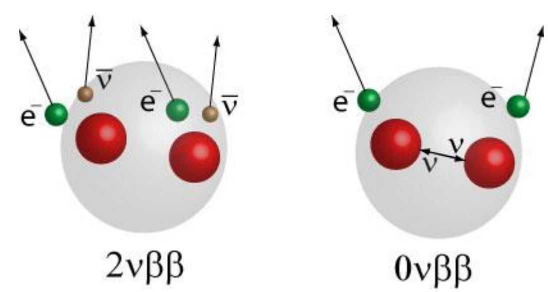

Forbidden in MSM
Lepton number violated
Neutrino enters as virtual particle, → $q \sim 0.5\ \mathrm{fm}^{-1}$

nuclear neutrino-less double-beta decay

0ν2β

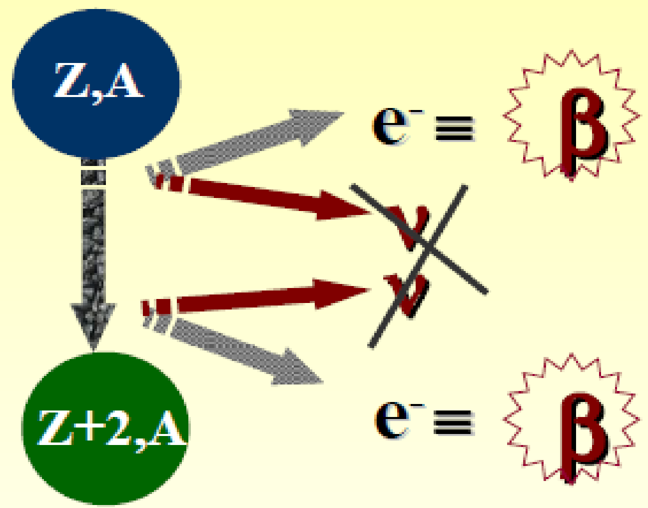

Majorana ν

$$decay\ rate \sim \left|NME^{0\nu 2\beta}\right|^2 \langle m_\nu \rangle^2$$

nuclear matrix element

Mass of Majorana neutrino!!

Approach

Study the spectroscopy of virtual states in the *2*-quantum process

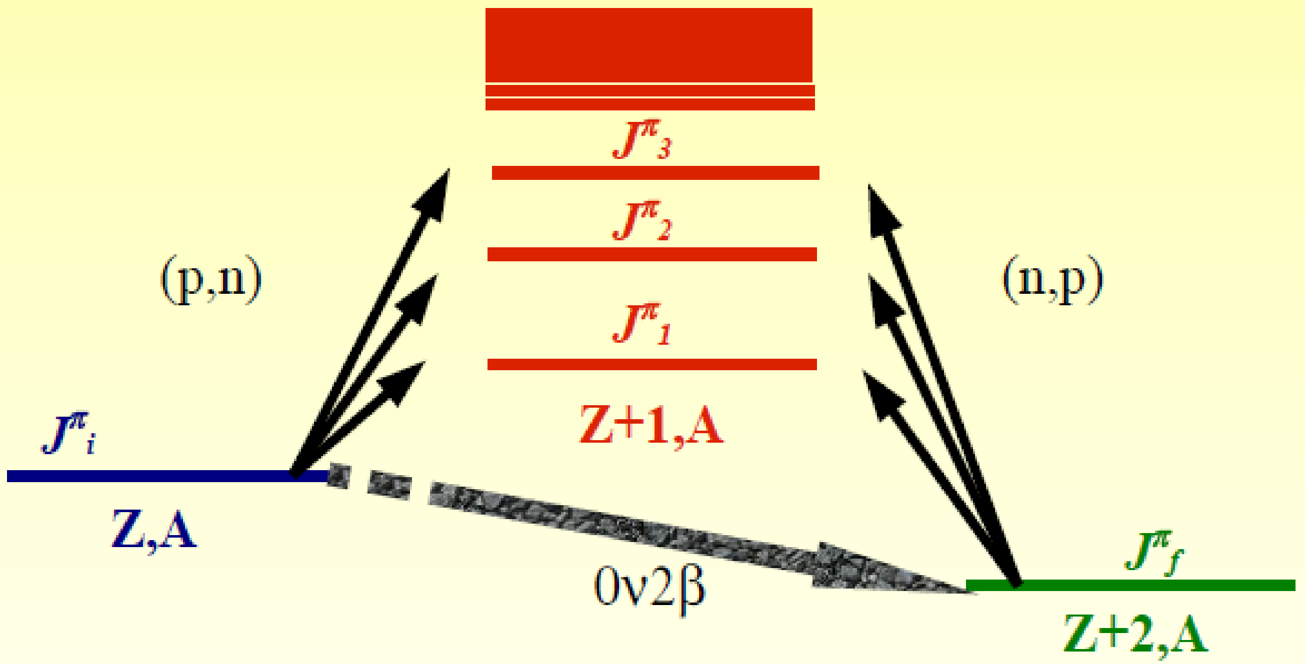

theory:

$$NME^{0\nu 2\beta} = \sum_m \frac{\langle J^\pi_i \| Operator \| J^\pi_m \rangle \langle J^\pi_m \| Operator \| J^\pi_f \rangle}{f(E_m)}$$

^{76}Ge - ^{76}As - ^{76}Se

- Intensively studied ββ-emitter
- $T_{1/2}$ determined by the Heidelberg-Moscow group: 1.55×10^{21}y
- $T_{1/2}$ deduced from (n,p) and (p,n) data with poor energy resolution

multipole decomposition: 7.4×10^{20}y

0°-6° subtraction method: 8.7×10^{21}y

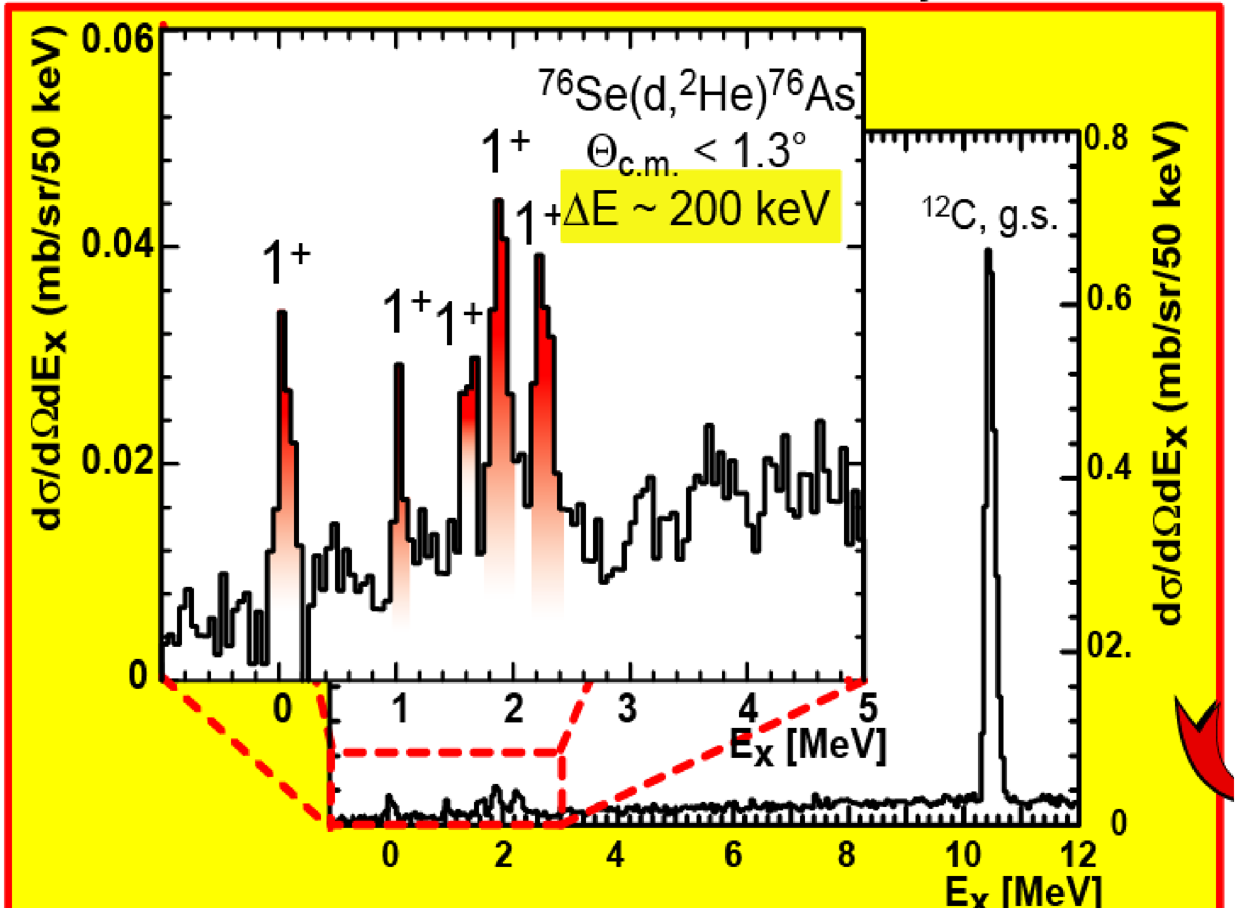

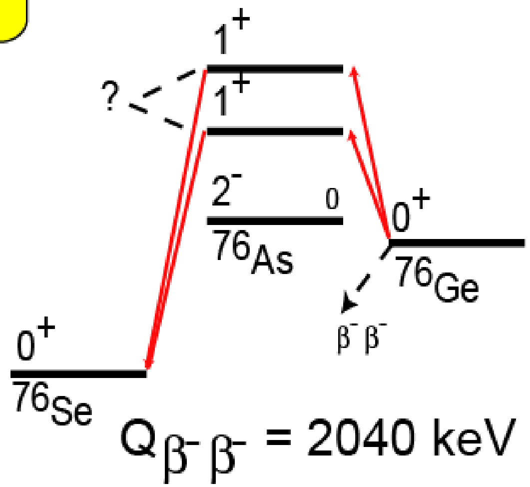

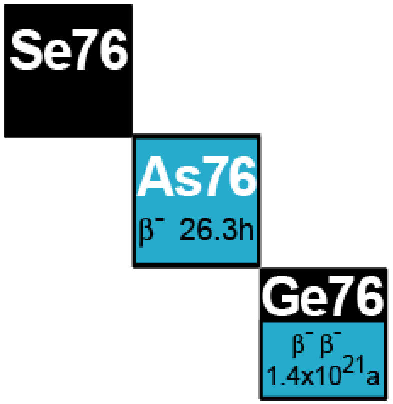

Σ B(GT+) ~ 0.56

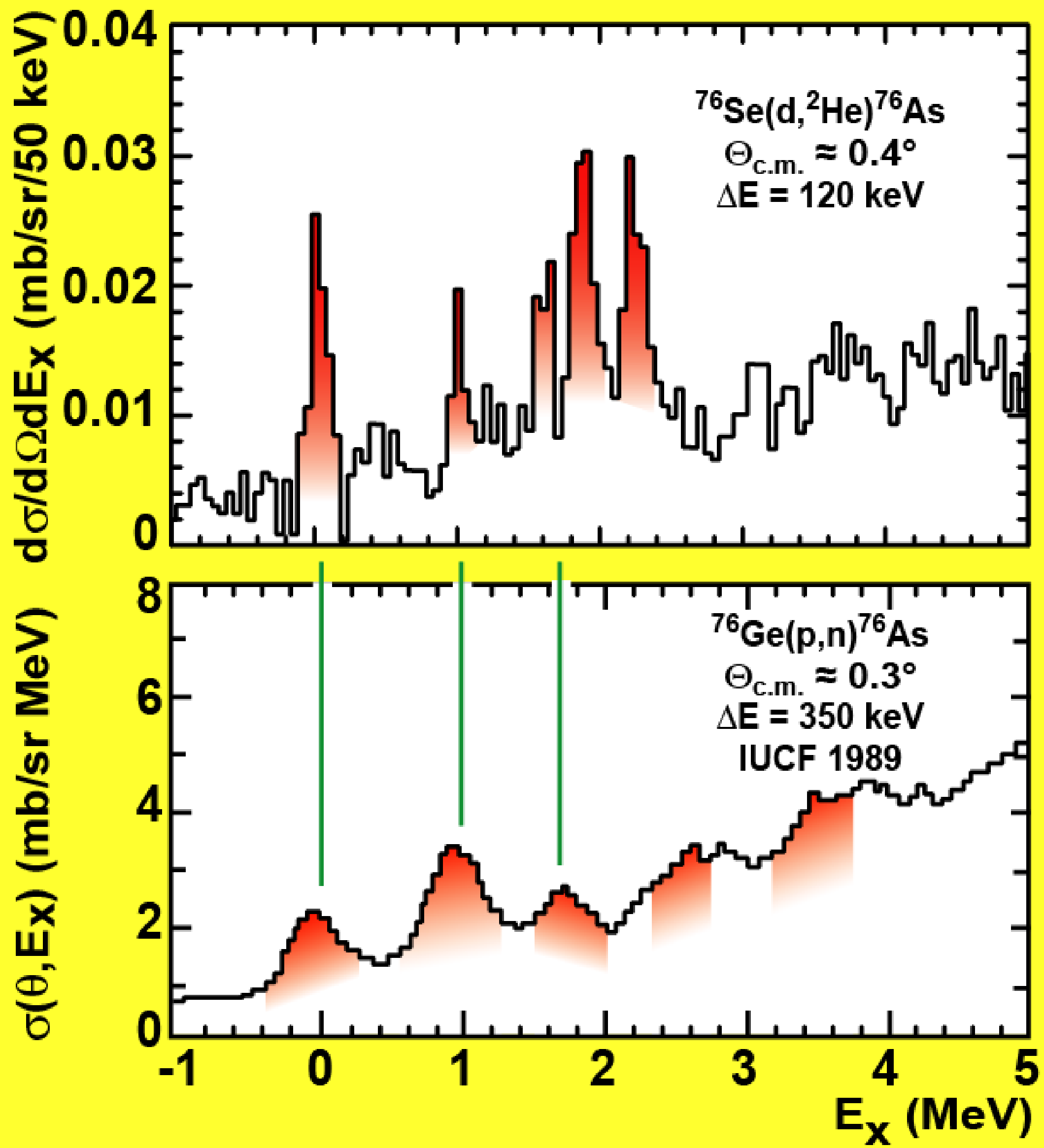

$2\nu\beta\beta$-matrix element

0.16 ± 0.04 MeV^{-1}

with

$G^{(2\nu)} = 3.4 \times 10^{-20}$ MeV^{2} a^{-1}

$2\nu\beta\beta$ - half-life

$(1.1 \pm 0.2) \times 10^{21}$ a

recommended. exp. value:

$(1.5 \pm 0.1) \times 10^{21}$ a

$G^{(2\nu)}$ taken from: J. Suhonen and O. Civitarese, Phys. Rep. 300, 123 (1998)

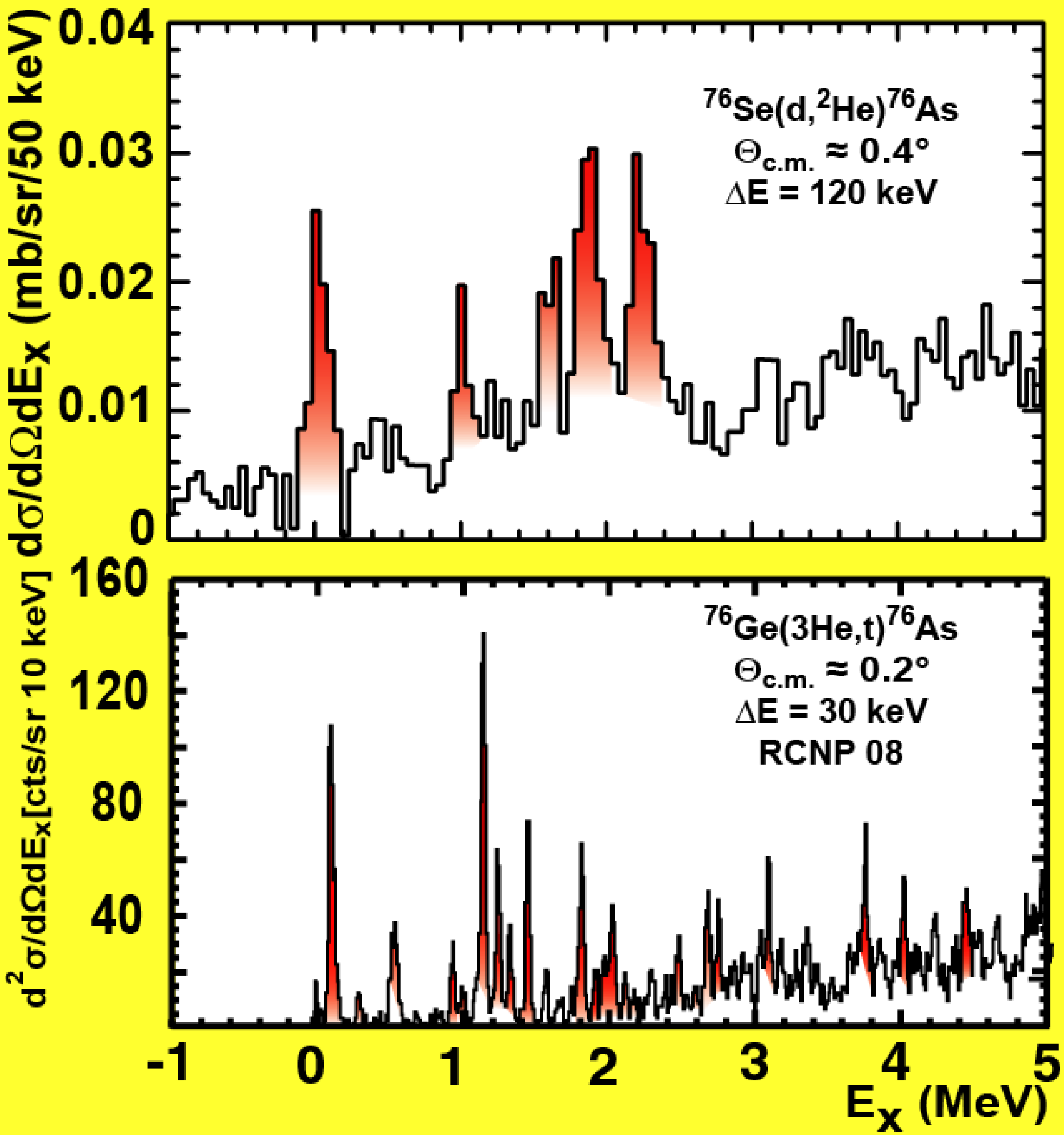

$2\nu\beta\beta$-matrix element

0.16 ± 0.04 MeV^{-1}

with

$G^{(2\nu)} = 3.4 \times 10^{-20}$ MeV^2 a^{-1}

$2\nu\beta\beta$ - half-life

$(1.1 \pm 0.2) \times 10^{21}$ a

recommended. exp. value:

$(1.5 \pm 0.1) \times 10^{21}$ a

$G^{(2\nu)}$ taken from: J. Suhonen and O. Civitarese, Phys. Rep. 300, 123 (1998)

^{96}Zr - ^{96}Nb - ^{96}Mo

- $T_{1/2}$ available:
  - counting experiments: 2.1×10^{19}y
  - geochemical methods: 9.4×10^{18}y
- g.s. transition forbidden
- strength concentrated in one transition

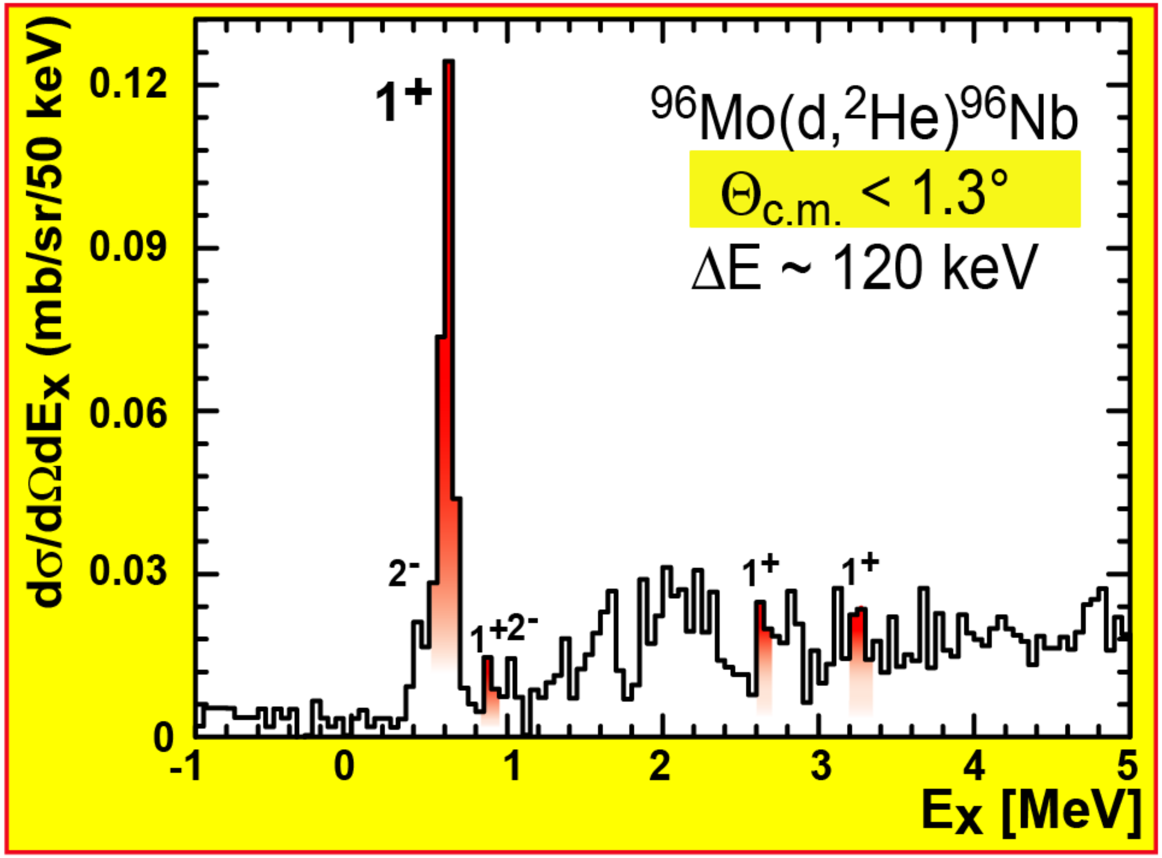

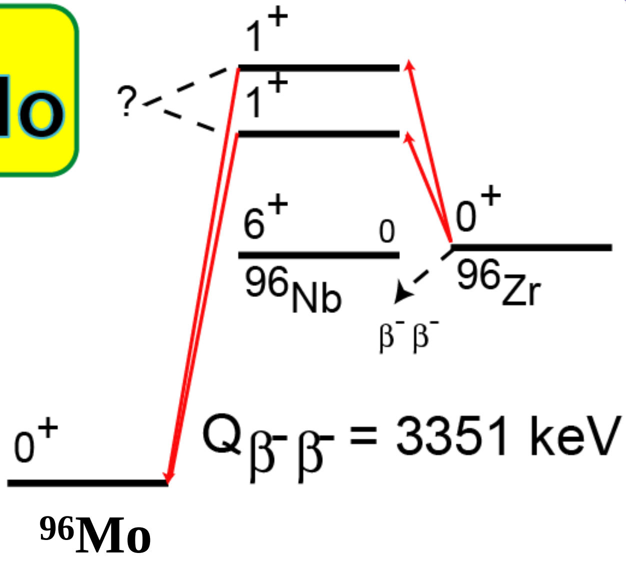

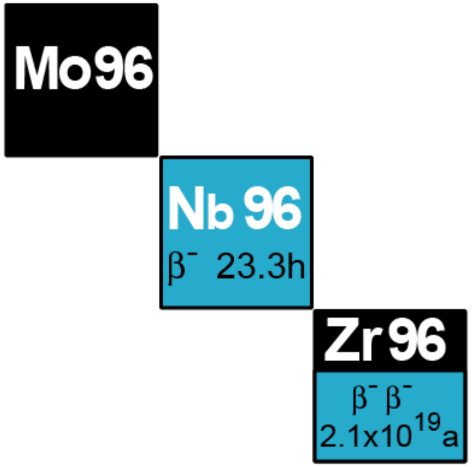

$B(GT^+) \sim 0.3$

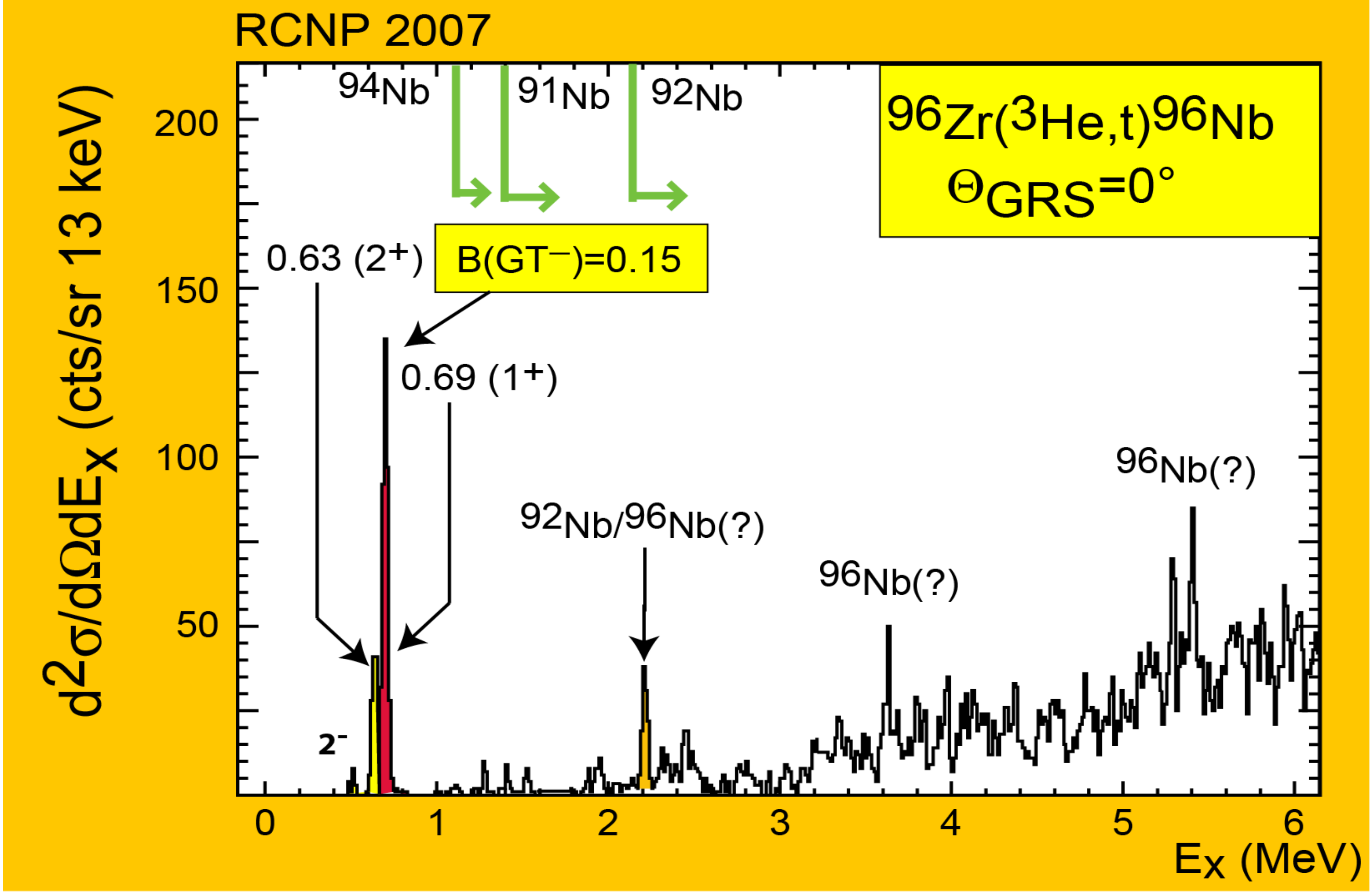

In (*p*,*n*) direction:

1 - exceptionally small *B(GT⁻)* below 6 MeV

2 - concentrated in one low-lying level only

$(d,{}^2He)$ — $({}^3He,t)$

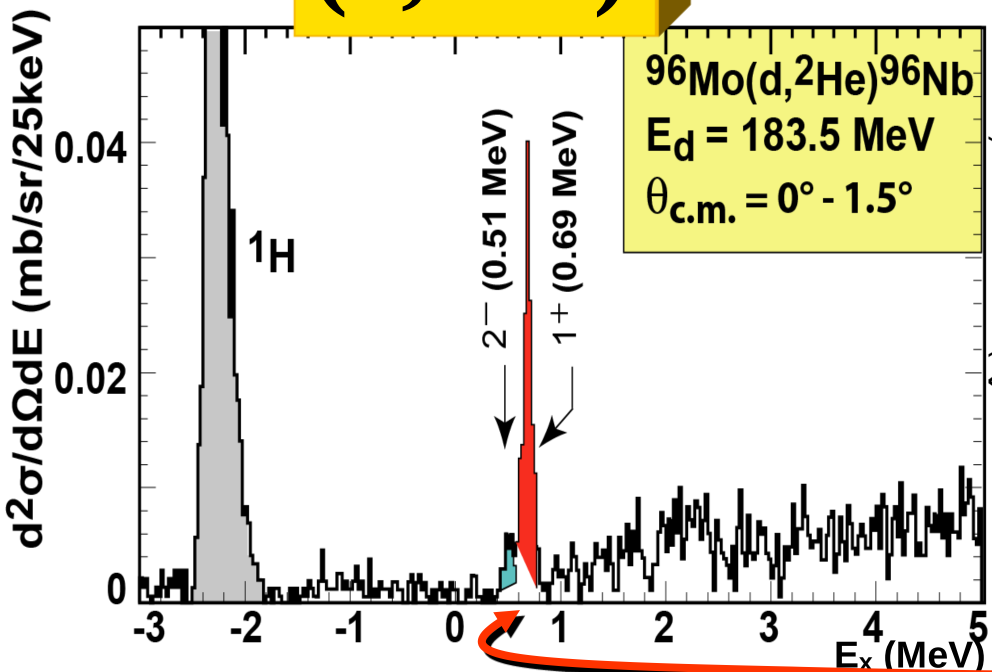

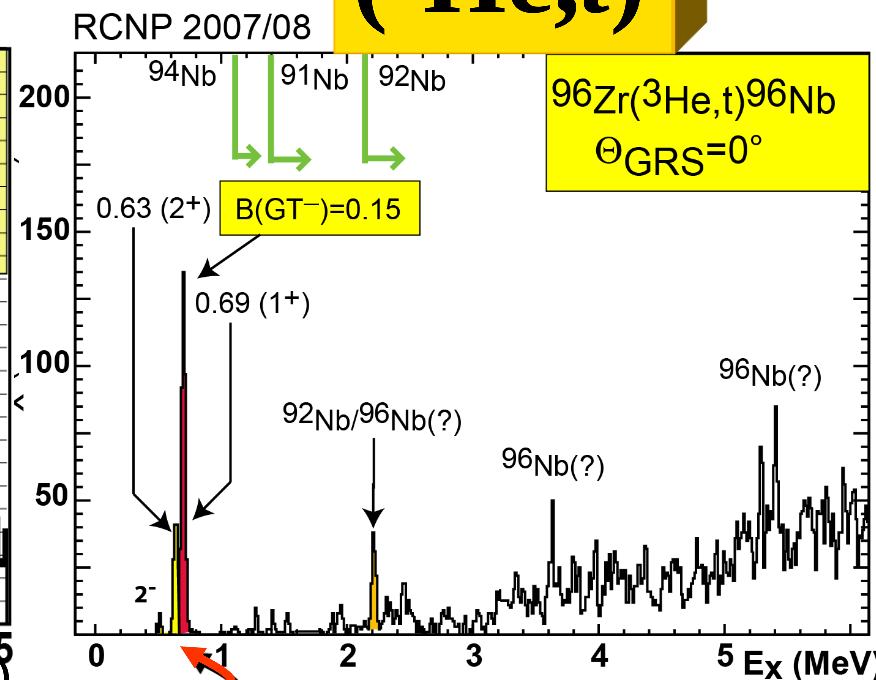

B(GT⁺) = 0.3

B(GT⁻) = 0.15

With this 1 level only

$$T_{1/2}^{calc.}(2\nu\beta\beta) = (2.4 \pm 0.3)\cdot 10^{19}\ \text{years}$$

$$T_{1/2}^{exp.}(2\nu\beta\beta = (2.2 \pm 0.4)\cdot 10^{19}\ \text{years} \quad \text{(NEMO3-result)}$$

Conclusions

- **Charge-exchange reactions provide important input for $2\nu\beta\beta$ decay ME; *i.e.* (d,^{2}He) (t,^{3}He) for GT^{+} leg and (^{3}He,t) for the GT^{-} leg**

- **^{96}Zr and ^{100}Mo exhibit Single-State Dominance (at 0.69 MeV (^{96}Zr) and g.s. (^{100}Mo))**

Physics case for 0ν2β study: ^{76}Ge

Claim of the observation of 0ν2β-decay in ^{76}Ge

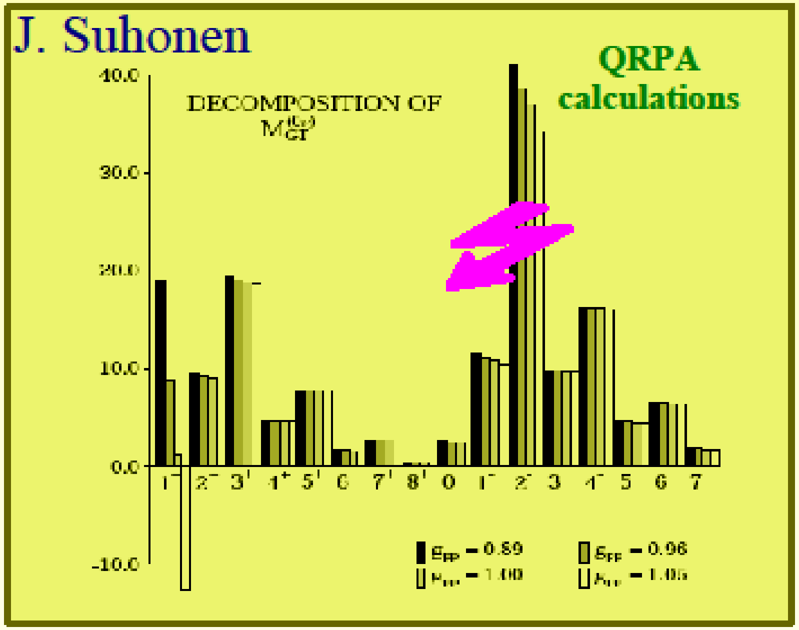

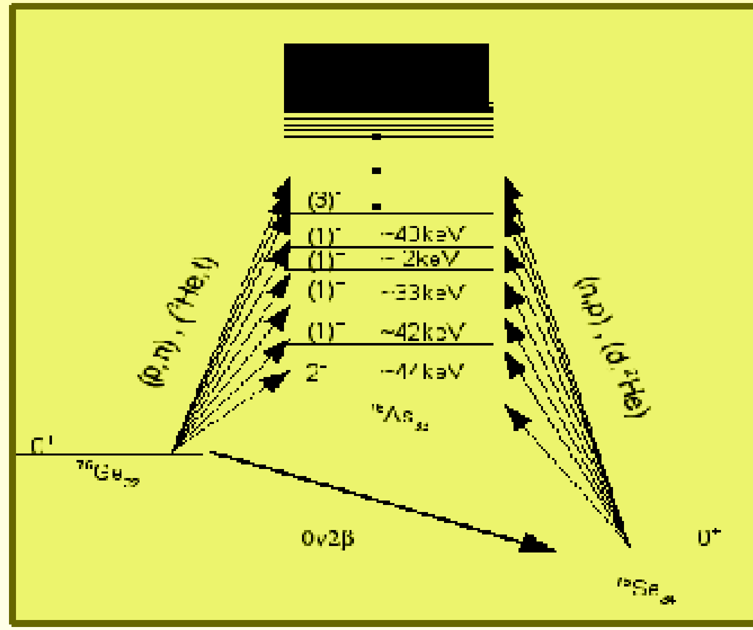

- contribution of many multi-poles
- dominance of dipole components
- the g_{pp} parameter affects mainly the $J^{\pi} = 1^{+}$ component
- it becomes imperative to study experimentally higher multi-pole components

Experiments at RCNP, Osaka University

- (^{3}He,*t*) reaction at 420 MeV
  - High-resolution spectrometer "Grand Raiden"
  - *ΔE* ~ 30 keV

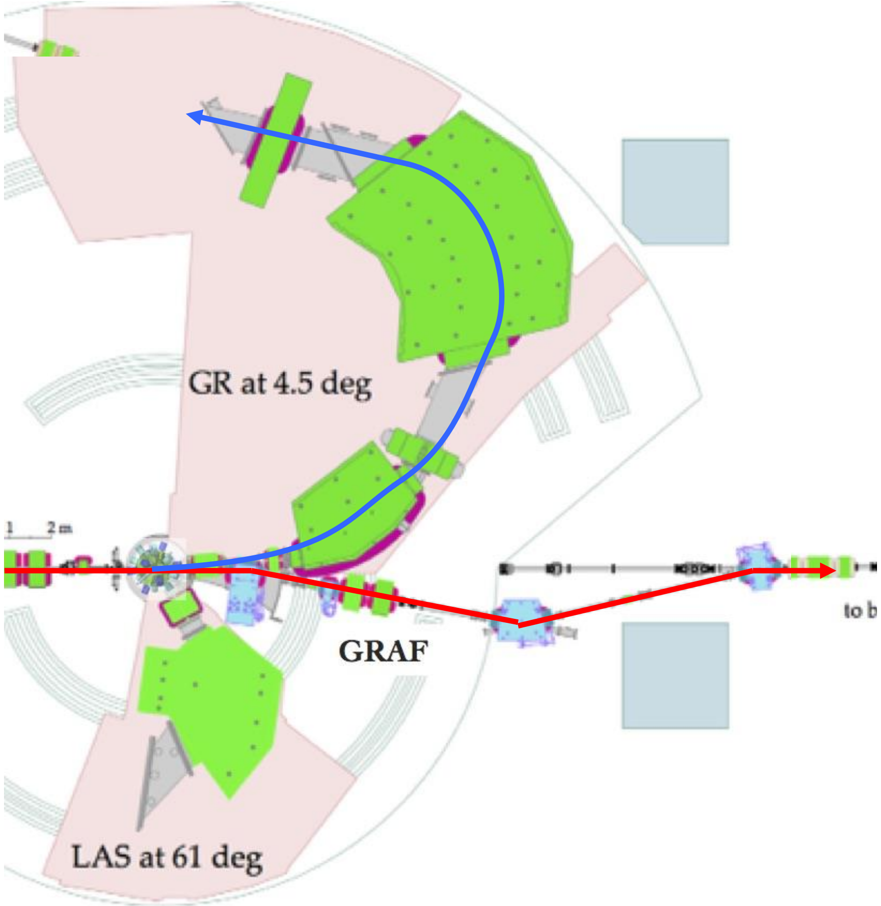

^{136}Xe(^{3}He,*t*)^{136}Cs

E(^{3}He) = 420 MeV

ΔE = 42 keV

B$_{exp}$(GT+) =

$$\frac{\mathrm{d}\sigma(q=0)}{d\Omega}\cdot\left[\frac{d\hat{\sigma}(GT)}{d\Omega}\right]^{-1}$$

extrapolated (DWBA)

unit cross section

***ΔL* = 2 & *ΔL* = 0 incoherent**

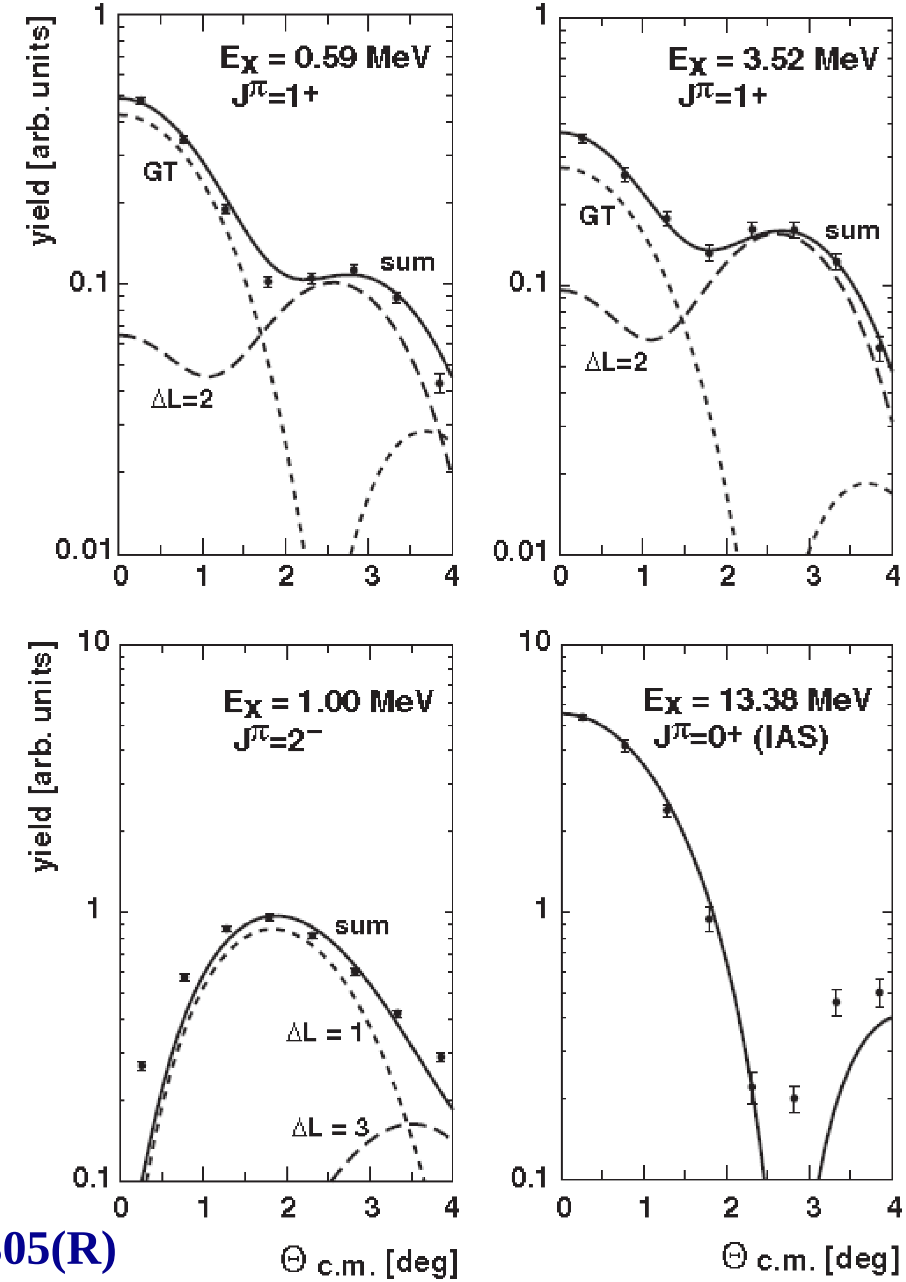

P. Puppe *et al*., Phys. Rev. C 84 (2011) 051305(R)

Double-beta decay nuclei ^{76}Ge, ^{82}Se, ^{100}Mo, ^{128}Te, ^{130}Te, ^{150}Nd show clear spin-dipole and Gamow-Teller states

- **RCNP high-resolution system is the unique and only opportunity to determine 2^- levels.**

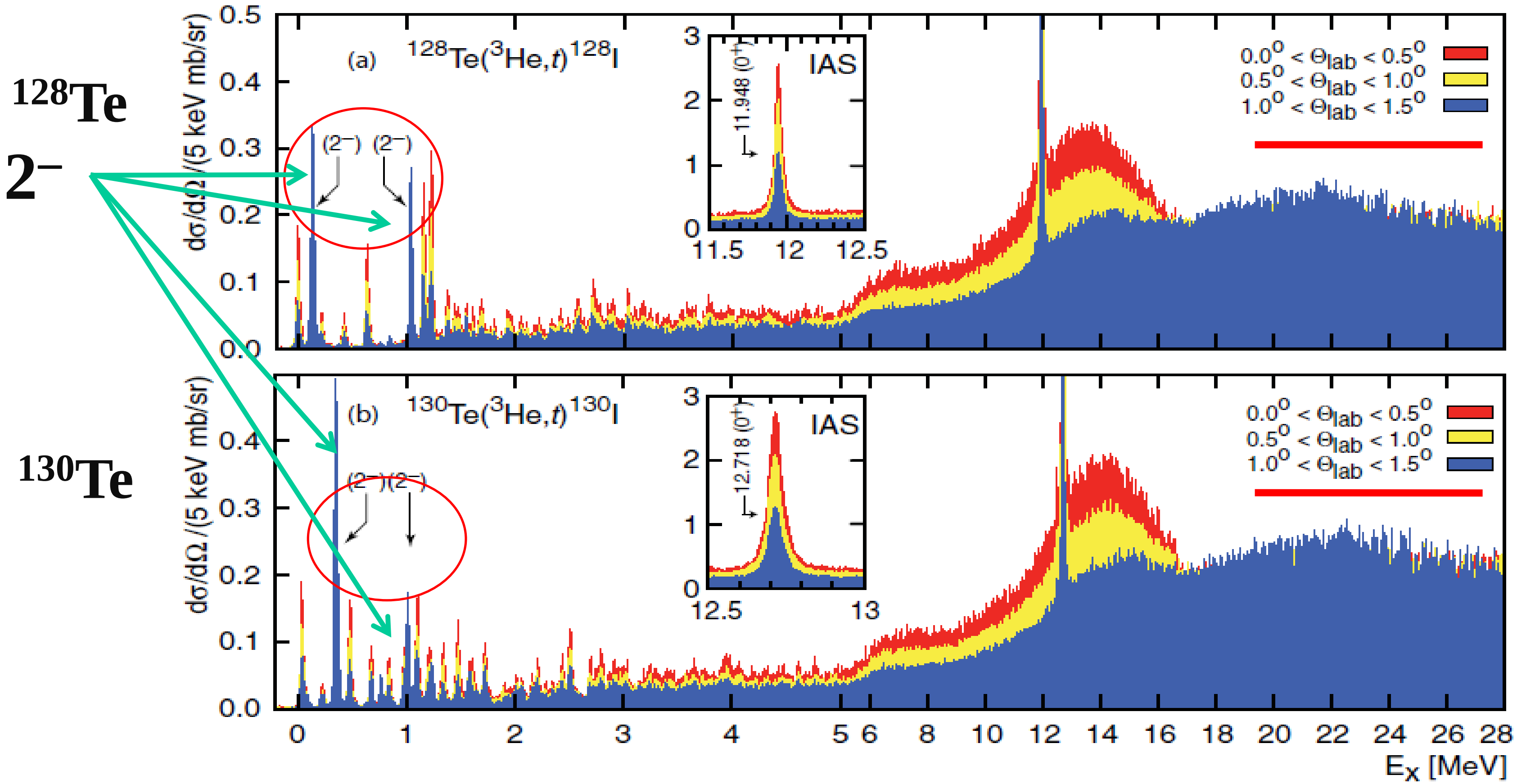

P. Puppe *et al*., Phys. Rev. C 86 (2012) 044603

Measured angular distributions

- **Select spin-dipole (SD) component and derive B(SD) from DWBA fit at the peak region where SD $\langle \sigma\tau Y_1 \rangle^{2-}$ is dominant.**
  - **Angular distributions of SD are peaked around 2 deg.**
  - **Small deviation of (0.1 mb/sr) at 0.5 deg!**

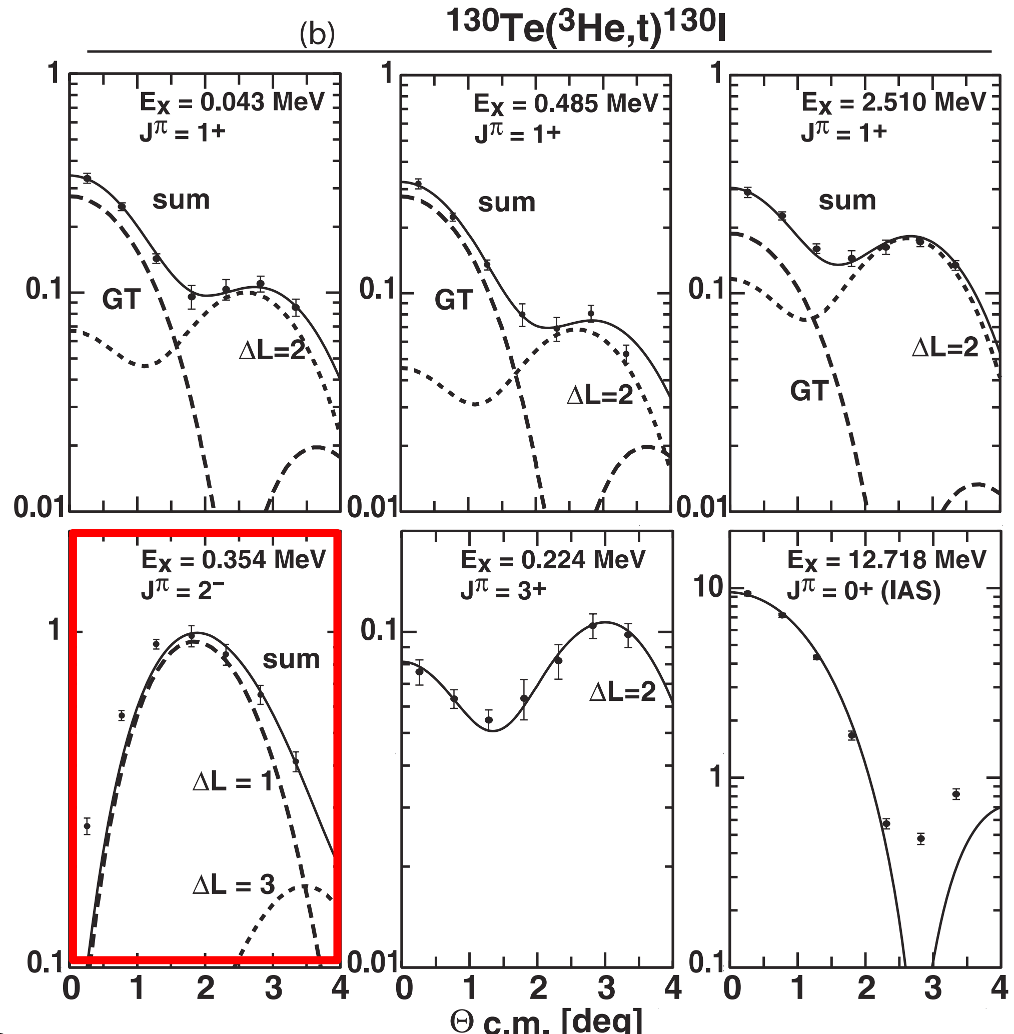

P. Puppe *et al*., Phys. Rev. C 86 (2012) 044603

IV(S)GDR & GTR
Neutron-Skin Thickness

Determining neutron-skin thickness from IVSGDR

Summed ΔL=1 strength depends on the neutron-skin thickness as follows:

$$S^{-}_{IVSGDR} - S^{+}_{IVSGDR} = \frac{9}{2\pi}\left(N\langle r^2\rangle_n - Z\langle r^2\rangle_p\right)$$

Here, S^{-} and S^{+} are the spin-dipole total strengths in β^{-} and β^{+} channels

Using the calculated $B = S^{+}/S^{-}$ ratios the neutron-skin thicknesses can be deduced

$$\langle r^2\rangle_n^{1/2} - \langle r^2\rangle_p^{1/2} = \frac{\alpha\sigma_{exp}(1-B) - (N-Z)\langle r^2\rangle_p}{2N\langle r^2\rangle_p^{1/2}}\ , \qquad (3)$$

^{A}Sn(^{3}He,*t*)

At 450 MeV

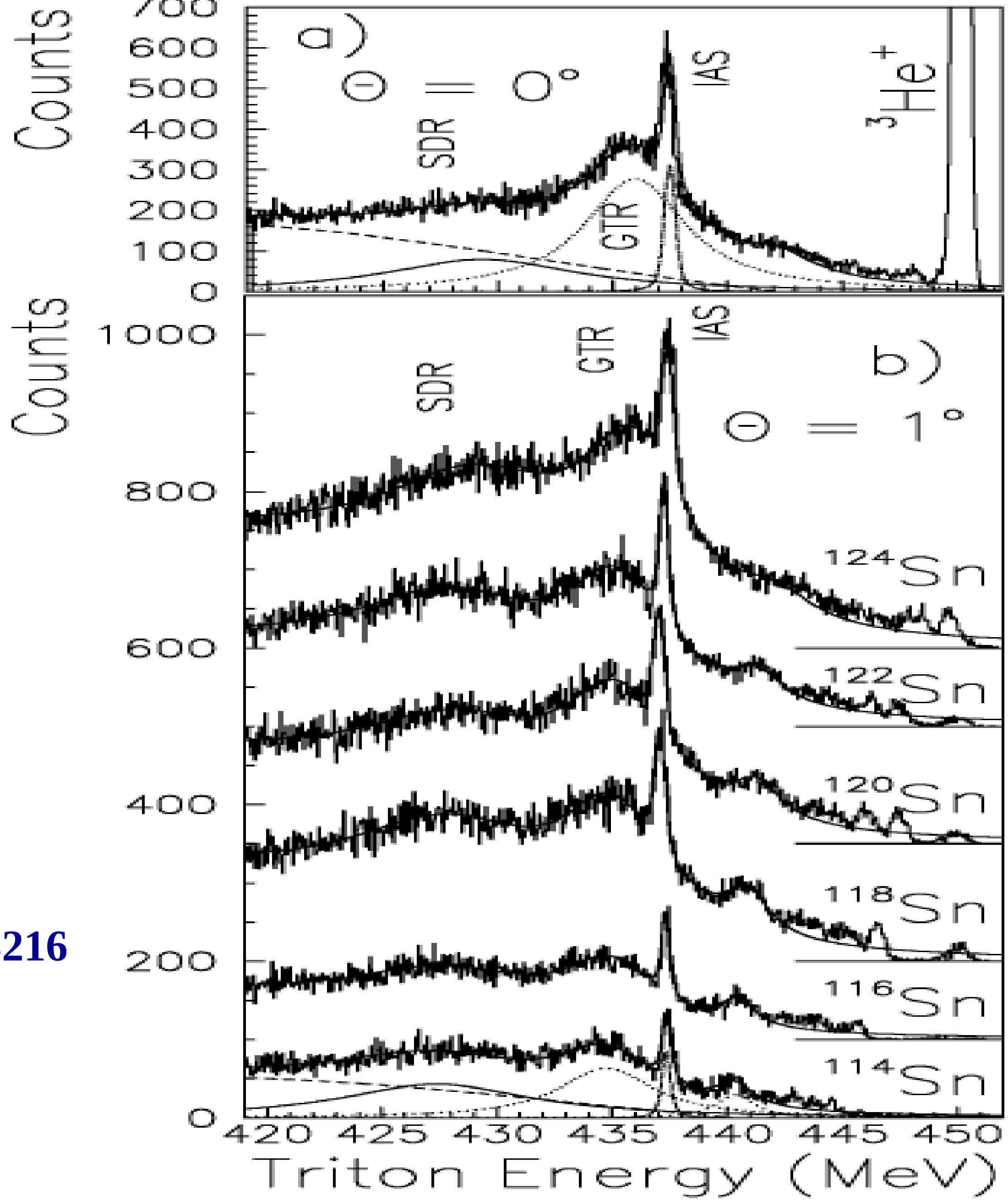

A. Krasznahorkay et al.,
Phys. Rev. Lett. 82 (1999) 3216

Summary of the neutron-skin thicknesses ($\langle r_n^2\rangle^{1/2} - \langle r_p^2\rangle^{1/2}$ in fm) obtained in different methods.

Isotope	(p,p) [4,5]	(p,p) [7]	GDR [16]	SDR [18]	antiproton [11]
^{112}Sn					0.09±0.02
^{114}Sn				≤0.09	
^{116}Sn	0.15±0.05		0.02±0.12	0.12±0.06	0.12±0.02
^{118}Sn				0.13±0.06	
^{120}Sn				0.18^{a})	0.12±0.02
^{122}Sn				0.22±0.07	
^{124}Sn	0.25±0.05		0.21±0.11	0.19±0.07	0.19±0.02
^{208}Pb	0.14±0.04	0.20±0.04	0.19±0.09		0.15±0.02

^{a}) Normalized to the theoretical value of Angeli et al. [21].

The full dots with error bars show the neutron-skin thicknesses of the Sn isotopes determined from the IVSGDR data as a function of the mass number. The experimental Values determined by the (*p*,p), And the antiprotonic methods are Shown as full triangles and full Squares with error bars, respectively. The numbered full lines represent different theoretical results.

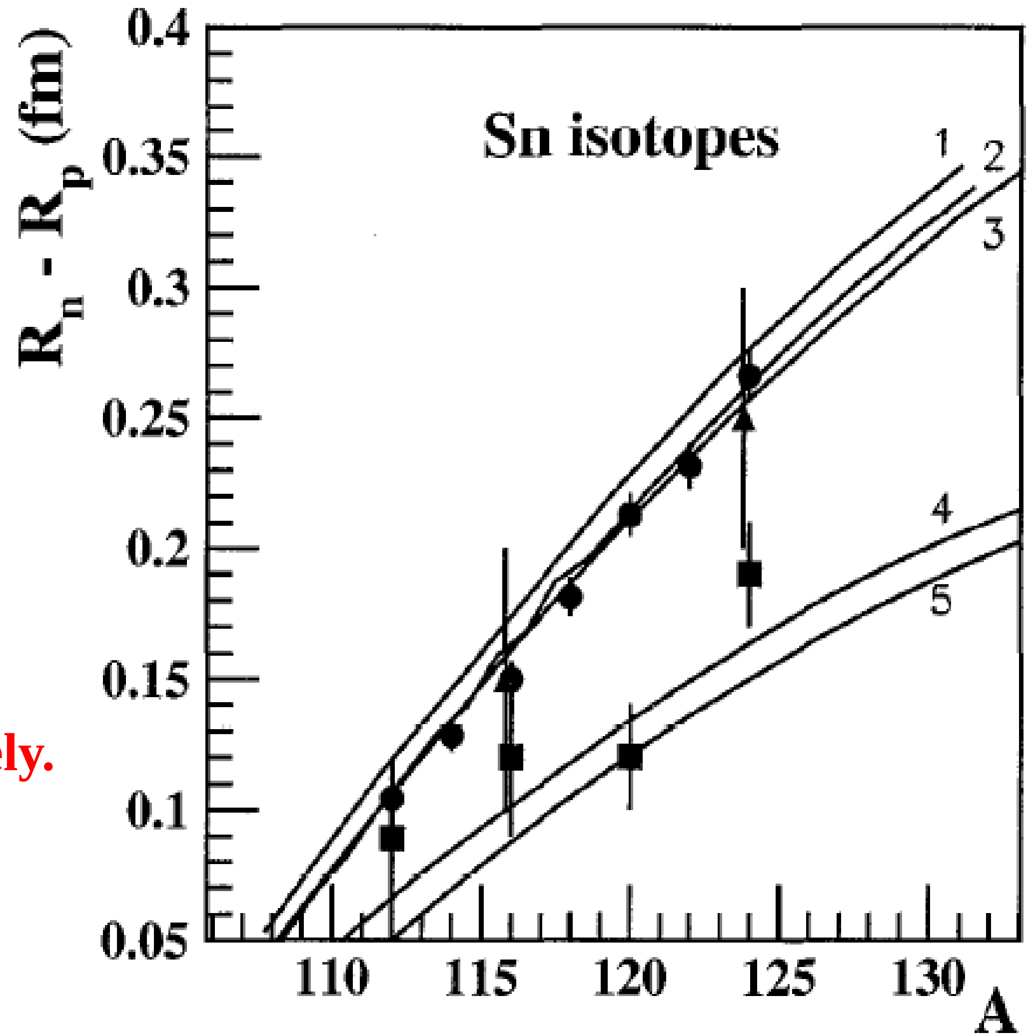

A. Krasznahorkay *et al.*, Nucl. Phys. A731 (2004) 224

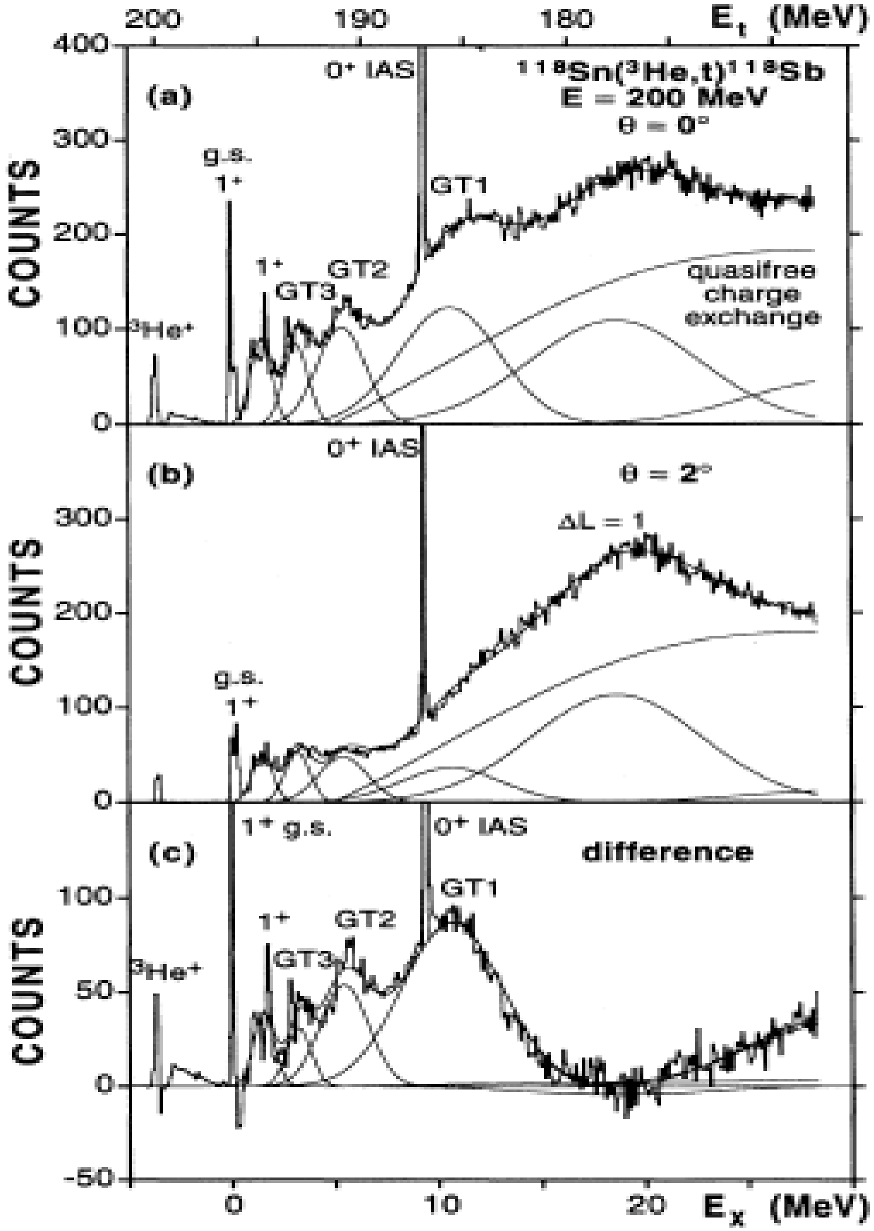

K. Pham *et al*., PRC 51 (1995) 526

(^{3}He,*t*) charge-exchange reaction on all stable Sn nuclei at IUCF, Bloomington
E(^{3}He) =200 MeV
Excitation-energy spectra are plotted relative to IAS.

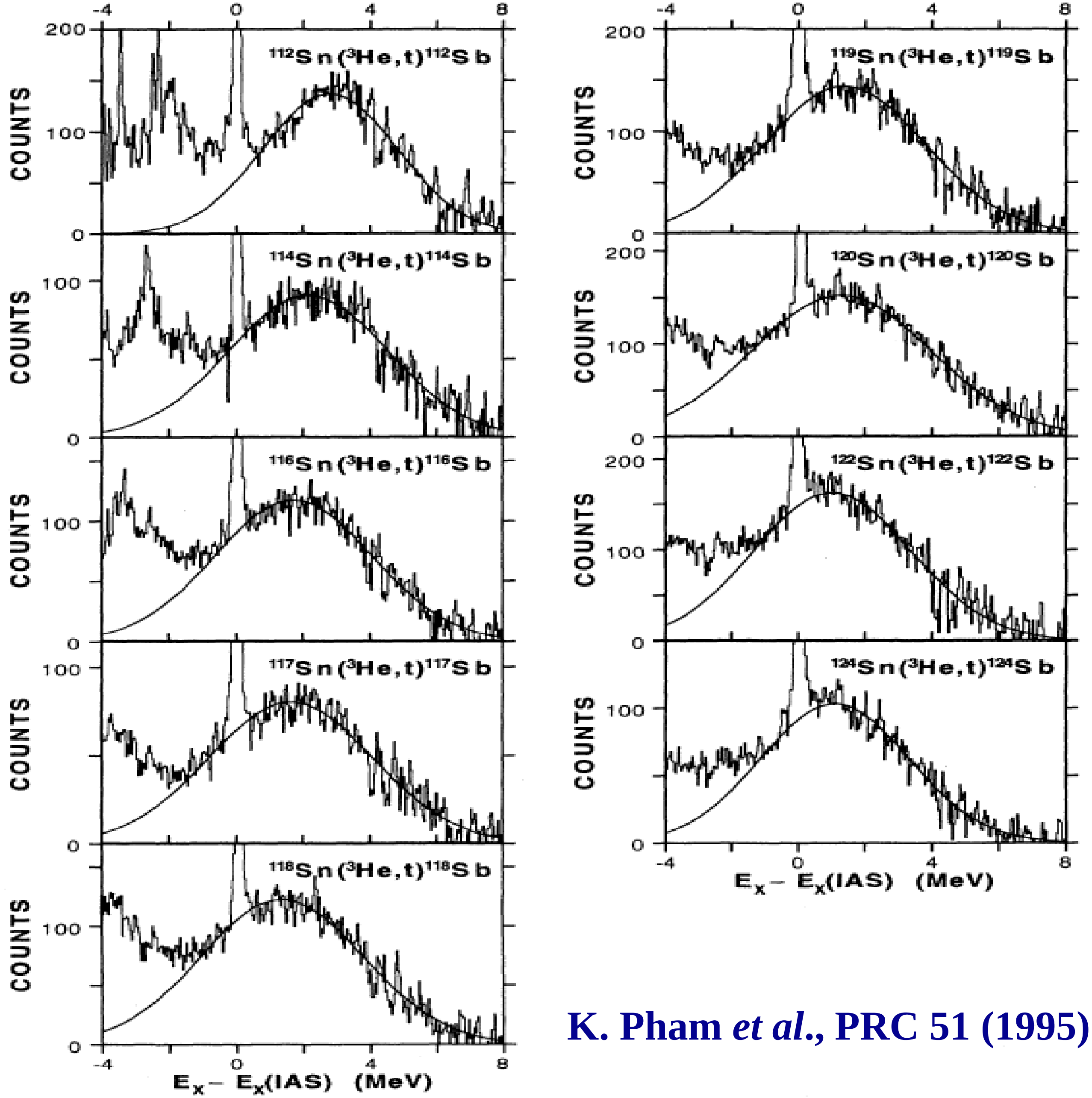

K. Pham *et al*., PRC 51 (1995) 526

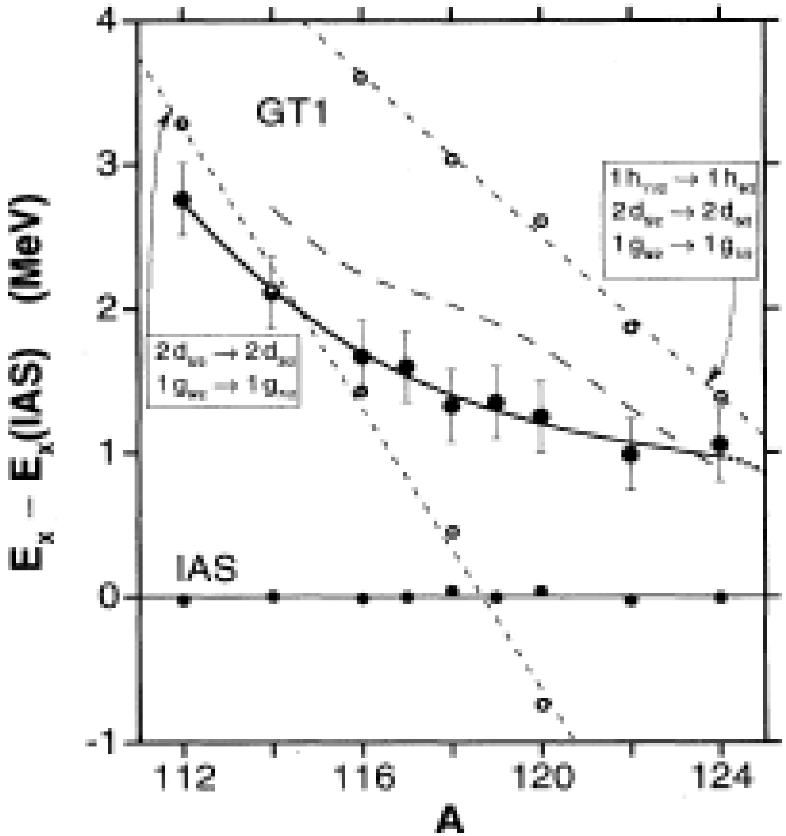

Excitation energy of main component of GTGR relative to IAS.

K. Pham *et al.*, Phys. Rev. C51 (1995) 526

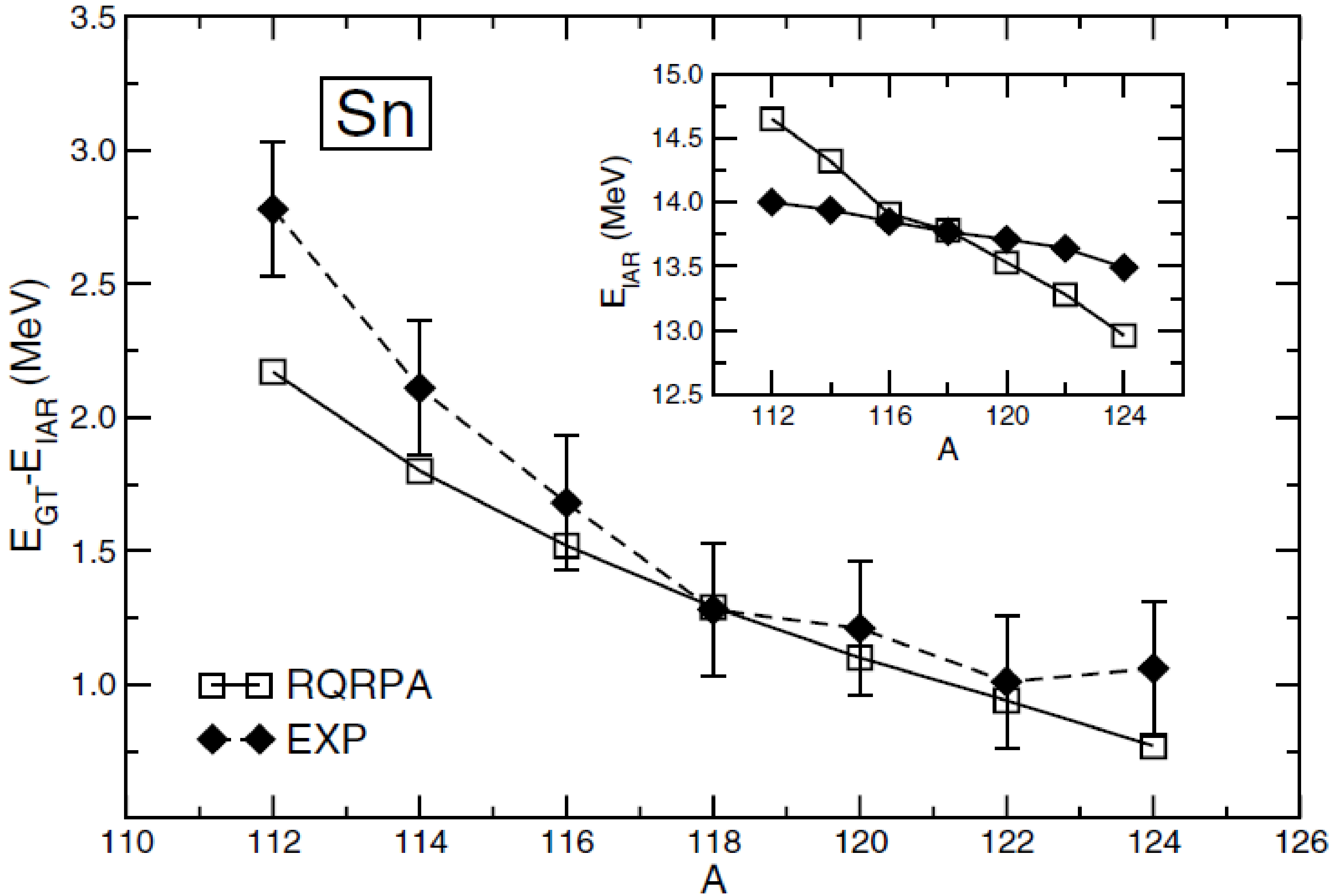

Comparison of theoretical calculations to experimental results for excitation energy of main component of GTGR relative to IAS. Inset shows IAS energies

D. Vretenar *et al*., Phys. Rev. Lett. 91 (2003) 262502

Theoretical pn-RQRPA and experimental differences of GTGR and IAS excitation energies as function of neutron-skin thickness (data from K. Pham). Lower panel shows comparison between theoretical neutron-skin thickness and experimental data (data from A. Krasznahorkay).

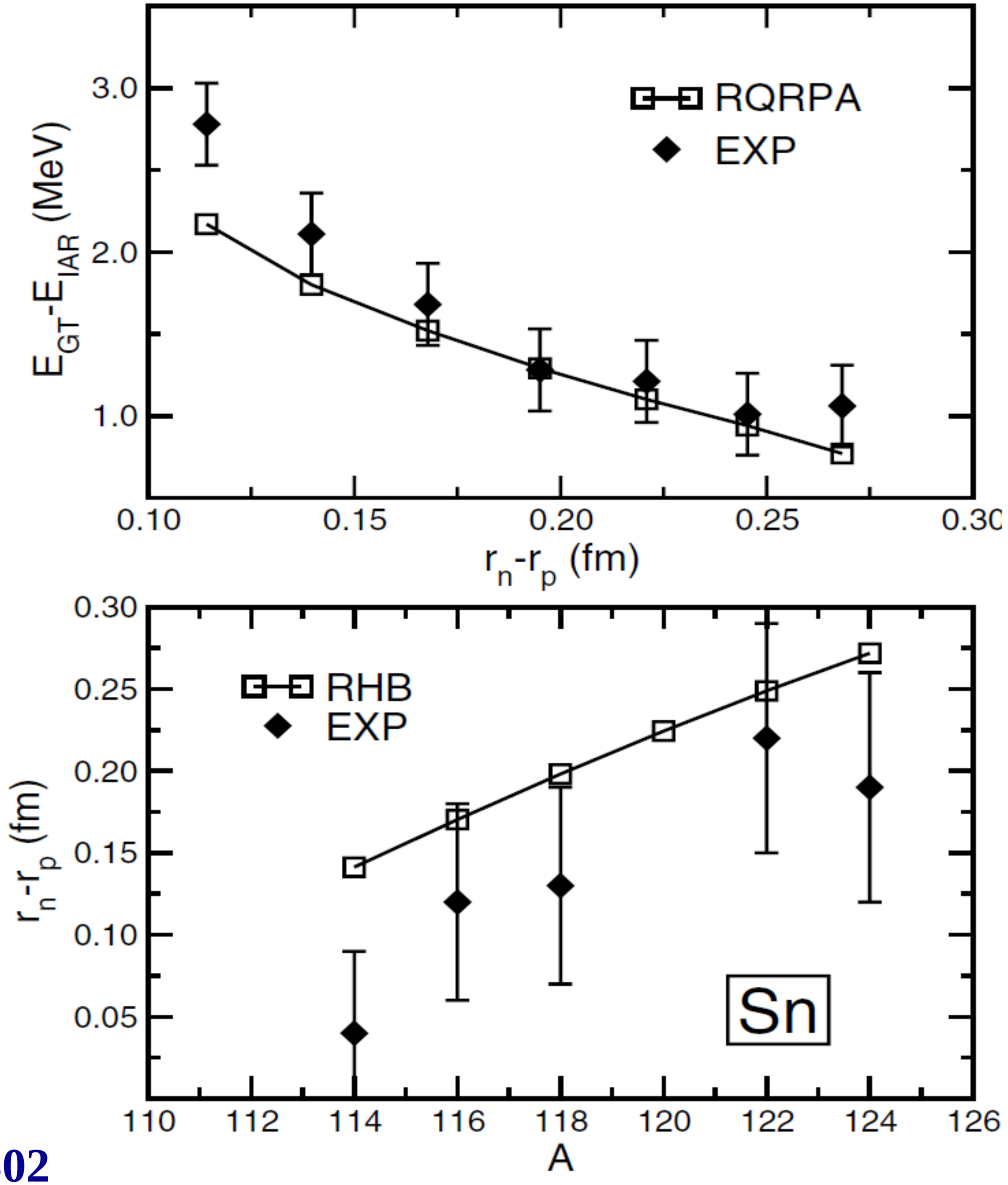

D. Vretenar *et al*., PRL 91 (2003) 262502

A. Krasznahorkay *et al*., PRL 83 (1999) 3216; r_n-r_p

Proton Decay
IAS, GTR, IVSGDR, IV(S)GMR

Microscopic Structure of GTR and IVSGDR in ^{208}Bi

- Proton decay of ^{208}Bi
  - Direct decay dominant
    - $E_x > E_{th}(n) > E_{th}(p)$
    - High Coulomb Barrier (Z=83)
  - Statistical proton decay negligible.
- Angular correlations
  - For IAS and GTR decay isotropic $\Delta L=0$
  - For IVSGDR anisotropic but not strongly
- Direct decay is influenced by:
  - Low *n*-decay threshold
  - High Coulomb barrier.

- $\Gamma_{GTR}{}^{\uparrow}/\Gamma \ll \Gamma_{IAS}{}^{\uparrow}/\Gamma \approx 0.5$
  - **IAS *n*-decay: isospin forbidden.**
  - **Centroid energy shift: cut off by Coulomb barrier**
- $\Gamma_{IVSGDR}{}^{\uparrow}/\Gamma > \Gamma_{GTR}{}^{\uparrow}/\Gamma$
  - **Higher proton energy**
- **Width** Γ

$$\Gamma = \Gamma^{\uparrow} + \Gamma^{\downarrow}$$

Escape: Direct decay
Spreading: Statistical Decay

$$\Gamma^{\uparrow} = \Gamma_p^{\uparrow} = \sum_i \Gamma^{\uparrow}_{pi}$$

Partial Escape Width

$$\frac{\Gamma^{\uparrow}_{pi}}{\Gamma} = \frac{\int d^2\sigma_{pi}/(d\Omega_t d\Omega_p) d\Omega_p}{d\sigma/d\Omega_t}$$

Branching ratio

Experiments

- RCNP facility
  K=400 MeV ring cyclotron
  Grand Raiden spectrometer
- Beam: $^{3}He^{++}$, 450 MeV

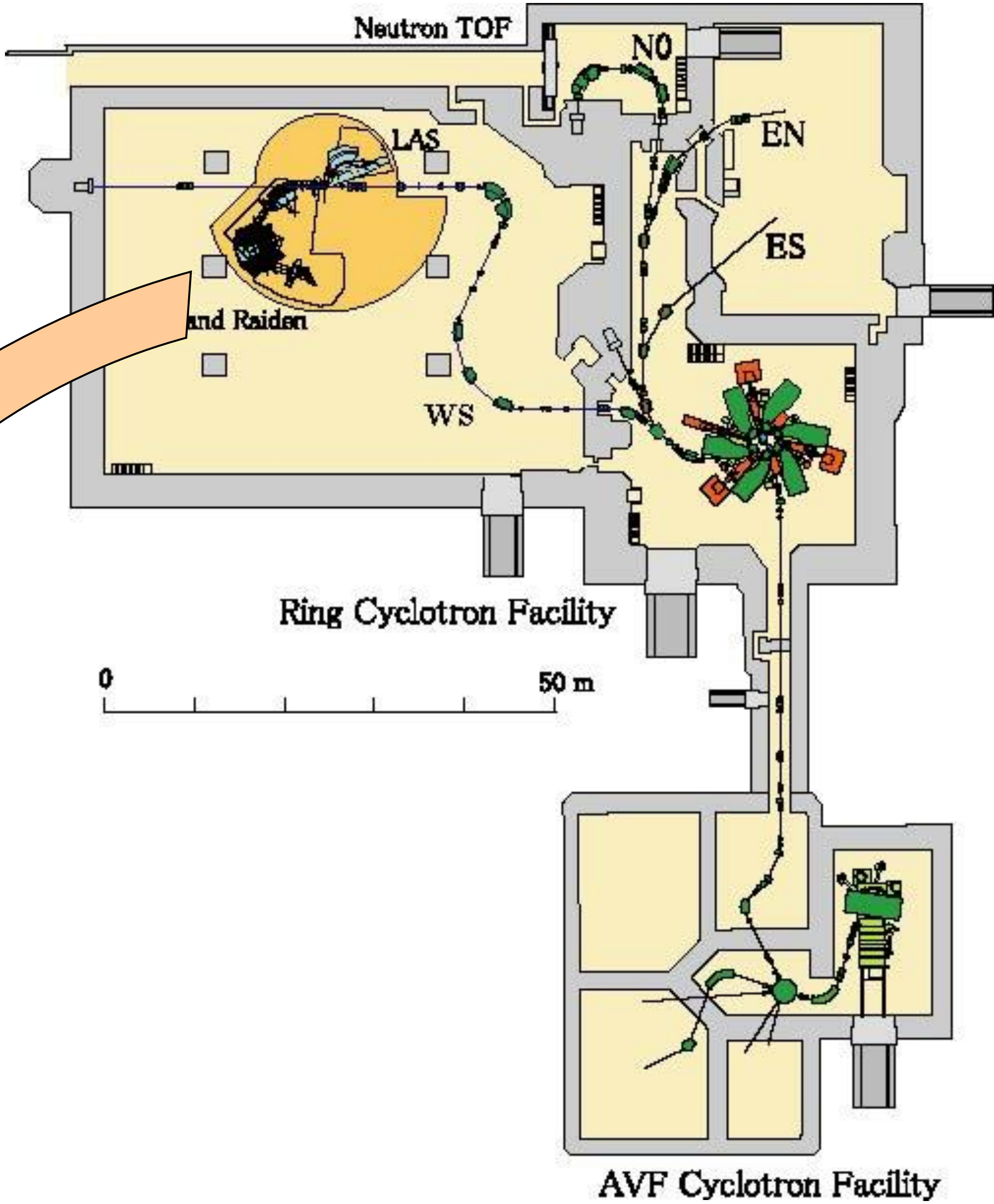

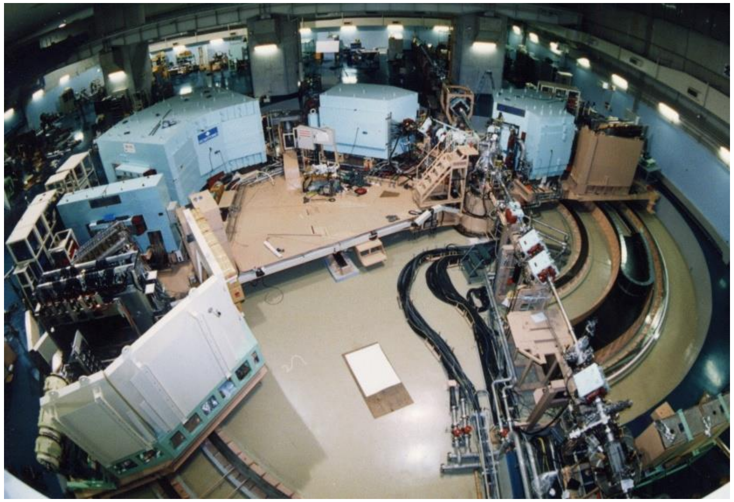

M. Fujiwara *et al.*, NIM A422 (1999) 484

Set-up of the Proton Counter

- Si(Li) detectors with a thickness of 5 mm, covering a solid angle of 5.7% in total.

- 35 keV (^{241}Am test)

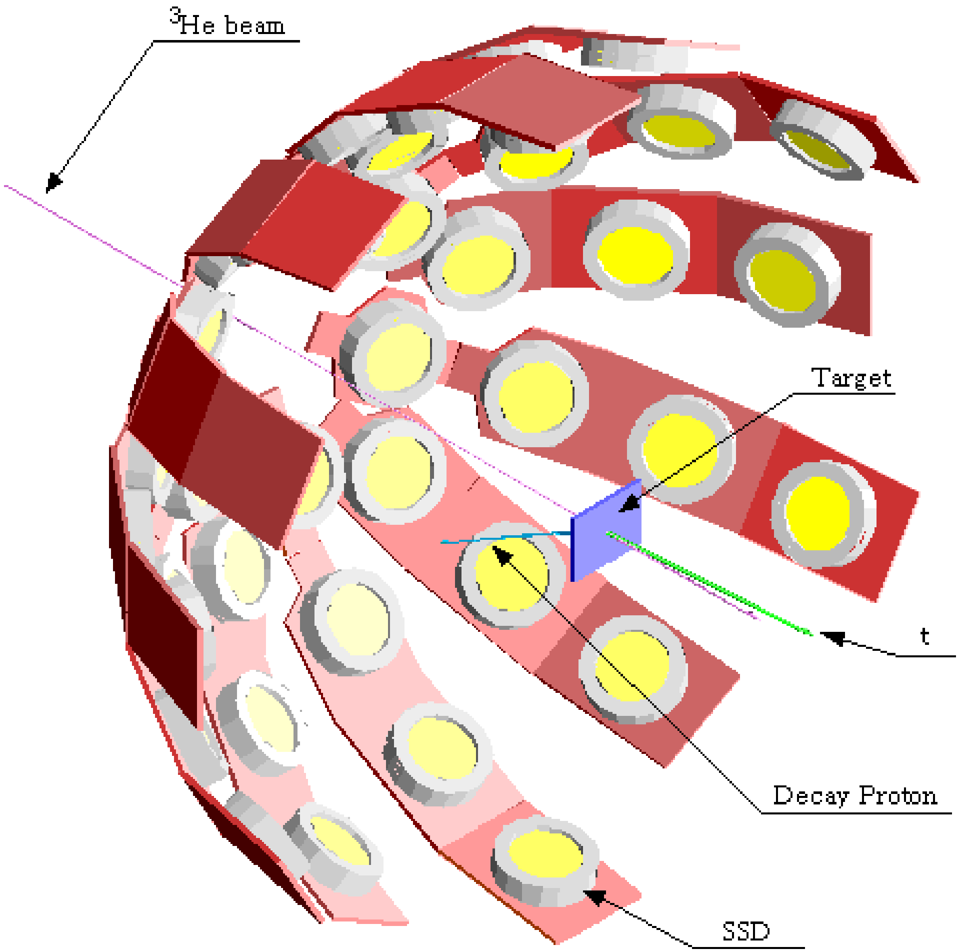

Spin-isospin-flip transitions in charge-exchange reactions and proton decay

A. Krasznahorkay et al., PRC 64 (2001) 067302.
A. Krasznahorkay et al., PRL 82 (1999) 3216.
H. Akimune et al., PRC 52 (1995) 604.
H. Akimune et al., Phys. Lett. B 233 (1994) 107

^{208}Pb(^{3}He,*t*) reactions E(^{3}He)=450 MeV

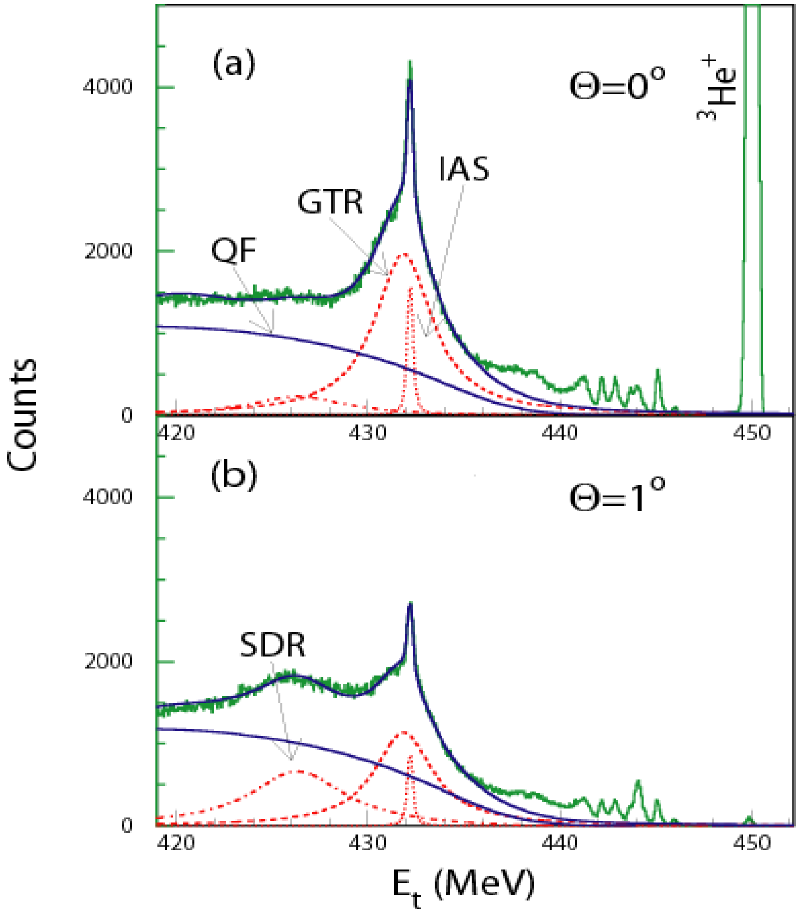

(^{3}He,*tp*) Coincidence data

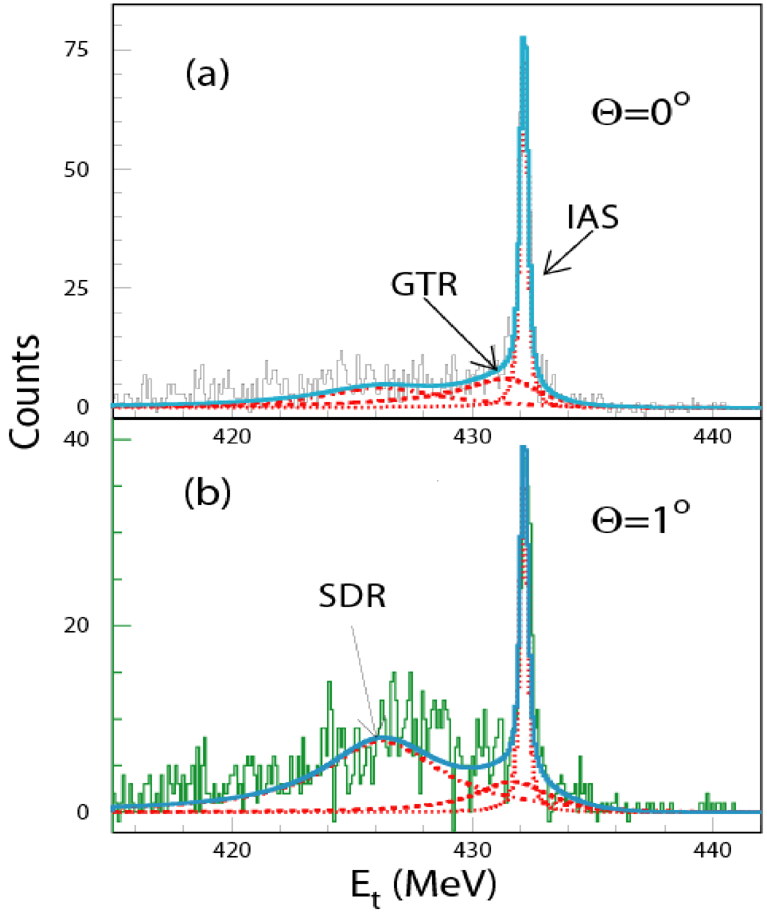

Experimental Results and Theoretical Calculations

➢ Partial escape width for GTR

		Theory	This work	
channel	E_x(keV)	$\Gamma_i^{\uparrow}$(keV)	$\Gamma_i^{\uparrow}$(keV)	branch (%)
$3p_{1/2}$	0	48,7	58.4 ± 19.8	1.8 ± 0.5
$2f_{5/2}$	570	46,2	inc. in $p_{3/2}$	
$3p_{3/2}$	898	44,7	101.5 ± 31.3	2.7 ± 0.6
$1i_{13/2}$	1633	0,87	8.3 ± 9.4	0.2 ± 0.2
$2f_{7/2}$	2340	5,89	15.6 ± 7.6	0.4 ± 0.2
$1h_{9/2}$	3413	0,24	–	–
Total		146,6	184 ± 49	4.9 ± 1.3

Theory:
E. Moukhai,
V.A. Rodin,
M.H. Urin
Continuum RPA

➢ Partial escape width for IVSGDR

		Theory		This work	
channel	E_x(keV	$\Gamma_i^{\uparrow}$(keV)	branch (%)	$\Gamma_i^{\uparrow}$(keV)	branch (%)
$3p_{1/2}$	0	103,4	1,23	83.4 ± 24.3	0.99 ± 0.29
$2f_{5/2}$	570	178,1	2,12	170.8 ± 49.3	2.12 ± 0.61
$3p_{3/2}$	898	210,1	2,5	240 ± 69.6	2.86 ± 0.83
$1i_{13/2}$	1633	299,8	3,57	330.4 ± 95.7	3.74 ± 1.08
$2f7_{/2}$	2340	249,3	2,97	282.2 ± 86.8	3.36 ± 0.97
$1h_{9/2}$	3413	52,6	0,63	86.7 ± 25.1	1.03 ± 0.29
Total		1209,6	14,4	1180 ± 340	14.1 ± 4.2

Summary: ^{208}Pb(^{3}He,*tp*)

- GTR: $\Gamma^{\uparrow}/\Gamma \sim 4.9\%$, $\Gamma^{\uparrow} = 184 \pm 49$ keV
  - Small branching ratio:
    - Spreading effect is very important.
    - Coupling to underlying 2p-2h states.
    - Centroid energy shift caused by
      High Coulomb barrier.
- IVSGDR: $\Gamma^{\uparrow}/\Gamma \sim 14.1\%$, $\Gamma^{\uparrow} = 1180 \pm 340$ keV
  - Larger p-decay $\Gamma^{\uparrow}/\Gamma$ compared to GTR.
    - E_p: enough higher than
      Coulomb barrier, centrifugal barrier.
  - Enhancement of decay to high-spin 1*n*-hole states

Isovector giant monopole resonances

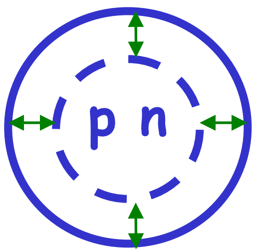

ΔL=0 ΔS=0 ΔT=0

ISGMR

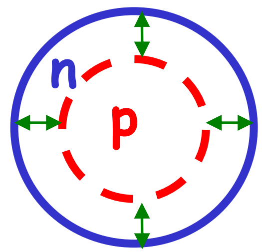

ΔL=0 ΔS=0 ΔT=1

IVGMR

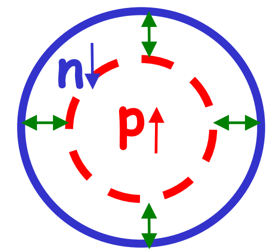

ΔL=0 ΔS=1 ΔT=1

IVSGMR

$O=r^{\lambda}[\sigma\otimes Y_L]_J\tau_-$

IAS: λ=0 S=0 L=0 J=0

GTR: λ=0 S=1 L=0 J=1

IVGMR: λ=0 S=0 L=0 J=0

IVSGMR: λ=0 S=1 L=0 J=1

IVSGDR: λ=1 S=1 L=1 J=0,1,2

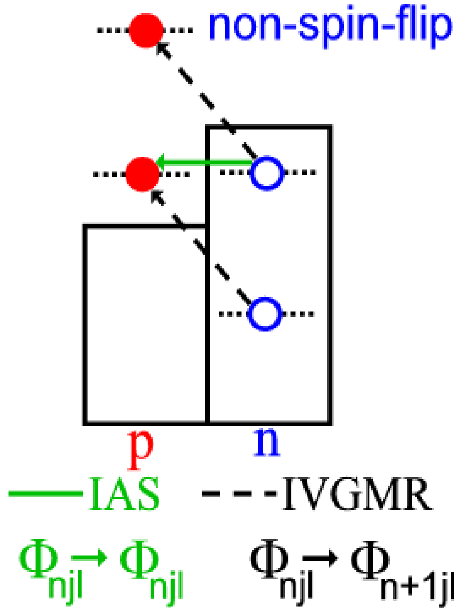

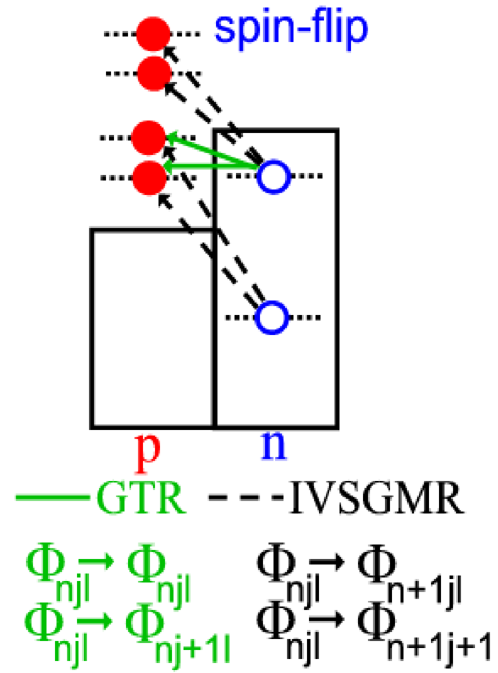

Decay studies

- **Successful:**
  - **GTR, IVSGDR in ^{208}Pb(^{3}He,*t*+*p*) at 450 MeV (Akimune *et al.*)**
  - **IVGMR/IVSGMR in Pb(^{3}He,*t*+*p*) at 177 MeV at KVI**

    & 410 MeV at RCNP (Zegers *et al.*)

- **Unsuccessful:**
  - **IVGMR/IVSGMR ^{124}Sn(^{3}He,*t*+*n*) at 200 MeV at IUCF**

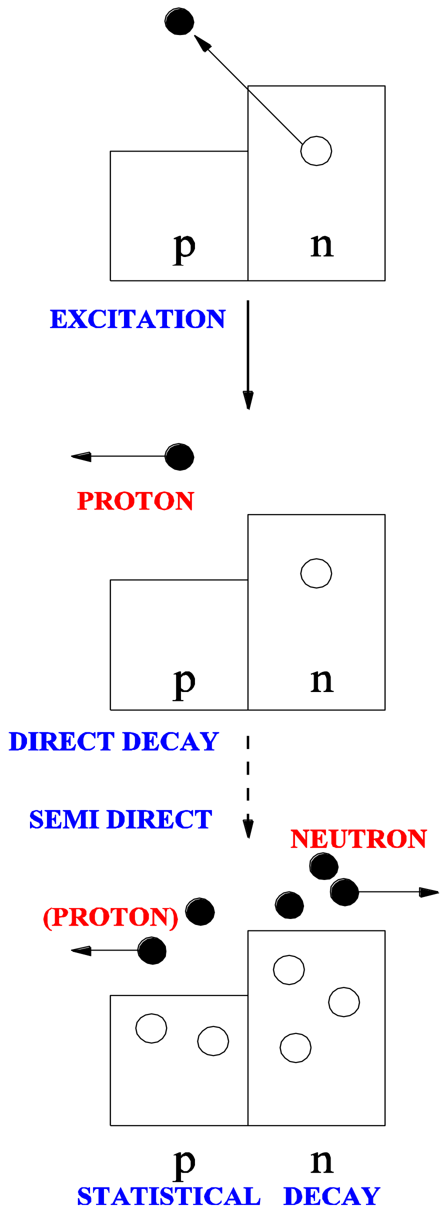

Proton decay from the IVSGMR

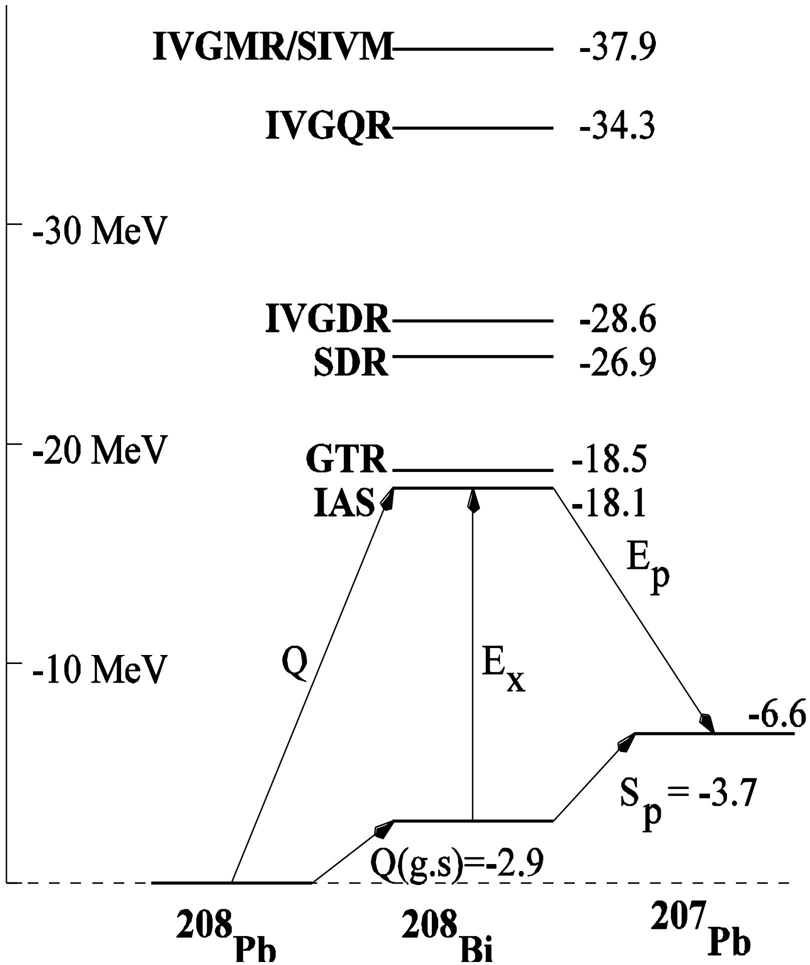

Measurement of IVSGMR via ^{208}Pb(^{3}He,*t*+*p*)

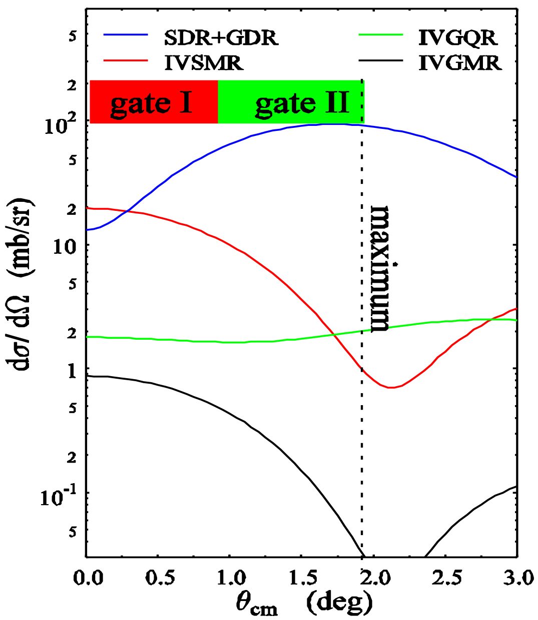

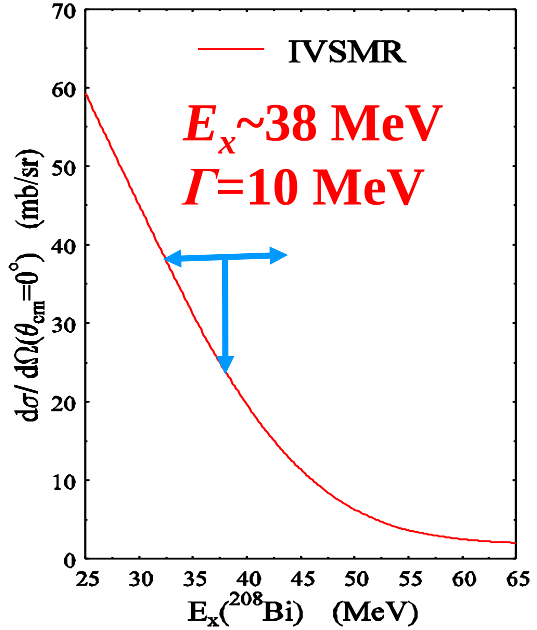

- **DW81 (Raynal)**
- **Effective ^{3}He-N potential**
  - **V_{τ}= 0.73±0.01 MeV (IAS)**
  - **$V_{\sigma\tau}$= -2.1±0.2 MeV (known ratio to V_{τ})**
  - **$V_{T\tau}$= -2.0 MeV/fm^{2}**
- **most coherent 1p-1h wave-function (normal modes).**

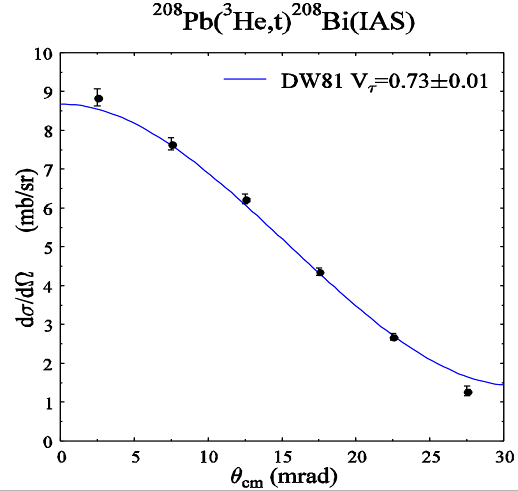

Use *difference-of-angle* to identify the monopole excitations

Results

R.G.T. Zegers et al., PRL 90 (2003) 202501

t singles

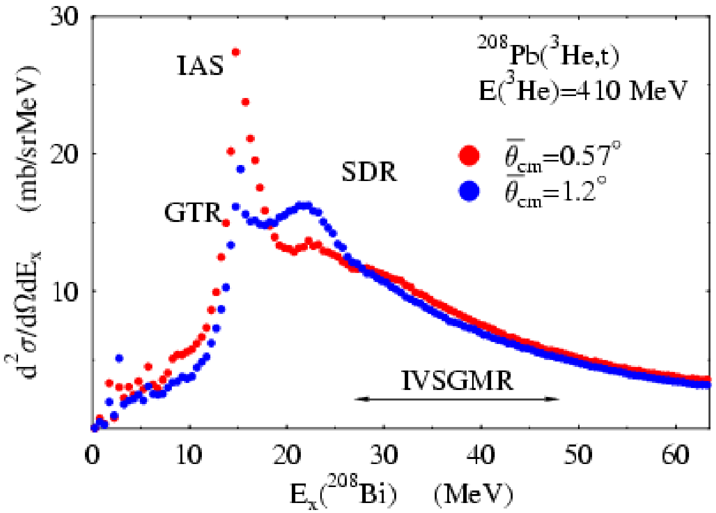

t-p coincidences

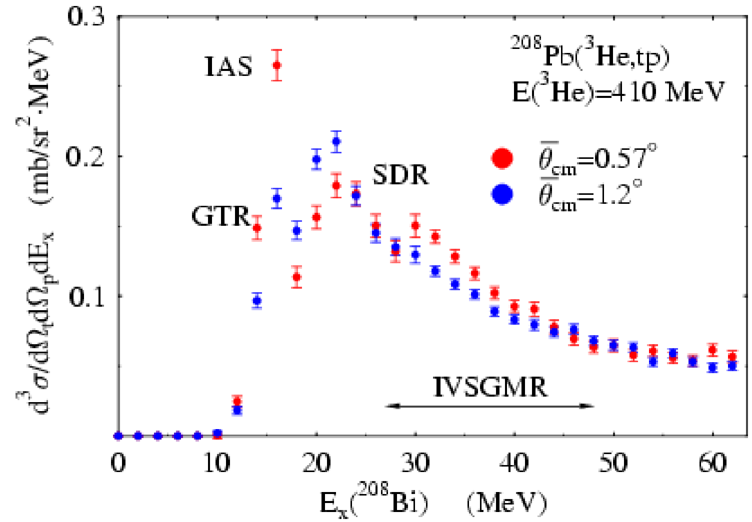

Difference of angles

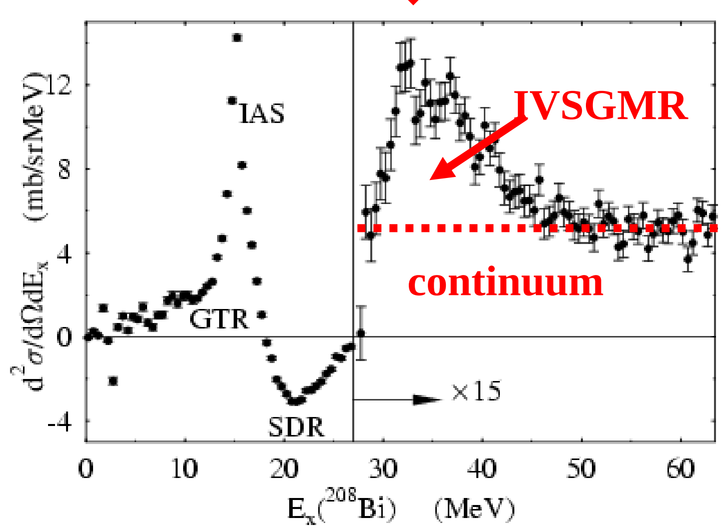

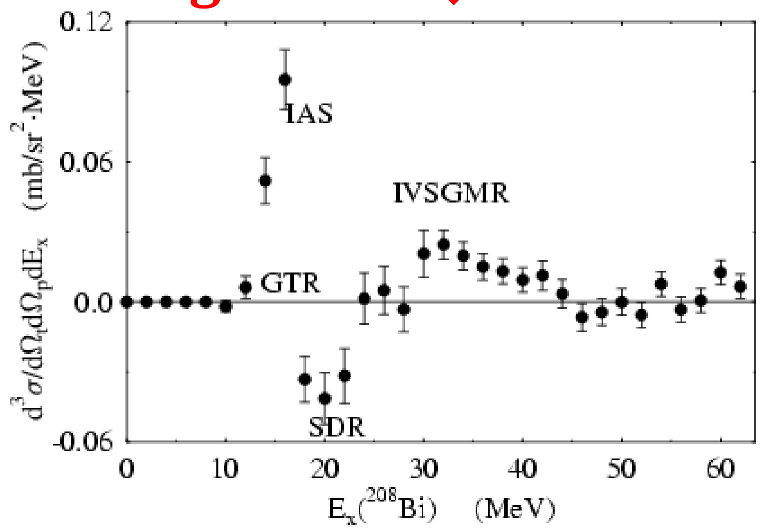

Angular distribution

Use difference-of-angle method between narrow angular bins to extract angular distribution of the resonance

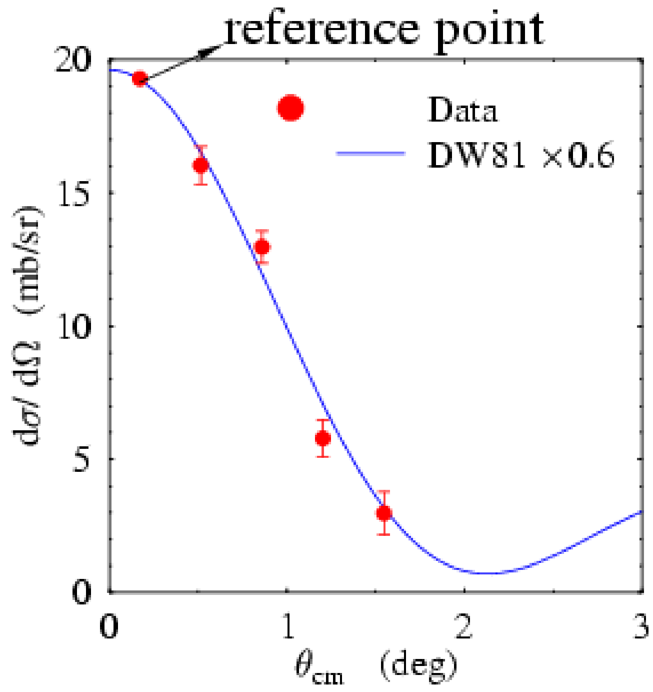

IVSGMR angular distribution confirmed

Strength exhaustion

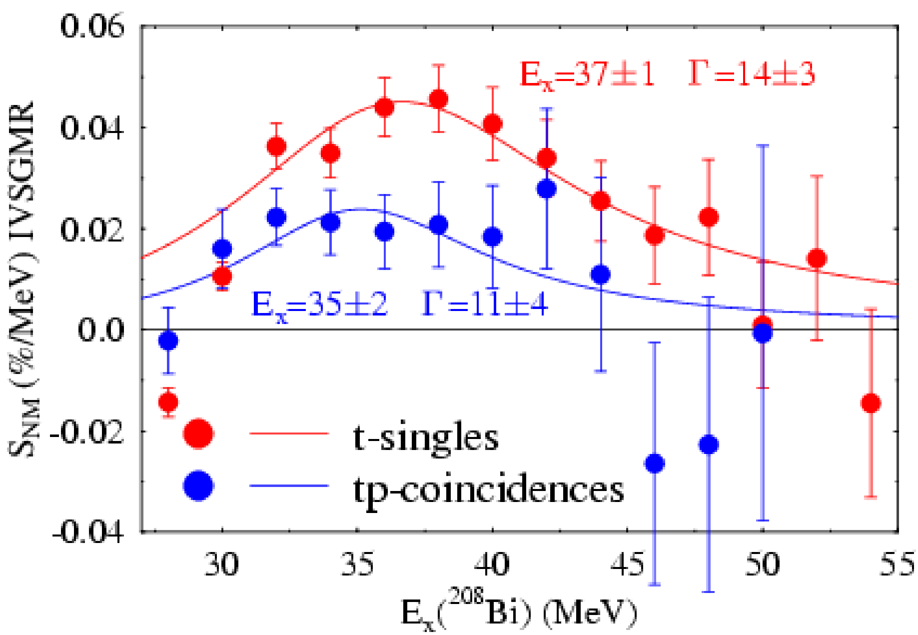

Summed strength: $(46\pm4\pm10)\cdot10^3$ fm^4
(contribution from IVGMR subtracted)

method	Exhaustion(%) ($\pm\sigma_{stat}$ $\pm\sigma_{sys}$)
Normal modes	60±5±14
Tamm-Dancoff Hamamoto & Sagawa PRC 62, 024319	68±6±17
Continuum RPA Rodin & Urin NPA 687, 276c	103±9±25
HF-RPA* Auerbach & Klein PRC 30, 1032	210±16±45

* Different operator, includes GT

Systematic errors

- extrapolation of continuum: 5%
- high-lying GT strength: small
- tail of the IVSGDR: 10%
- DWBA: 10% of measured value

Final state spectra

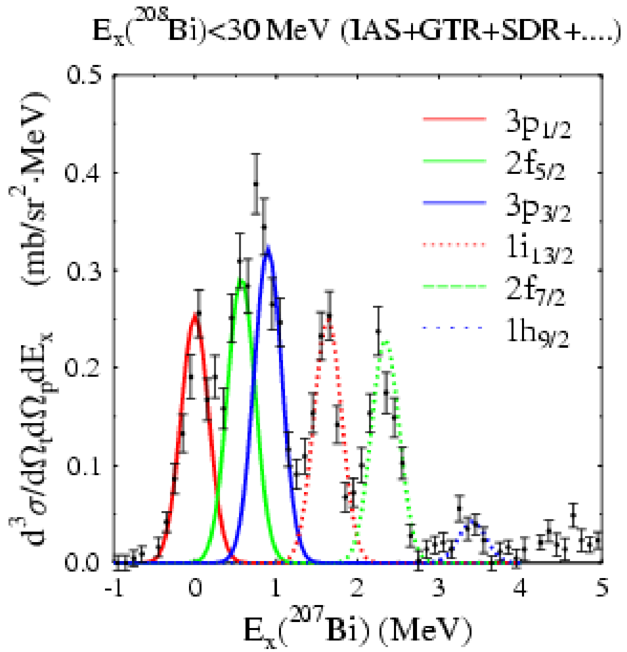

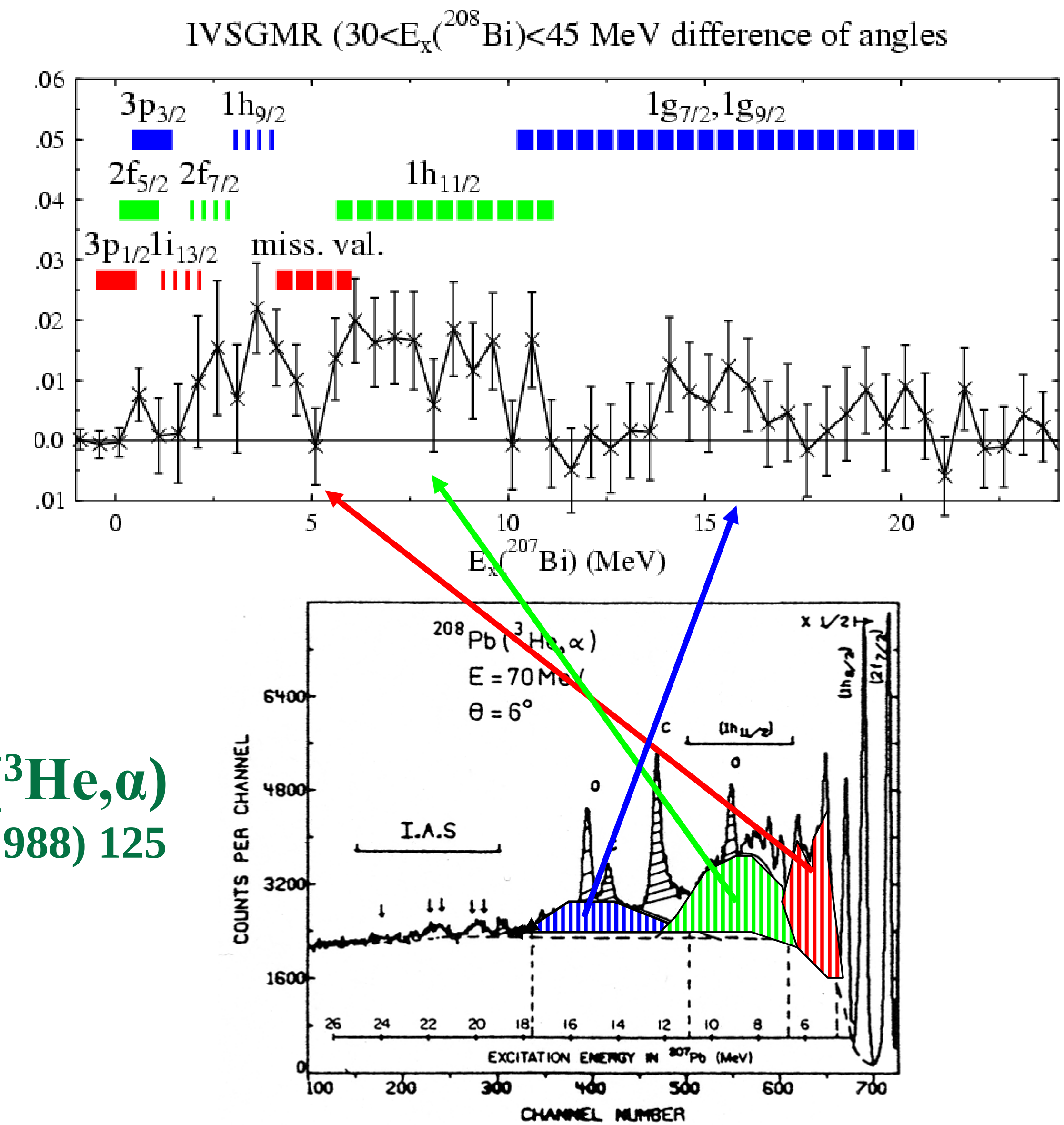

Comparison with $^{208}Pb(^3He,\alpha)$

S. Galès *et al.*, Phys. Rep. 166 (1988) 125

Final state population in ^{207}Pb

Final state	Data(%)	Theory(%)*
$3p_{1/2}$ $2f_{5/2}$ $3p_{3/2}$	< 3	11.3
$1i_{13/2}$		21.4
$2f_{7/2}$ $1h_{9/2}$	13±5	9.5
$1h_{11/2}$	22±8	22.8
$1g_{7/2}$ $1g_{9/2}$	17±8	
All	52±12	66

*Rodin & Urin NPA 687, 276c (continuum RPA)

Large discrepancies for partial branchings!!

Outlook

Radioactive ion beams will be available at energies where it will be possible to study GT transitions (RIKEN, NSCL, FAIR, EURISOL)

- **Determine GT strength in unstable *sd* & *fp* shell nuclei**
- **Measure ISGMR and ISGDR in extended isotope chain**
- **Unravel the nature of the pygmy dipole resonance**
- **Use IV(S)GDR as tool to determine *n*-skin [IV(S)GDR]**
- **Exotic excitations such as double GT (SHARAQ)**

Thank you for your attention